Journal of Statistical Physics, Vol. 49, Nos. 1/2, 1987

Cellular Automata and Statistical Mechanical Models

Pål Rujån[1,2]

Received January 16, 1987; revision received June 1, 1987

We elaborate on the analogy between the transfer matrix of usual lattice models and the master equation describing the time development of cellular automata. Transient and stationary properties of probabilistic automata are linked to surface and bulk properties, respectively, of restricted statistical mechanical systems. It is demonstrated that methods of statistical physics can be successfully used to describe the dynamic and the stationary behavior of such automata. Some exact results are derived, including duality transformations, exact mappings, "disorder," and "linear" solutions. Many examples are worked out in detail to demonstrate how to use statistical physics in order to construct cellular automata with desired properties. This approach is considered to be a first step toward the design of fully parallel, *probabilistic* systems whose computational abilities rely on the cooperative behavior of their components.

KEY WORDS: Cellular automata; multispin Ising models; static and dynamic critical phenomena; duality relations; exact solutions; stochastic processes; predictible behavior; topological invariants; microcanonical simulations.

1. INTRODUCTION

A cellular automaton (CA) is a lattice model with discrete variables which are updated in discrete time steps according to a specified set of local rules. The dynamic behavior of systems containing many discrete elements with local interactions can be conveniently modeled in this way. One of the earliest applications was for biological systems; actually, the concept was

[1] Institut für Festkörperforschung der Kernforschungsanlage Jülich GmbH, D-5170 Jülich, Federal Republic of Germany.

[2] On leave from Institute for Theoretical Physics, Roland Eötvös University, Budapest, Hungary.

0022-4715/87/1000-0139$05.00/0 © 1987 Plenum Publishing Corporation

introduced by von Neumann and Ulam[1],[3] in an attempt to distill in a mathematical form the "logical structure of life." A survey of papers published in the last 10 years on the subject[4] shows that, besides many mathematical papers, most applications of concepts of cellular automata can be found in biology[3] and in the theory of automata.[4] Physicists became active in this field only relatively recently,[6],[5] motivated in part by the expected proliferation of special-purpose machines built for stochastic simulations of very highly time-consuming problems (see Ref. 7 for reviews) and partly by the study of models for neuronal networks[8],[6] and failure-resistant machines.[10]

The definition of a cellular automaton given above is usually supplemented with the requirement of a *deterministic, simultaneous updating* (dynamics). In this paper we emphasize *probabilistic* cellular automata: we hope to convince those who dislike such an extended definition that this generalization is an extremely useful one. Many interesting phenomena, such as changes from an n-cycle to an $(n+1)$-cycle behavior, phase transitions, etc., can be achieved *only* if one has some probabilistic elements in the CA rules. On the other hand, such an extension is very general: any proper Monte Carlo simulation, quasirandom number generator,[11] etc., might be labeled as a cellular automaton. Any Markovian process defined on a lattice is also a good candidate for a CA, so the topic is overhelmingly abundant. This fact is partly expressed by the size of this article in spite of the efforts by the author to select and present here only the most illustrative examples.

The main goal of this paper is to make an extensive use of the similarity between the usual transfer matrix formalism and the time evolution operator (master equation) of the cellular automata. Finding an analogy between two different fields usually benefits both. In our case, defining appropriate cellular automata rules for statistical physical systems is equivalent to finding an importance sampling procedure for the Green function Monte Carlo method[12] giving exact results for the ground-state energy and ground-state correlation functions. This leads to a very accurate and powerful numerical method for studying statistical physical systems. Moreover, by using deterministic CA that conserve some macroscopic

[3] For books on cellular automata see Refs. 2.

[4] This was done through a search of the PDOC a database, containing documents on parallel computing, parallel processing, and high-speed computing maintained by J. Hake, ZAM KFA Jülich (Manual KFA-ZAM-0055 DB, 1986).

[5] For a recent collection of reprints see Wolfram.[5] See also the full volume of *Physica D* **10** (1984).

[6] For a cellular automaton model see Refs. 9.

quantities, it is possible to simulate hydrodynamics[13] or thermodynamics[7] using "microcanonical" ensembles. On the other hand, the study of dynamical systems such as cellular automata may be undertaken using standard methods developed in statistical physics, especially the ones dealing with cooperative critical behavior near continuous phase transitions. Some of these methods are analytical in nature and lead to exact relations; others are numerical methods especially useful when studying complicated rules or the critical behavior of CA.

The paper is organized basically in two main parts: Sections 2–4 form a theoretical basis for the applications discussed in Section 5. In Section 2 we discuss the transfer matrix formalism and the master equation approach, pointing out the common features. A few pedagogical examples illustrating the basic concepts are given and some theorems on finite CA are briefly summarized. The classification of different CA from the point of view of their time-developing operators leads in a natural way to the discussion of different possible mechanisms for phase transitions. Section 3 contains most of our exact results. The notion of duality is generalized to models with many spin interactions, including odd-spin and negative interactions. In general, the model dual to a cellular automaton has more degrees of freedom than the original one—often its parameters are complex ("unphysical" regime). Two distinct classes of exactly soluble CA are discussed: disorder solutions and linear (free) models. Both represent a valid starting point for series expansions. Finally, we show that the condition of exact integrability—involving here the existence of an infinite number of integrals of motion (conserved charges)—has a specific form in the case of CA models. In Section 4 we discuss numerical finite-size lattice calculations and extrapolation through the phenomenological renormalization group method: as an example, we consider the "Hamiltonian limit" or the sequential updating version of the directed percolation problem. Our numerical results indicate that the critical behavior is not affected by the change in dynamics.

The second part of the paper (Sections 5–6) is quite unusual. In Section 5 we address the question of how to design rules leading to an *a priori* desired behavior. This question rests more in the realm of engineering than on that of statistical mechanics. Accordingly, I have selected a few representative examples centered around four topics I consider of major importance for *practical applications* of CA (Section 6).

[7] The observation made by Pomeau[14] that Fredkin's reversible Q2R[15] rule conserves the energy of two decoupled Ising models has been used by Herrmann[16] to devise a very fast microcanonical simulation algorithm. See also Goles and Vichniac.[17]

1. The question of phase transitions in CA is considered in some detail; we show how to design rules leading to special types of critical exponents.

2. For many practical applications the question of *conserved quantities* may be crucial: we give a few examples and in particular discuss a simple local automaton conserving the *topological structure* of a given initial configuration.

3. Sometimes it is useful to have a system that can change from a limit cycle of given length to a different limit cycle, such transitions correspond to a change from a commensurate phase to another commensurate phase: two examples are explicitly worked out.

4. Finally, we emphasize that one may easily build parallel networks of cellular automata with a quite complex behavior by linking together two different, but simple, rules. One such class are the "substitution" and "hierarchical" automata; here *probabilistic* rules are changed *deterministically* in time according to the state of a parallelly running deterministic automaton. Another case of such structures corresponds to quenched random networks of automata, with a very complicated behavior. Although very important, random networks of automata will be given here a limited space, mainly because of the topic has a strong overlap with the area of research regarding neural networks and spin-glass models, which is abundantly and well represented in the recent physics literature.

Finally, in Section 6 we summarize the results of our paper by speculating on the feasibility of fully parallel *probabilistic* automata networks, whose computing abilities are provided through the cooperative behavior of their components. I call this concept a *probabilistic computer*; others call it a Boltzmann machine.[18] At the moment one can put forward only little more than speculations on this subject, presented with the firm convinction that physics, and especially statistical physics, has an important role to play in understanding the basic features and the main functional principles of such networks.

2. GENERAL FORMALISM AND (0+1)-DIMENSIONAL EXAMPLES

2.1. Generalities

Consider a regular lattice in $d+1$ dimensions. Here we follow the field-theoretic notation; d is the dimension of the "space," 1 is the dimension of "time." In (classical) statistical physics we have then a $(d+1)$-

dimensional lattice whose transfer operator will "transfer" the interactions from a d-dimensional space slice at time t to the next space slice at time $t+\tau$. For simplicity, we consider the square lattice shown in Fig. 1a and we suppose that at each lattice point we have an Ising-like variable $s_{i,j} = \pm 1$. Generalization to other variables is straightforward, but in this paper we shall consider only discrete variables with q (mostly $q=2$) possible states. The spins of Fig. 1 interact with other spins located around a basic face of the square lattice (interaction-round-a-face = IRF model).[19] As will soon become evident, not all forms of interactions are suitable for constructing cellular automata. Another typical interaction form is the checkerboard lattice shown in Fig. 2a; only in the full squares are all possible interactions between the corner spins allowed. The partition function depends on all the couplings of the different interaction terms of the energy function (*interaction representation*) or, equivalently, on all independent Boltzmann factors

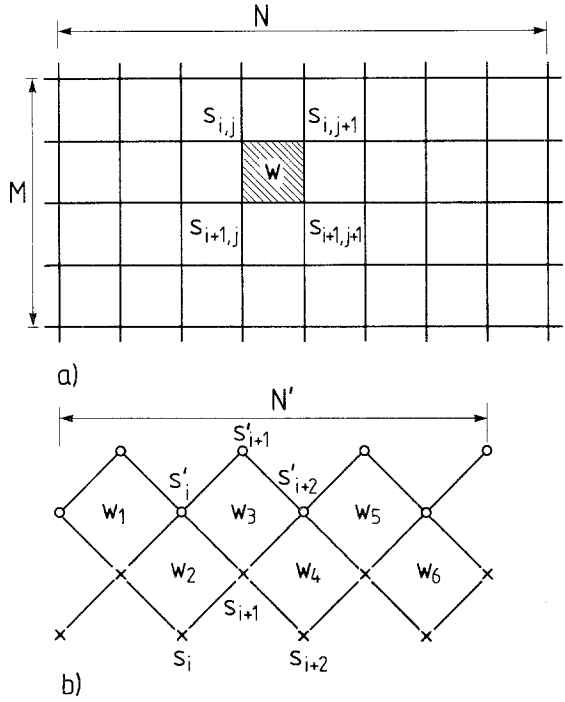

Fig. 1. The interactions-round-a-face (IRF) model and the diagonal-to-diagonal transfer matrix. (a) All possible interactions are allowed between the four corner spins forming an elementary face of the square lattice (hatched square). (b) The portion of the square lattice whose Boltzmann factor constitutes the element of the diagonal-to-diagonal transfer matrix corresponding to a given configuration of spins denoted by circles and crosses, respectively.

associated with an elementary face $w(s_{i,j}, s_{i+1,j} | s_{i+1,j+1}, s_{i,j+1})$ (*weight representation*). The partition function of an $N \times M$ lattice is defined as

$$Z_{NM}(w) = \sum_{\{s_{i,j}\}} \prod_{(\mathrm{nn})} w(s_{i,j}, s_{i+1,j} | s_{i+1,j+1}, s_{i,j+1}) \tag{2.1}$$

The sums can be "ordered" in some way—for example, row after row or diagonal after diagonal—and a proper repartitioning of the product in (2.1) leads to the well known expression[19]

$$Z_{NM}(w) = \mathrm{Tr}[T^{M'}] = \sum_{\alpha=1}^{q^{N'}} t_\alpha^{M'} \tag{2.2}$$

where N' is the number of spins in a layer (row or diagonal), M' is the number of layers, and

$$T_{\{\mathbf{s}\},\{\mathbf{s}'\}}$$

is a matrix of dimensions $q^{N'}$ with eigenvalues t_α. In Fig. 1b the diagonal-to-diagonal transfer matrix is also depicted graphically and equals

$$T^{\mathrm{D\text{-}D}} = W_1 W_3 \cdots W_{2k+1} W_2 W_4 \cdots W_{N'} \tag{2.3}$$

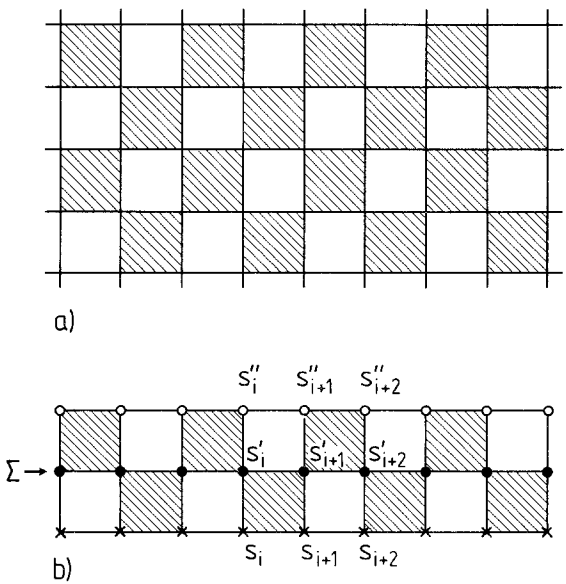

Fig. 2. The checkerboard lattice and the corresponding row-to-row transfer matrix. (a) All possible interactions are allowed within the hatched squares; the white squares contain no interaction. (b) An element of the row-to-row transfer matrix is obtained by summing over all possible configurations of the second row.

where

$$W_k = \delta_{s_1, s_1'} \cdots \delta_{s_k, s_k'} w(s_k, s_{k+1}, s_{k+2} | s_k', s_{k+1}', s_{k+2}') \, \delta_{s_{k+2}, s_{k+2}'} \cdots \delta_{s_{N'}, s_{N'}'}$$

The row-to-row transfer matrix of the checkerboard lattice is indicated in Fig. 2b and has the definition

$$T^{\mathrm{R\text{-}R}}_{\mathbf{s},\mathbf{s}''} = \sum_{\{\mathbf{s}'\}} (T_1)_{\mathbf{s},\mathbf{s}'} (T_2)_{\mathbf{s}',\mathbf{s}''}$$

$$= \sum_{\{\mathbf{s}'\}} \prod_{i=1}^{N} w_{\blacksquare}(s_i, s_{i+1} | s_i', s_{i+1}') \times w_{\blacksquare}(s_{i+1}', s_{i+2}' | s_{i+1}'', s_{i+2}'') \quad (2.4)$$

where $w_{\blacksquare}$ indicates the weight of a hatched face in Fig. 2.

In general T is a nonsymmetric, real matrix and its spectral decomposition is $(t_1 \geqslant t_2 \geqslant t_3 \cdots)$

$$\hat{T} = \sum_{\alpha=1}^{q^{N'}} |R_\alpha\rangle \, t_\alpha \langle L_\alpha| \quad (2.5)$$

where the left $\langle L_\alpha|$ and the right $|R_\beta\rangle$ eigenvectors are biorthogonal

$$\langle L_\alpha | R_\beta \rangle = \delta_{\alpha,\beta}$$

When $M' \to \infty$ and t_1 is nondegenerate (also t_k, $k > 1$ is not *exponentially* degenerate), any function $A(\mathbf{s})$ of spins lying on the same "space" layer has the expectation value

$$\langle A(\mathbf{s}) \rangle = \langle L_1(\mathbf{s})| \, A(\mathbf{s}) \, |R_1(\mathbf{s})\rangle \quad (2.6)$$

while correlations of functions $B(\mathbf{s}_i) \times C(\mathbf{s}_{i+R})$ involving spin variables on layers separated by a distance R are given by

$$\langle B(\mathbf{s}_i) \, C(\mathbf{s}_{i+R}) \rangle = \sum_{\alpha} \left(\frac{t_\alpha}{t_1}\right)^R \langle L_1| \, B(\mathbf{s}) \, |R_\alpha\rangle \langle L_\alpha| \, C(\mathbf{s}) \, |R_1\rangle$$

$$\xrightarrow[M > R \to \infty]{} \left(\frac{t_2}{t_1}\right)^R \langle L_1| \, B(\mathbf{s}) \, |R_2\rangle \langle L_2| \, C(\mathbf{s}) \, |R_1\rangle \quad (2.7)$$

These equations are all valid only for matrices of simple structure when $\langle L_1| \, B, C \, |R_1\rangle = 0$ and can be easily generalized when some eigenvalues are degenerate; this will be shortly discussed in the context of phase transition mechanisms.

From Eqs. (2.2), (2.6), and (2.7) it is obvious that the knowledge of a few largest eigenvalues and of the corresponding left and right eigenvectors is sufficient for the calculation of thermodynamic quantities and of the

correlation lengths parallel and perpendicular to the chosen layers. Since the operator T is real, positive (all its elements are Boltzmann weights), and irreducible (see later exceptions), the Frobenius–Perron theorem[20] ensures that the largest eigenvalue is not degenerate and the corresponding eigenvector is nodeless, as long as the matrix is finite. Phase transitions occur when in the $N' \to \infty$ limit the largest eigenvalue becomes degenerate. Any operator that has nonzero matrix elements between the two (or more) degenerate states is a good candidate for an order parameter, provided one does not have a simple crossing of eigenvalues (first-order transition).

It is very seldom that one can diagonalize exactly the transfer matrix.[19] In general one relies on various numerical methods, such as variational approaches,[21],[8] renormalization group methods,[23] or finite-size extrapolation of exact numerical diagonalization results.[24],[9] However, the exact diagonalization of very large matrices sometimes becomes intractable before the extrapolation procedure converges. In such cases one may compromise on the accuracy of the largest eigenvalues (and notably on that of the corresponding eigenvectors) and apply a stochastic diagonalization procedure known as the Green function Monte Carlo (GFMC) method.[12,26] Equation (2.2) can be viewed as the sum of all possible paths running randomly in the space of the transfer matrix indices and returning to their starting position after M' steps. The large majority of these random walks give a small contribution to the partition function. This suggests the choice of a transition probability that is proportional to the value of the transfer matrix elements. This probability distribution is normalized as follows. Suppose one knows the *left eigenvector* $\langle L_1|$ corresponding to t_1; denote its elements by $\{L_1(i)\}$. The matrix

$$P_{i,k} = \frac{1}{t_1} L_1(i)\, T_{i,k} L_1^{-1}(k) \tag{2.8}$$

is a stochastic matrix, i.e., $\sum_i P_{i,k} = 1$. Thus, *any single walk* in the index space of P will give the *exact* t_1 with variance zero. In practice, of course, it is more difficult to obtain $\langle L_1|$ than t_1. The basic idea of importance sampling is that using an appropriate *Ansatz* will make P almost stochastic[12,26] and will reduce drastically the variance of the measured t_1.

Since P is a stochastic operator, we might reinterpret it as a discrete-time developing operator for a cellular automaton defined on one layer (space) of N' spins. Starting with some initial *right vector* $|R(\{\mathbf{s}\}, t=0)\rangle \equiv$

[8] For an application of variational principles to estimate the dynamic critical exponent see Haake and Thol.[22]

[9] For a review see Barber.[25]

$R^{(0)}$, which we call the *initial configuration*, and iterating in discrete time steps, one obtains [see Eq. (2.4) and Fig. 2b]

$$R(\{\mathbf{s}''\}, t+2\tau) = \sum_{\{\mathbf{s}\}} [P^{\text{R-R}}(\mathbf{s}''|\mathbf{s})\, R(\{\mathbf{s}\}, t)] \tag{2.9}$$

for the "row-to-row" rules and a similar equation involving $P^{\text{D-D}}$ for the "diagonal-to-diagonal" rules (Fig. 1b). Here $P^{\text{D-D}}$ and $P^{\text{R-R}}$ are the stochastic matrices constructed from the transfer operators $T^{\text{D-D}}$ and $T^{\text{R-R}}$, respectively, and involve in both cases a two-step recursion in time. These processes may be split into two one-step recursions with alternating time development operators.

From Eq. (2.8) it follows that there is no difficulty in defining appropriate cellular automata dynamic rules for any statistical physical model with a finite and tractable transfer matrix (see the following examples). The main question is what happens in higher dimensions, where usually the transfer matrix is infinite. Is it possible, for example, to start from exactly soluble models[19] and construct dynamic rules? The answer is *yes* and *no*. In principle, the knowledge of the left eigenvector with largest eigenvalue is sufficient for constructing the stochastic matrix P whose elements give the probability that a given configuration of "children" has been born from a given configuration of "parents." In this sense every single "child" spin depends on the *whole generation* of its parents and of its peers. For any practical purpose, however, one would like to set all spins at some time t_0 *independently of each other* and depending only on the values of the spins within the (usually short range) of the rules at time $t_0 - \tau$. These conditions both can be satisfied if the transfer matrix has the following structure:

$$T_{\mathbf{s},\mathbf{s}'} = \prod w(s_{i_1}, \ldots, s_{i_k} | s'_{I_1}, \ldots, s'_{I_K}) \tag{2.10}$$

where the elementary faces w may interpenetrate *except at the base* (spins $\mathbf{s}$) and

$$\sum_{s_{i_1}, \ldots, s_{i_k}} w(s_{i_1}, \ldots, s_{i_k} | s'_{I_1}, \ldots, s'_{I_K}) = \text{const} \tag{2.11}$$

When expanding the solution of (2.10)–(2.11), w must contain, besides a constant 1/2, all possible spin products that include *at least* one s_{i_a}, $a = 1, 2, \ldots, k$, spin.

A few possibilities for w faces are shown in Fig. 3. This particular form of the w faces involves a constant left eigenvector $\langle L_1|$. Equations (2.10)–(2.11) are known in statistical physics as *disorder line conditions.*[10]

[10] For reviews on the subject of disorder lines see Refs. 27.

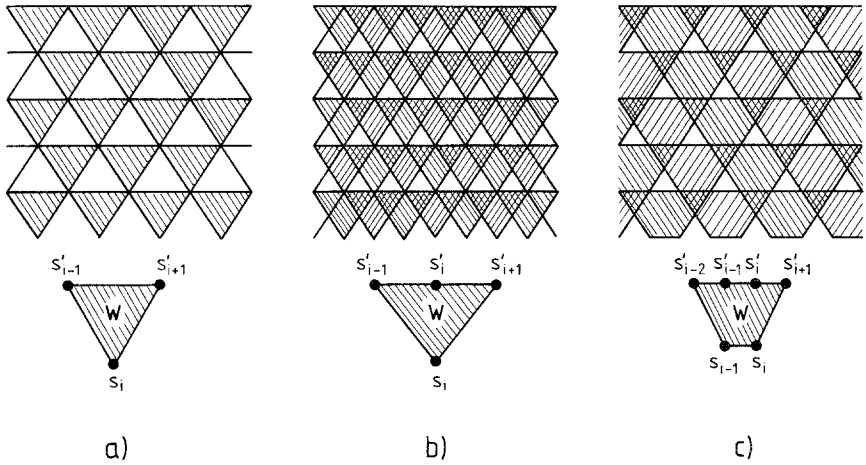

Fig. 3. Two-dimensional statistical mechanical models with different Boltzmann faces. (a) Checkerboard triangular lattice, (b) simple model with interpenetrating faces, (c) a more general model with interpenetrating faces. The faces end on the bottom row without having common lattice points. Note the periodic boundary conditions in the "space" direction.

Strictly speaking, this name is appropriate only in $(0+1)$- and $(1+1)$-dimensional CA with symmetric transfer matrices (*symmetric* CA)[11]; there are no phase transitions for temperatures $T>0$, and hence the name disorder line (see Section 3 for a discussion on this point). We refer in what follows to Eq. (2.11) as to the *cellular automaton* condition.

Once the original statistical mechanical problem is solved by diagonalizing a transfer matrix, it is often possible to do this also for other choices of transfer matrices. The same basic solution may be used in setting different "dynamic" rules. An extreme example is shown in Fig. 4, exhibiting the sparse Kramers–Wannier[29] transfer matrix with skew boundary conditions. In this formulation the spins are set sequentially and depend on the value of the spins set in the last $(N+1)\tau$ steps:

$$tR(s_1, s_2, \ldots, s'_k, \ldots, s_{N+1}) = \sum_{s_k} [\bar{w}(s_k \mid s_{k-1}, s'_k, s_{k+1})\, R(s_1, s_2, \ldots, s_k, \ldots, s_{N+1})] \tag{2.12}$$

where $\bar{w}(a \mid b, c, d)$ can be interpreted as a conditional probability if Eq. (2.11) is fulfilled. An important advantage of this formulation is the fact

[11] By a *symmetric* CA we mean a cellular automaton whose elementary interaction face is invariant when the time direction is reversed, or if its face can be recast in a symmetric form by a repartition of couplings. If the rules are *deterministic*, such a CA is *reversible*. The role of irreversibility in deterministic CA was exposed by Bennett and Grinstein.[28]

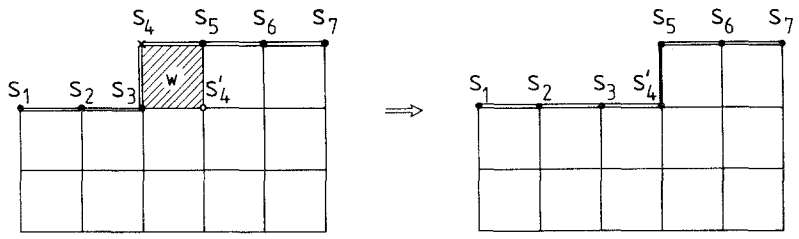

Fig. 4. Graphical representation of the eigenvalue equation for the sparse Kramers–Wannier transfer matrix applied to the IRF model. The spin s'_4 is summed up on the left-hand side of the equation. The double line denotes the $|R_1\rangle$ state: all possible interactions with the same symmetry as that of the original Hamiltonian are allowed between the spins lying on this line. From the point of view of the cellular automaton rule, this procedure has the important advantage that the spins can be updated one at a time.

that the spins can be updated independently of each other even for long-range rules.

A different but equivalent form of Eq. (2.9) is

$$R(\{\mathbf{s}'\}, t+2\tau) - R(\{\mathbf{s}\}, t) = \sum_{\{\mathbf{s}\}} P(\mathbf{s}'|\mathbf{s})\, R(\{\mathbf{s}\}, t) - \sum_{\{\mathbf{s}\}} P(\mathbf{s}|\mathbf{s}')\, R(\{\mathbf{s}'\}, t) \tag{2.13}$$

Here $P(\mathbf{s}|\mathbf{s}')$ is the conditional probability given by the element

$$P_{\{\mathbf{s}'\},\{\mathbf{s}\}}$$

of the stochastic matrix. This *discrete time master equation* follows directly from Eq. (2.9) by using the normalization conditions

$$\sum_{\{\mathbf{s}\}} P(\mathbf{s}|\mathbf{s}') = \sum_{\{\mathbf{s}\}} R(\mathbf{s}, t) = 1$$

The stationary probability distribution of Eqs. (2.9)–(2.10) is just $|R_1\rangle$ with elements $R^{(1)}(\mathbf{s})$, which, according to the Perron–Frobenius theorem, are positive. The expectation value of equal-time operators in the stationary state follows from Eq. (2.6) as

$$\lim_{T\to\infty} \langle A(\mathbf{s})\rangle_T = \langle L_1(\mathbf{s})|\, A(\mathbf{s})\, |R_1(\mathbf{s})\rangle = \sum_{\mathbf{s}} A(\mathbf{s})\, R_1(\mathbf{s}) \tag{2.14}$$

while the stationary expectation values of non-equal-time operators are given by

$$\lim_{T\to\infty} \langle A(\mathbf{s}, T)\, B(\mathbf{s}, t+T)\rangle = \sum_{\alpha} \langle L_1|\, A\, |R_\alpha\rangle\, p'_\alpha \langle L_\alpha|\, B\, |R_1\rangle \tag{2.15}$$

where $p_\alpha \leqslant 1$ are the eigenvalues of the operator P. Relations (2.14)–(2.6) and (2.15)–(2.7) make the analogy between the transfer matrix formalism and the master equation approach complete as far as the *stationary properties* are concerned. Note that our statistical system had originally periodic boundary conditions, whereas the time evolution of CA starts from some fixed boundary conditions. Thus, the *transient phenomena* in cellular automata are related to *surface effects* in the corresponding statistical mechanical system and decay in time according to the eigenvalues of the P operator, only the largest ones surviving at long times. Let $|R^{(0)}\rangle$ be the initial right-side vector describing the boundary conditions at the surface. Then in general

$$\langle A(T)\, B(T+t)\rangle = \sum_\alpha \sum_\beta \langle L_1|\, A\, |R_\alpha\rangle\, p_\alpha^T \langle L_\alpha|\, B\, |R_\beta\rangle\, p_\beta^t \langle L_\beta|\, R^{(0)}\rangle \tag{2.16}$$

from which all previous results follow by taking into account that $p_1 = 1 > p_\alpha$ $(\alpha > 1)$ and the normalization condition $\langle L_1|\, R^{(0)}\rangle = 1$.

2.2. A Few (0+1)-Dimensional Examples

To make the formalism more transparent, we give here a few examples of $(0+1)$-dimensional cellular automata constructed *from* the transfer matrix formalism. This also gives the opportunity to introduce in a natural way some notations used in the theory of cellular automata.

Example 1. Incommensurate Modulations in Time. Consider a linear chain of length N with competing first and second interactions:

$$-\beta H = K_1 \sum_{i=1}^{N} s_i s_{i+1} - K_2 \sum_{i=1}^{N} s_i s_{i+2}; \qquad K_{1,2} > 0; \qquad \beta = \frac{1}{k_B T} \tag{2.17}$$

Since the interaction extends to two neighbours, the transfer matrix is a 4×4 matrix whose elements are

$$T = \begin{bmatrix} e^{2K_1 - 2K_2} & 1 & e^{-2K_1} & e^{2K_2} \\ 1 & e^{-2K_1 - 2K_2} & e^{2K_2} & e^{2K_1} \\ e^{2K_1} & e^{2K_2} & e^{-2K_1 - 2K_2} & 1 \\ e^{2K_2} & e^{-2K_1} & 1 & e^{2K_1 - 2K_2} \end{bmatrix} \tag{2.18}$$

Using the symmetry of T under flipping all the spins, one can obtain the four eigenvalues $t_{1,2}^{\text{even}}$ and $t_{1,2}^{\text{odd}}$ corresponding to the even eigenfunctions and to the odd eigenfunctions, respectively. The stochastic matrix

corresponding to T is constructed following Eq. (2.8) and describes the time development of an automaton consisting of two sites. After some algebra one obtains that the matrix P is amenable to the following block structure:

$$P = \begin{bmatrix} a & b & 0 & 0 \\ 1-a & 1-b & 0 & 0 \\ 0 & 0 & c & d \\ 0 & 0 & e & f \end{bmatrix} \tag{2.19}$$

where a, b,..., f are given functions of $K_{1,2}$. It is worth noting that the symmetry reduction shows clearly that the largest eigenvalue comes from the even (upper) block, which is still stochastic, while the odd block is not. The stationary distribution is given by the right eigenvector of P corresponding to the eigenvalue one:

$$|\bar{R}_1\rangle \sim \begin{bmatrix} b \\ 1-a \\ 0 \\ 0 \end{bmatrix} \geqslant |0\rangle$$

or, in the *original spin basis of the matrix* (2.18)

$$|R_1\rangle \sim A \exp(\kappa \sigma_1^z \sigma_2^z)\,|0\rangle; \qquad |0\rangle = \tfrac{1}{2}(|\uparrow\uparrow\rangle + |\uparrow\downarrow\rangle + |\downarrow\uparrow\rangle + |\downarrow\downarrow\rangle) \tag{2.20}$$

with $A = [b(1-a)]^{1/2}$ and $\kappa = \ln[b/(1-a)]^{1/2}$. Here σ_i^z is the Pauli matrix acting on spin i: $\sigma^z|\uparrow\rangle = |\uparrow\rangle$; $\sigma^z|\downarrow\rangle = -|\downarrow\rangle$. From (2.20) the expectation value of $\lim_{t\to\infty}\langle s_1(t)\, s_2(t)\rangle$ is easily computed. The non-equal-time spin–spin correlation function decays exponentially with the relaxation time $\tau \sim -(\ln p_{\max}^{\text{odd}})^{-1}$. Beyond the branching point $p_1^{\text{odd}} = p_2^{\text{odd}}$, given in terms of the $K_{1,2}$ as

$$(\cosh 2K_1)_+ = e^{4K_2} + (e^{4K_2} - 1) \qquad \text{or} \qquad \tanh K_2 = \tanh^2 K_1 \tag{2.21}$$

the odd eigenvalues are complex conjugated and the exponential decay of spin–spin correlations is modulated with a frequency depending continuously on the parameters. Except for special values of the couplings, the modulation is *incommensurate* with the length of the elementary time step.[30] The relaxation time has a cusp and is smallest at the branching (disorder) points (2.21). Note that one can interpret (2.19) as the dynamics

of a two-spin system described by the effective Hamiltonian given in Eq. (2.20): $H^{\text{eff}} = \exp(\kappa s_1 s_2)$.[31]

As the temperature $T \to 0$, some elements of T become zero and one must carefully check whether the conditions for the transformation (2.8) are still valid. The model (2.16) has two ground states, a ferromagnetic state ($\uparrow\uparrow\uparrow\uparrow\cdots$ or $\downarrow\downarrow\downarrow\downarrow\cdots$) and a $\langle 2, 2\rangle$ state, the spins forming one of the four possible $\uparrow\uparrow\downarrow\downarrow\uparrow\uparrow\downarrow\downarrow\cdots$ configurations. In the $\langle 2, 2\rangle$ ground state the transfer matrix is *imprimitive*, since $P^2 = 1$, and this corresponds to a two-cycle stationary behavior. Increasing further the size of the automaton, one may produce more and more stationary limit cycles at $T = 0$. Other ways of obtaining a large set of limit cycles will be discussed in Section 5.

Example 2. An Enumeration Problem. Consider the problem of counting all possible configurations of particles in a linear chain of length N, provided two nearest neighbor sites cannot be empty.[32] This problem is equivalent to calculating the partition function of a one-dimensional antiferromagnetic Ising model in the critical external field at $T = 0$.[33] After factorizing out the ground-state energy $\exp(|K|)$, one has for the transfer matrix the form

$$T = \begin{bmatrix} 0 & 1 \\ 1 & 1 \end{bmatrix} \tag{2.22}$$

leading to $t_{\pm} = (1 \pm \sqrt{5})/2$; $Z_N = t_+^N + t_-^N$ for periodic boundary conditions. Note that the successive partition functions Z_N form a Fibonacci sequence: $Z_N = Z_{N-1} + Z_{N-2}$, $Z_0 = 2$, $Z_1 = 1$. The automaton rules are easily derived to be

$$P = \begin{bmatrix} 0 & x^{-2} \\ 1 & x^{-1} \end{bmatrix} \tag{2.23}$$

($x = t_+$), which will produce an exponentially decaying correlation function with the relaxation time $\tau^{-1} = \ln[(\sqrt{5}+1)/(\sqrt{5}-1)] \equiv -\ln \lambda$. When some transition probabilities are zero or one (as in the present case), the model has some constraints and only special classes of configurations are allowed. If *all* the elements of P are zero or one, the rules of the cellular automaton are *deterministic*. Otherwise they are *probabilistic*.

Iterating the matrix P for a long time, one obtains a chain of events where clusters of occupied sites are delimited by empty sites. Call an occupied site a living site and a cluster of occupied sites a living (or directed) "lattice animal." The life span of these animals is given by the length of

the corresponding cluster. Now different questions may be asked: What is the average life expectancy? What is the (average) number of animals living exactly L iterations (time units)? In the one-dimensional case the animals do not have a structure, but in higher dimensions they may change their shape in time, and the number of questions one may ask varies accordingly.

The probability of finding a cluster of empty cells with exactly the length L is given by the correlation function $\langle (1-n_i)\, n_{i+1} n_{i+2},\ldots, n_{i+L+1}(1-n_{i+L+2})\rangle$. An elementary calculation of this *nonlocal* correlation function gives

$$\langle (1-n_i)\, n_{i+1} n_{i+2},\ldots, n_{i+L+1}(1-n_{i+L+2})\rangle = \frac{\lambda^L}{(1+t_+^2)(1+t_-^2)} \tag{2.24}$$

In one dimension, of course, there is no problem in calculating such correlations. In higher dimensions, however, this is usually impossible. It is much simpler to calculate a *two-point* correlation function instead of (2.24); the two are related through a duality transformation (see the next section). A well-known problem in polymer physics is to enumerate the number of distinct directed animals (living clusters with different shapes) containing exactly n living sites, g_n, without taking into account their interactions. In one dimension the answer is simply $g_n = 1$. The animal-generating function is defined as

$$A(z) = \sum_{n=1}^{\infty} g_n z^n = \sum_{n=1}^{\infty} z^n = \frac{z}{1-z} \tag{2.25}$$

For living (directed) animals the generating function has a simple recursive property related to causality. After being born (source), the sites may be occupied at time $L+1$ only if at least one of the predecessor sites at L was occupied:

$$A(z) = z[1 + A(z)] \tag{2.26}$$

leading again to the result (2.25).

2.3. Finite Cellular Automata: Elementary Facts

Here we review some well-known theorems regarding (finite) stochastic matrices[20] and Perron–Frobenius operators.[34] In general a stochastic matrix may be *reducible* or *irreducible*, depending on whether it may or may be not reduced to a block form by the same permutation of rows and columns. This condition is best represented in graphical terms: if

one associates a directed graph pointing from i to j with the matrix element $P_{i,j} > 0$, then the condition for irreducibility is that the graph of the matrix P must be connected, that is, in the space of indices $\{i, j\}$ from each point one can reach any other point. Otherwise, there would be points or groups of points one can reach but no longer leave. Such points are called *attractors* (more precisely, they form the *support* of the attractors) and the dynamics is said to be *contracting*. The directed graph of the matrix contains important information about the dynamics of the system,[35] including the support of the attractors, their basin of attraction, number of possible cycles, etc. The main question concerning cellular automata is related to the existence of a proper "thermodynamic" limit: as the size of the automaton increases, one wold like to make statements about the attractors and their basin of attraction. Is it possible to define a *density* of points on these attractors? I failed in obtaining such a stationary density for "class IV"[6] deterministic CA such as Conway's *Life*[36] by using the methods of nonlinear dynamics.[12] The interesting "zoo" of configurations leading to a "class IV"[6] behavior seems to have a zero Hausdorff dimension.

The matrix elements of $\lim_{N \to \infty} P^N$ are called *limit probabilities* and they correspond to the probabilities to reach i from j in ∞ time. If the largest eigenvalue of the matrix (which for normalized P matrices is unity) is not degenerate, the matrix is *primitive*; if there are q eigenvalues with unity modulus, the matrix is *q-imprimitive*. The matrix has a *limit distribution* if the right eigenvector corresponding to the eigenvalue 1 is nondegenerate and nonnegative. Some states are *negligible* if they correspond to columns with positive elements on the right of some other main diagonal blocks (see Fig. 5a). When iterating P many times, the weight of these states diminishes and disappears in the $N \to \infty$ limit. If a reducible matrix consists of several primitive blocks and some negligible states, then the limit probabilities $\{P^{\infty}_{i,j}\}$ exist, and also have zero elements corresponding to the negligible states.

When the matrix is irreducible, there are only two possibilities (Figs. 5b and 5c): the matrix is primitive and then the limit distribution exists (ergodic Markov chain) or the matrix is *q-imprimitive* and one has the so-called q-island case (Fig. 5c). In this case P has q right vectors χ_m with disjoint support such that $P\chi_m = \chi_{m+1 \bmod(q)}$ and the right eigenvectors ϕ_k corresponding to the q-eigenvalues on the complex unit circle are given by

$$\phi_k = \sum_{m=0}^{q-1} e^{2\pi i m k/q} \chi_m, \qquad k = 0,..., q-1 \tag{2.27}$$

[12] For applying discrete nonlinear dynamics to CA problems see Ref. 37; for the random Ising chain see Refs. 38.

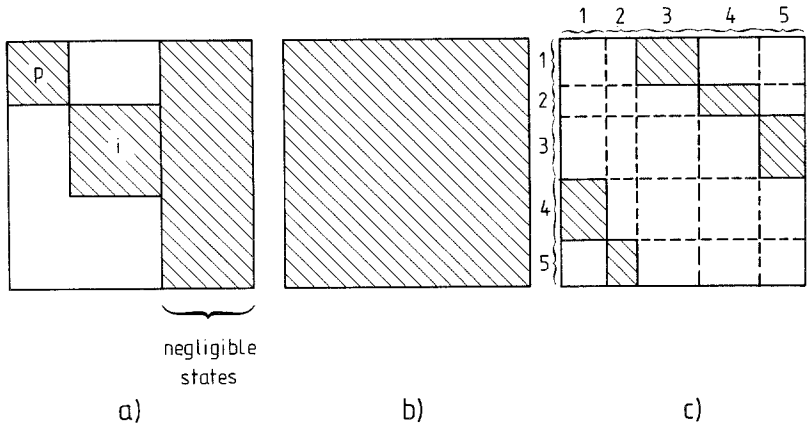

Fig. 5. Classification of stochastic matrices. (a) Reducible matrices: i and p stand for imprimitive and primitive blocks, respectively. (b) Irreducible, primitive matrix. (c) The q-island case: a q-imprimitive irreducible matrix. In the example shown the $q = 5$ cycle is $(1 \to 3 \to 5 \to 2 \to 4 \to 1)$.

Regarding every block (see Fig. 5c) as a single element, one gets a permutation matrix.

These theorems are quite useful when dealing with finite cellular automata and can be appropriately generalized to probability-conserving integral operators.[34] Moreover, they allow us to discuss the possible mechanism of phase transitions occurring in such systems.

2.4. Phase Transition Mechanisms in Cellular Automata

Our definition of a phase transition is related to the definition of the "partition function" (2.2), where we now group the eigenvalues according to their multiplicity $D(\alpha)$: $Z_{N,M} = \sum_\alpha D(\alpha)\, p_\alpha^M$. The main contribution to this partition function in the large-(M, N) limit comes from the eigenvalues with largest modulus. A phase transition occurs when, as some external parameter(s) is (are) varied, *the number of eigenvalues with unity modulus changes*, or, as explained later, when the degeneracy of a subleading eigenvalue becomes exponentially large with N. Static phase transitions can be classified as first-order and as continuous phase transitions. Dynamic systems may have additional phase transitions, such as purely dynamic transitions,[39] where the correlations change from an exponential to an algebraic decay in *time*, but not in *space*, or transitions in nonequilibrium states.[40],[13] Dynamics is also much richer in universality classes, depending

[13] For another example of nonequilibrium transitions in lattice-gas models see J. Marro *et al.*[41]

on the macroscopic conservation laws.[42] According to our mapping (2.8), we may expect to find this rich structure in our "static" $(d+1)$-dimensional models. Almost all phase transitions encountered in CA models have a pronounced anisotropic character: the scaling (if there is scaling at all!) of time is different from that of space.

Our discussion of phase transition mechanisms will follow closely the classification of stochastic matrices shown in Fig. 5. The most "regular" form is when P is primitive and irreducible (fully probabilistic cellular automata). In this case no phase transition can occur for finite systems when the temperature $T>0$. In order to have phase transitions in such finite systems one has to violate some of the conditions of the Perron–Frobenius theorem.[20] This may happen by letting some elements become zero (e.g., $T\to 0$), so that the matrix becomes imprimitive (see Example 2), or by continuing some of the parameters to unphysical values, as shown in the next example.

Example 3. Phase Transition in 0+1 Dimensions. In this example we discuss a typical phase transition that may happen in a finite CA through an example given by Wu.[43] In this automaton we have a single variable l, which may assume the values $l=0, 1,..., q-1$ and is updated in time according to the rules

$$P_{i,i}=a; \qquad P_{i,j}=\frac{1-a}{q-1}; \qquad i\neq j; \qquad i, j=0, 1,..., q-1 \tag{2.28}$$

This dynamics corresponds to the transfer matrix of a one-dimensional q-state antiferromagnetic Potts model. P can be diagonalized by a Fourier transform and one obtains two distinct eigenvalues: $\lambda_1=1$ and $\lambda_{2-(q-1)}=(qa-1)/(q-1)$. The two eigenvalues are equal in magnitude $(\lambda_1=-\lambda_{2,...,q-1})$ when

$$0\leqslant a_c=\frac{2-q}{q}\leqslant 1$$

implying a transition for $1\leqslant q\leqslant 2$. For integer values of q this happens either for $a=1$ or 0, corresponding to $T_c=\infty$ and, respectively, to $T_c=0$. Continuing q to real values, one encounters a phase transition at some $T_c>0$ temperature, with critical properties characteristic for one-dimensional static models.[44] Since the eigenvectors of P, (2.28), do not depend on a, from the point of view of the CA this transition is purely *dynamic*.

A different type of phase transition occurs when continuing the interactions constants to *complex values*. Going back to Example 1, the largest eigenvalue of the upper block of P given in Eq. (2.19) becomes com-

plex at the branching point $a = 1 + b$, and so does the partition function. In the cellular automaton description this is again a *dynamic* transition corresponding to the (static) Lee–Yang edge singularity.[45]

If the conditions of the Perron–Frobenius theorem are met, the right eigenvector $|R_1\rangle$ corresponding to the eigenvalue 1 must be positive and can be rewritten as

$$|R_1\{\mathbf{s}\}\rangle \equiv A \exp[\hat{H}^{\text{eff}}(\{\boldsymbol{\sigma}^z\})]\,|0\rangle = A \exp[H^{(d-1)}(\{\mathbf{s}\})] \qquad (2.29)$$

where $\sigma_k^x |0\rangle = |0\rangle\ \forall k$ and $H^{(d-1)}$ is an effective $(d-1)$-dimensional Hamilton function. In analogy to the kinetic Ising model,[46] we will denote the problem defined by the $H^{(d-1)}$ as the *static* problem whose partition function is given by

$$Z^{(d-1)} = \langle L_1 | R_1 \rangle = \sum_{\{\mathbf{s}\}} \exp[H^{(d-1)}(\{\mathbf{s}\})]$$

This definition of statics leads also to a natural way of defining the *entropy* of a state $|R_1\rangle$ as the entropy related to the $Z^{(d-1)}$.

The time evolution of a cellular automaton involves only implicitly the *static* problem: what one can easily mesure is the *gap* $G \equiv \tau^{-1}$, the inverse of the longest relaxation time. Applying the dynamic scaling hypothesis,[42] or equivalently, the *anisotropic scaling* formalism,[47] one can, however, determine both the static and the dynamic exponents (see Section 4). Renormalization group studies[31,48] show that the dynamic transition is in the same universality class as for the corresponding class of (sequential) dynamics for usual statistical models.[42] From the point of view of the $(d+1)$-dimensional model, however, the critical behavior corresponds to a Lifschitz tricritical point.[49] The critical behavior of fully probabilistic CA is not necessarely related to a *static* transition as described by the stationary distribution $|R_1\rangle$. In Section 5 we will present a $(1+1)$-dimensional CA that exhibits a purely *dynamic* transition, the possibility of which has been pointed out recently[39] in connection with diffusion on fractal objects.

Going back to Fig. 5, let us consider the *q-island* problem, which corresponds to a $T = 0$ commensurate phase of q-periodicity in the time direction. Usually, transitions from a commensurate phase to another commensurate phase are of first order, especially in three or higher dimensions. Moreover, continuous *surface* (such as wetting or roughening) transitions can still occur within the bulk commensurate phases or at first-order bulk transitions. A typical example studied in this context is a ferromagnetic Ising model with all spins fixed to point down (up) at the top (bottom) layer and with the first row of interactions antiferromagnetic. A domain wall is created at low temperatures at the top row: increasing the tem-

peratures will eventually result in a delocalization of the wall. In analogy to this picture, one may imagine a cellular automaton where for the first time step the rules are different from the following steps: starting from an initial configuration with all spins down, the transient behavior of this CA will be different in the case of a localized or a delocalized wall.

The next case is that of a reducible matrix. If the matrix consists of primitive blocks, the same analysis as above applies to each of the blocks. A more interesting case is when the matrix consists of one primitive block and negligible states. A typical example is the transfer matrix corresponding to the directed percolation.[30,50] Its distinctive feature is the existence of a so-called *absorbing* state, a state which is reproduced with probability one during iterations. In directed percolation once the system is "dry" (every site is empty) it remains so forever. From the theorems mentioned in Section 2.3 it follows that for finite matrices of this sort the absorbing state is always stationary. A phase transition may happen only in the thermodynamic limit when either: (a) the "escape" rate from the "infected" states into the absorbing state becomes negligible, leading to a reducible matrix with two distinct primitive blocks, or (b) when the density of negligible states becomes high enough so that

$$\lim_{N \to \infty} \lambda_1^N = \lim_{N \to \infty} \sum_{\alpha > 1} \lambda_\alpha^N$$

Let us discuss in some detail both possibilities.

(a) If the matrix has two or more primitive blocks, then each block is in itself a stochastic matrix, so there are as many positive but disjoint right eigenvectors, which correspond to the eigenvalue 1 of each primitive block. Denote by $|R_1^{(\alpha)}\rangle$ and by $\langle L_1^{(\alpha)}|$ the set of biorthogonal right and left eigenvectors with eigenvalues of unity modulus. Following Hamer,[51] define as order parameter any physical quantity A for which $\langle L_1^{(\alpha)}| A |R_1^{(\beta)}\rangle \neq 0$ $(\alpha \neq \beta)$. Then introducing $P' = P + h_A A$ (h_A is the field conjugate to A), an elementary degenerate perturbation scheme shows that one has to find the spectral decomposition of the matrix

$$\begin{bmatrix} \langle L_1^{(\alpha)}| A |R_1^{(\alpha)}\rangle; & \langle L_1^{(\alpha)}| A |R_1^{(\beta)}\rangle \\ \langle L_1^{(\beta)}| A |R_1^{(\alpha)}\rangle; & \langle L_1^{(\beta)}| A |R_1^{(\beta)}\rangle \end{bmatrix} \tag{2.30}$$

The right and left eigenvectors corresponding to the largest eigenvalue of this equation determine all the coefficients in the linear combinations

$$|R_1\rangle = a_1 |R_1^{(\alpha)}\rangle + a_2 |R_1^{(\beta)}\rangle; \qquad \langle L_1| = b_1 \langle L_1^{(\alpha)}| + b_2 \langle L_1^{(\beta)}| \tag{2.31}$$

Finally, in terms of these coefficients the order parameter is given as

$$\langle L_1|\, A\, |R_1\rangle = a_1 b_1 \langle L_1^{(\alpha)}|\, A\, |R_1^{(\alpha)}\rangle + a_2 b_2 \langle L_1^{(\beta)}|\, A\, |R_1^{(\beta)}\rangle + a_2 b_1 \langle L_1^{(\alpha)}|\, A\, |R_1^{(\beta)}\rangle + a_1 b_2 \langle L_1^{(\beta)}|\, A\, |R_1^{(\alpha)}\rangle \tag{2.32}$$

Note that if the operator A is such that $A\,|R_1^{(\alpha)}\rangle = 0$, then $\langle A\rangle = \langle L_1^{(\beta)}|\, A\, |R_1^{(\beta)}\rangle$. This phase transition does not break any symmetry; however, it might be a continuous one. A test regarding the universality of this phase transition mechanism is performed in Section 4.

(b) The other possible mechanism for a phase transition is more subtle and *does not* require a change in the number of eigenvalues with modulus one. The simplest scenario for such a transition is that a subleading eigenvalue of the transfer matrix becomes exponentially degenerate. This degeneracy factor may boost this eigenvalue to become the leading term in the sum (2.2). Physically such a mechanism will happen when the metastable state corresponding to the subleading eigenvalue is highly degenerate; in other words, it has a lot of entropy. Entropy-driven transitions are common in hard-core liquids and usually are of first order.[52] In order to have a better understanding of such a mechanism, consider the following example.

Example 4. Thermodynamic Limit from the Transfer Matrix Formalism—A Few Subtleties. Consider the problem of finding all possible close-packed configurations on a square lattice for a lattice gas with nearest and next nearest neighbor exclusion. Equivalently, one must count in how many ways one can cover an N by M (N, M are even) lattice with squares of side twice the lattice constant. Let us use the row-to-row transfer matrix. If the number of columns is N, then there are $2\times 2^{N/2}-1$ allowed states: every second site is empty or full ($2^{N/2}$), times the number of sublattices (2), minus 1 (the completely empty state has no pair). Among these states there are three, namely the empty state $(0000\cdots 0)\equiv|0\rangle$, the every-second-up state $(1010\cdots 0)\equiv|1\rangle$, and its shifted pair $(0101\cdots 1)\equiv|2\rangle$, which form a 3-cycle. Since $T^2\,|0\rangle = T(|1\rangle+|2\rangle)=2\,|0\rangle$ in this subspace, $T^2=2$, leading to two degenerate $\pm\sqrt{2}$ and one zero eigenvalues. All other states form pairs of 2-cycles involving eigenvalues ± 1. However, their degeneracy equals $2\times 2^{N/2}-4$. Taking into account the corresponding multiplicities, we find for the partition function form

$$Z_{N,M} = \mathrm{Tr}(T)^M = [2(2^M)^{1/2} + 2(2^{N/2}-2)] = 2[(2^M)^{1/2} + (2^N)^{1/2} - 2] \tag{2.33}$$

as also given by a direct counting. What one can learn here is that the result depends on the way the thermodynamic limit $M, N\to\infty$ is taken!

Taking either $M \to \infty$ or $N \to \infty$ first leads to erroneous results: one must take $M \sim N \to \infty$ simultaneously!

In the same spirit, one may imagine a situation when the leading eigenvalues of the transfer matrix are $\lambda_1 = \varepsilon_1^N$ and $\lambda_2 = \varepsilon_1^N \rho$, where $\rho < 1$ is due to one-particle excitations. Let us assume that the degeneracy of λ_2 is $D(2) \sim a^N$, $a > 1$. Hence $\mathrm{Tr}(T^M) \sim \lambda_1^M (1 + a^N \rho^M)$. If $M \to \infty$ first, then the partition function is given always by the λ_1^M, while if $N \to \infty$ first, then it is given by the degeneracy of λ_2. Obviously, the thermodynamic limit depends on the way $N \sim M \to \infty$ is taken, predicting a phase transition when $a\rho \sim 1$. More generally, such a situation may occur when a group (band) of nonleading eigenvalues have exponential degeneracy. I am not aware of any microscopic model calculation displaying explicitly this mechanism. I am, however, aware of a few examples where this point might have been missed.

After this lengthy excursion, let us go back again to Fig. 5. The case of a *q-island* imprimitive block and some negligible states is very similar to the situation discussed above. This can be most easily seen by considering the operator $\dot{P}^q$, which will consist again of an imprimitive block and negligible states. Apart from some modulations, one expects the critical behavior to be in the same universality class with the directed percolation problem. The same observation applies to more complicated structures involving many different imprimitive blocks with different periodicities and negligible states (P has to be raised to the smallest common multiplier of these periodicities). A quite different critical behavior is expected for nested imprimitive blocks, or when there are matrix elements coupling blocks with different periodicities.

3. EXACT RESULTS FOR PROBABILISTIC CELLULAR AUTOMATA

In this section we present a few exact results concerning probabilistic CA in $(d+1)$ dimensions. Some of these results have been presented previously in different contexts,[27,53–60] but will be summarized here from a unified point of view. First we discuss the problem of *symmetric* CA; in this case we show that the stationary distribution has a short-ranged direct product form and that the equal-time correlations in the stationary state can be calculated from a *d-dimensional* static problem. Second, we treat a class of CA we call *linear* or *free* models because the equations for the correlations decouple. For these models the dynamic critical exponent equals exactly $z = 2$. Generalizing the notion of duality, we show how to construct duality relations for CA, and, finally, we briefly discuss the

integrability conditions for statistical physical models with interpenetrating faces. Throughout this section we shall often use as illustration the $(1+1)$-dimensional automaton shown in Fig. 3b.

3.1. Disorder Solutions

Many statistical physical models with *competing* short-range interactions can be solved partially—which in our context means that one obtains the stationary distribution $|R_1\rangle$ and related equal-time correlations—on special subspaces of the external parameter space.[27,56–58] Such solutions have been found independently in many fields, for example, in the theory of crystal growth,[54] quantum chains,[55] and models for adsorbate systems (for review see Ref. 59). In the context of CA they were mentioned first by Domany and Kinzel.[50] The name "disorder" is not always appropriate and was given for historical reasons, since the first solutions were found in one- and two-dimensional exactly soluble statistical models.[53] Here the presence of a unique stationary state implies that this subspace lies on the paramagnetic (disordered) phase. However, it became clear that in some cases a duality transformation will map these solution into solutions lying on the ordered (ferro- or antiferromagnetic) phase.[60,27] The study of these solutions is a field of active interest, since they provide (at minimal cost) strong insights into the phase diagram of complex models,[55] allow for the exact calculation of the generating function of directed animals in two and three dimensions,[61],[14] shed light on unexpected symmetries,[64] and constitute the starting points for systematic expansions.[65]

The disorder-type solutions are related to an exact dimensionality reduction to a $(d-1)$- or a 0-dimensional static problem as defined by $|R_1\rangle \equiv A \exp[H^{\text{eff}}(\{\mathbf{s}\})]$, where H^{eff} is an effective Hamiltonian with *short-range interactions.* This is the case for *all time-symmetric* CA. In order to see how this comes about, consider two types of characteristically shaped $w(s|\{s'\})$ interaction faces. The most typical one is that of Fig. 3b, which is also shown in detail in Fig. 6a. This type of face has a "conical" structure allowing explicitly for the construction of contracting processes. Throughout this subsection we shall work on the *interaction representation,* the independent parameters of the partition function being the couplings of the energy functional. If the energy of a face contains only one- and two-spin interactions between "children" spins and "parent" spins, then the interactions between parent spins can be redistributed in such a way as to obtain a symmetric transfer matrix. Let us explain this on the automaton

[14] For a direct calculation see Hakim and Nadal[62]; for compact animals see Derrida and Nadal.[63]

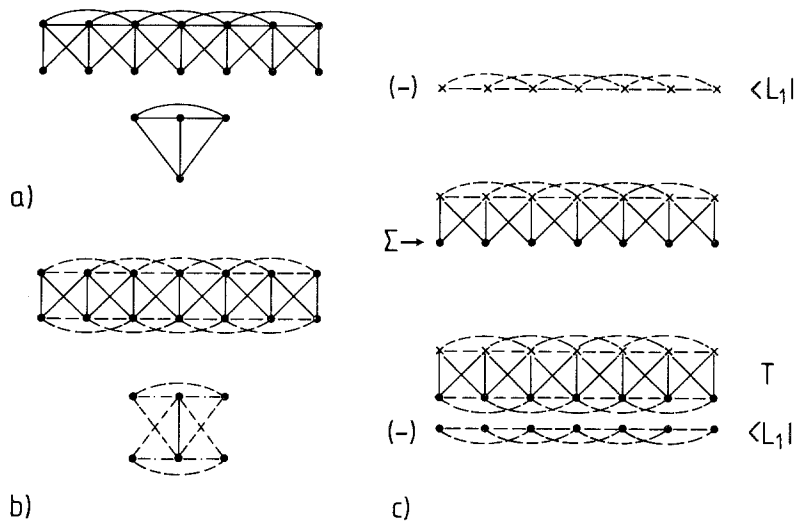

Fig. 6. Graphical picture of the disorder solution. (a) The graphical representation of the original stochastic matrix and the corresponding elementary face. (b) The repartitioning of couplings G leading to a symmetric matrix and to a symmetric elementary face. Note that dashed (dashed-dot) lines are one-half (one-quarter) of the coupling value represented by a heavy line. (c) From bottom up: acting with the left eigenvector removes the bonds between bottom spins, which are then summed up. As a result, the left eigenvector moves one time step upward.

shown in Fig. 6. Consider first the part of the face weight $\bar{w}$ that contains only the interactions between the spin s_i and the spins $(s'_{i-1}, s'_i, s'_{i+1})$:

$$\sum_{s_i} \bar{w}(s_i, s'_{i-1}, s'_i, s'_{i+1}) = \exp[G(s'_{i-1}, s'_i, s'_{i+1})]$$

$$= \exp\left[A + \left(\sum_{j=i-1,i,i+1} H_j s'_j\right) + K_{12} s'_{i-1} s'_i + K_{23} s'_i s'_{i+1} + K_{13} s_{i-1} s_{i+1} + L s'_{i-1} s'_i s'_{i+1}\right] \tag{3.1}$$

All the parameters in the expansion of G are functions of the original couplings contained in $\bar{w}$. By construction, the full face weight of the CA [which satisfies the normalization condition (2.11)] is

$$w(s_i | s'_{i-1}, s'_i, s'_{i+1}) = \bar{w}(s_i, s'_{i-1}, s'_i, s'_{i+1}) \exp[-G(s'_{i-1}, s'_i, s'_{i+1})] \tag{3.2}$$

As indicated in Fig. 6b, the interactions contained in G are split in half, half being assigned to the top row, half to the bottom row. The resulting

symmetric transfer matrix is no longer stochastic. The elementary face is now given by

$$w^{\mathrm{sym}}(s_{i-1}, s_i, s_{i+1}; s'_{i-1}, s'_i, s'_{i+1})$$
$$= w(s_i | s'_{i-1}, s'_i, s'_{i+1}) \exp[-\tfrac{1}{2}G(s_{i-1}, s_i, s_{i+1})] \exp[-\tfrac{1}{2}G(s'_{i-1}, s'_i, s'_{i+1})]$$

Acting with this operator on the vectors

$$\begin{aligned} \langle L_1| &= \exp[\tfrac{1}{2}G(s_{i-1}, s_i, s_{i+1})] \\ |R_1\rangle &= \exp[\tfrac{1}{2}G(s'_{i-1}, s'_i, s'_{i+1})] \end{aligned} \tag{3.3}$$

one finds that the bonds moved to the bottom row and the bonds remaining on the top row will be exactly cancelled by $\langle L_1|$ and $|R_1\rangle$, respectively. By summing up all the remaining uncoupled spins, one recovers the same left and right eigenvectors [use Eq. (3.1)]. The Perron–Frobenius theorem identifies the *positive* vectors (3.3) to be the ones corresponding to the largest eigenvalue (one)—this completes the proof. The calculation of equal-time correlations involves the solution of the static problem defined by the effective Hamiltonian H^{eff}, which in this case corresponds to the $(d-1)=1$-dimensional problem:

$$Z^{(d-1)} = \langle L_1 | R_1 \rangle = \sum_{\{\mathbf{s}\}} \prod_i \exp[G(s_{i-1}, s_i, s_{i+1})]$$

This problem is similar to the problem considered in Example 1, so the static problem corresponds to a $(0+1)$-dimensional CA, illustrating the $(d) \to (d-1)$ dimensionality reduction. Moreover, for $H=L=0$ and at the disorder point (2.21) the *spacelike* correlations of the $(1+1)$-dimensional CA will change in character and become incommensurately modulated.

The second example is the chekcerboard lattice of Fig. 2a, also displayed in Fig. 7a. There are two distinct possibilities for disorder-type solutions in such models. The first class consists again of models with one- and two-spin interactions only. In this case the distinction between hatched and white squares is purely arbitrary. If all the couplings are assigned to the hatched squares, the condition (2.11) reads

$$\sum_{s_1, s_2} w_{\blacksquare}(s_1, s_2 | s'_1 s'_2) = 1$$

If they are assigned to the white faces, the very same condition is

$$\sum_{s'_1, s'_2} w_{\square}(s_1, s_2 | s'_1 s'_2) = 1$$

This symmetry corresponds to the reversal of time for the *two-time-step* transfer matrix (2.4) or to the (time revesal + elementary space shift) for the *one-time step* transfer matrices. The correlation function of two spins on the same row (time slice) is obtained by summing the upper part of the lattice in the usual way (summing over $w_{\blacksquare}$) and the lower part of the lattice using now the white squares ($w_{\square}$); for the static problem one ends up with a one-dimensional Ising problem with alternating couplings,[66] as illustrated in Fig. 7a. The second class of solutions may be obtained when the hatched squares contain quite complicated couplings but $w_{\blacksquare}(s_1, s_2 | s_1' s_2') = w_{\blacksquare}(s_1', s_2' | s_1, s_2)$. The same method as the one discussed before again can be applied, since the left and right wave functions have the following form:

$$\langle L_1| = \exp\left[\sum_{i=1}^{N/2}\left(-Hs_i - \frac{K_3}{2}s_{2i}s_{2i+1} + \frac{K_1}{2}s_{2i-1}s_{2i}\right)\right]$$

$$|R_1\rangle = \exp\left[\sum_{i=1}^{N/2}\left(-H's_i - \frac{K_1}{2}s_{2i-1}s_{2i} + \frac{K_3}{2}s_{2i}s_{2i+1}\right)\right]$$

The couplings $K_1/2$ and $K_3/2$ cancel the bonds connecting the top and bottom rows of spins of the white faces. After summing the pairs of (independent) spins on the top (or bottom) row of spins, one regains the

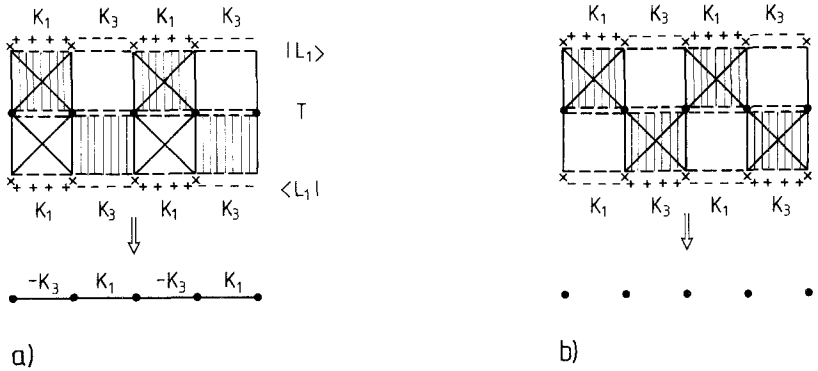

Fig. 7. Disorder solution for the checkerboard lattice. (a) First, the two-spin couplings K_1 and K_3 are split in half, one half being included in $w_{\blacksquare}$, the other half belonging to $w_{\square}$. (b) When the left eigenvector acts on the bottom (top) rows of the white squares it cancels the half-couplings [the "+" ("−") lines correspond to plus (minus) half of the original couplings] belonging to $w_{\blacksquare}$ (bottom) and $w_{\square}$ (top). A chain with alternating couplings results after summing over the crossed faces. (b) For time-symmetric faces $w_{\blacksquare}(s_1, s_2 | s_1', s_2')$ only the $w_{\blacksquare}$ are summed up; the notations are the same as in (a). A row of independent spins results.

vectors (3.3), but shifted by a lattice constant. Since the full faces have the symmetry $w_{\blacksquare}(s_1, s_2 | s_1' s_2') = w_{\blacksquare}(s_1', s_2' | s_1, s_2)$, the one-step transfer matrices are now *invariant* under time reversal. The calculation of equal-time correlations is shown in Fig. 7b and leads to

$$Z^{(d=0)} = \langle L_1 | R_1 \rangle = \sum_{\{s\}} \exp \left\{ - \sum_i [(H + H') s_i] \right\}$$

This example illustrates a reduction to a 0-dimensional problem, since $Z^{(d=0)}$ is equivalent to a static problem of independent spins in an external field.[60] This way of finding disorder-type solutions in staggered models works in any $(d+1)$ dimension.[58] The underlying static problem is (d)- or (0)-dimensional.

Finally, consider a rotated square face with a diamond shape, as shown in Fig. 1b. For the IRF model a general condition for the existence of a disorder solution was given by Baxter.[58] As in (3.1)–(3.3), one can show that this condition can be also rewritten in the form (2.11) by a proper reassignment of the edge bonds. The diamond face must be symmetric:

$$w(s_i | s_{i-1}', s_i', s_{i+1}') = w(s_i' | s_{i-1}', s_i', s_{i+1}')$$

and the dimensionality reduction is again from $(1+1)$ to 1 dimension.

For $(1+1)$-dimensional time-symmetric CA one has therefore an underlying one-dimensional static problem with short-range interactions, which does not have a phase transition at $T > 0$. For $(2+1)$-dimensional CA, however, such a transition may exist and the calculation of $|R_1\rangle(H^{\text{eff}})$ is useful when determining the transition point (see Domany[57]). Here the name "disorder solution" is not misplaced: it is downright wrong.

A very similar approach can be applied to continuum models and it has been successful in giving an alternative treatment of the problem of critical dynamics.[48]

In concluding this part on disorder solutions, let us summarize our findings:

(a) CA with "conical" faces are symmetric under time reversal *iff* in the interaction representation the face Boltzmann factor w contains only one- and two-spin interactions between the two different time slices it connects.

(b) CA with checkerboard-type faces or with diamond-type faces are symmetric in time *iff* their Hamiltonians contain only one- and two-spin interactions $\vee$ if their faces are symmetric when reflected on the time direction.

(c) Every probabilistic CA that is symmetric under time reversal has a corresponding *static* Hamiltonian whose interactions extend at most to the maximal spatial length of the original face.

Points (a)–(c) generalize the result of Grinstein *et al.*[31] Furthermore:

(d) As a consequence, probabilistic $(1+1)$ CA that are symmetric under time reversal do not have phase transitions for temperatures $T>0$.

3.2. Linear Models

By linear models we mean CA models whose elementary faces contain in the *weight representation* only two-spin products:

$$P(\{s_i\}, \{s_i'\}) = \prod_i w(s_i | \{s_I'\}); \qquad w(s_i | \{s_I'\}) = \frac{1}{2}\left(1 + \sum_i a_I s_i s_I'\right) \geqslant 0 \tag{3.4}$$

where $s_i = \pm 1$, and I indexes the spins $\mathbf{s}'$ interacting with s_i. The form (3.4) can be easily generalized to any q-state model; then the constant changes to $1/q$ and the term $s_i s_I'$ to $\delta_{s_i, s_I'}$, with δ being the Kronecker delta-function and $s_i = 0, 1, \ldots, q-1$. An elementary calculation shows that

$$\begin{aligned}
\langle s_k \rangle_{t+\tau} &\equiv \sum_{\{\mathbf{s}\}} s_k R(\{\mathbf{s}\}, t+\tau) \\
&= \sum_{\{\mathbf{s}\}} \sum_{\{\mathbf{s}'\}} s_k \prod_i w(s_i | \{s_I'\})\, R(\{\mathbf{s}'\}, t) \\
&= \sum_{\{\mathbf{s}\}} \left[\sum_{\{\mathbf{s}'\}} s_k' \prod_i w(s_i' | \{s_I\}) \right] R(\{\mathbf{s}\}, t) \\
&= \left\langle \sum_{s_k'} s_k' w(s_k' | \{s_K\}) \right\rangle_t \\
&= \sum_K a_K \langle s_K \rangle_t
\end{aligned} \tag{3.5}$$

We have used only the gauge symmetry $\sum_s f(s) = \sum_s f(-s)$, the normalization condition $\sum_s w(s | \{s_I'\}) = 1$, and Eq. (3.4). Similar equations can be obtained for multispin correlations; for example, for two-spin correlations one obtains

$$\langle s_k s_l \rangle_{t+\tau} = \left\langle \sum_{s_k', s_l'} s_k' s_l' w(s_k' | \{s_K\})\, w(s_l' | \{s_L\}) \right\rangle_t = \sum_K \sum_L a_K a_L \langle s_K s_L \rangle_t \tag{3.6}$$

In this "spin correlation" basis the transfer matrix splits up in blocks. Within each block it can be diagonalized by the generating function

method,[46] or, in the continuum limit, by a Fourier transform. This decoupling of correlation functions suggests that the continuum limit of this model is related to a free field theory with an analytic gap, as reflected by the fact that the dynamic critical exponent always assumes its mean field value $z = 2$.

The derivation given here can be repeated for any discrete (or continuous) variables. A special case of these models has been discussed by Choi and Huberman.[67] The interest in these linear models is motivated by two facts: first, such models may constitute a fair approximation of more complicated models, in the same way as the free fermion approximation have been found useful in deriving phase boundaries in statistical physical models.[68] Second, they may constitute a standard starting point for diagramatic and/or series expansions when the nonlinear part of w is small compared to (3.4). It might be of some interest to consider the statistical physical models whose face Boltzmann factors are such linear functions of the variables: they are exactly soluble models in any dimension.

A further generalization of the (3.4) form seems possible when nonlocal (disorder-like) operators are introduced.[40] The correlation functions are still decoupled, but Eq. (3.6) will contain terms proportional to the distance between the two spins.

3.3. Duality Transformations

Duality transformations have been quite useful in statistical mechanical systems. Such transformations relate the high-temperature behavior of a given model to the low-temperature behavior of another (the dual) model. If the two models are identical, it has the property of *self-duality*, which allows for the determination of the critical point and for values of thermodynamic functions at criticality when the model under consideration has only two distinct phases. Moreover, duality may shed light on the nature of low-temperature excitations, hence laying the ground for a more physical approach to the problem.

In the context of CA one must distinguish two main possibilities: if the static problem is known and the corresponding Hamiltonian is short-ranged, as is the case for time-symmetric CA, then in principle the d-dimensional *static* problem may have a duality transformation on its own: we call it a *static duality transformation.* On a more general level, the full $(d+1)$-dimensional problem (2.1) might also have a duality transformation, which we shall call a *dynamic duality transformation.* The main difficulty in deriving such a general duality transformation is related to two facts inherent in CA models: complicated multispin interactions *including*

odd products of spins. In addition, some of them are necessarily negative ("antiferromagnetic"). When performing a dynamic duality transformation for the full $(d+1)$ CA Hamiltonian (which we shall call a *dynamic duality transformation*) one often obtains a dual model more complicated than the original one, with couplings that might be outside the physical regime (they assume complex values). However, this establishes a correspondence between the nature of phase transitions in CA and phase transitions taking place for complex values of interactions.[61–63,69]

The duality relation is performed by graphical methods or within the transfer matrix formalism (see Ref. 70 for a review). Recently, a simple algebraic method was applied to models having odd interactions,[71] a fact important for models with complicated interactions. However, the derivation used implicitly the fact that the couplings are positive. In the next example we show how to generalize the method when one has also negative couplings.

Example 5. Duality Transformation for a (1 + 1) CA. Consider a triangular lattice, represented as a square lattice with diagonals in one direction only (Fig. 8a). Let us consider as interactions an external field, a three-spin interaction term in the triangles pointing in the SW direction only, and the diagonal two-spin interactions. Thus, the partition function will be the trace over the products of local Boltzmann weights shown in Fig. 8a and given by

$$\begin{aligned} w(s_1, s_2, s_3, s_4) &= e^{Hs_1 + Ls_1s_2s_3 + Ks_2s_3} \\ &= \cosh(H)\cosh(L)\cosh(K) \\ &\quad \times [(1 + v_H v_L v_K) + (v_H + v_L v_K)\, s_1 \\ &\quad + (v_L + v_H v_K)\, s_1 s_2 s_3 + (v_K + v_H v_L)\, s_2 s_3] \end{aligned} \tag{3.7}$$

where $v_X \equiv \tanh(X)$. Note that the different spin products in the Hamiltonian form a cyclic subgroup and that the CA condition for this model is simply

$$v_K + v_H v_L = 0 \tag{3.8}$$

implying that either one or all three coupling constants H, L, K are negative. Following the method of Giacomini,[71] one introduces a *link* variable for *every* spin product in (3.7): these link variables assume the value 1 or 0, depending on whether in the product of w a given term is present or not. One gathers next all the link variables connected to a given spin, as shown in Fig. 8b. The term corresponding to (3.6) and spin s_1 is

$$\cosh(H)\cosh(L)\cosh(K)(1 + v_H)\, e^{Ln_1 + Km_1} s_1^{n_1 + n_2 + n_4 + m_2 + m_4} \tag{3.9}$$

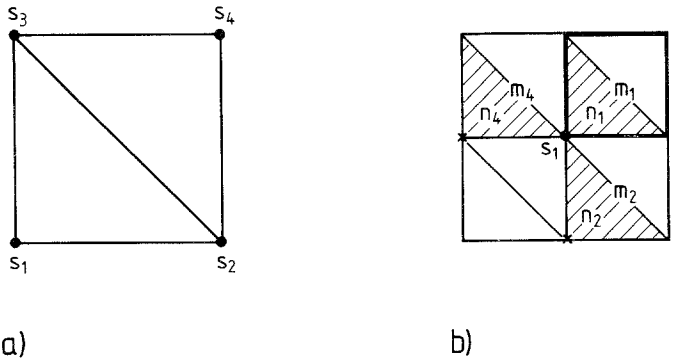

Fig. 8. Duality transformation for models with complicated interactions. (a) The elementary face for a triangular lattice; three different interactions are allowed on the triangle s_1, s_2, s_3. (b) All link variables connected to spin s_1: $m_{1,2,4}$ are related to the two spin couplings along the SE-NW diagonal; $n_{1,2,4}$ are link variables for the three-spin interactions (hatched-triangles).

with the indices shown in Fig. 8b. By using the identity ($m=0, 1$, $\mu=\pm 1=1-2m$)

$$v^m=(|v|)^{1/2}\,\mu^{\Theta(-x)}e^{K^*\mu};\qquad e^{-2K^*}=|v|$$

where

$$\Theta(x)=\begin{cases}1 & \text{if } x>0\\ 0 & \text{if } x\leqslant 0\end{cases}$$

and the μ's are spinlike link variables ($m\to\mu$, $n\to v$). The summation over the original spins leads to

$$\left(\frac{\sinh(2H)\sinh(2L)\sinh(2K)}{8}\right)^{1/2}\pi\exp(L^*v_1+K^*\mu_1+H^*v_1v_2v_4\mu_2\mu_4) \tag{3.10}$$

where π contains the product of link spins corresponding to negative couplings. If, for example, $K<0$, then $\pi=\mu_1$. Using the gauge transformation $v_i=\mu_i v_i$, $i=1, 2, 4$, one finds that the spin μ_1 decouples and can be summed up. The π factor in front of the exponential leads to a sinh function instead of the usual cosh. Defining

$$S_1=2\sinh(H^*+L^*+K^*);\qquad S_2=2\sinh(-H^*-L^*+K^*)$$
$$S_3=2\sinh(H^*-L^*+K^*);\qquad S_4=2\sinh(-H^*+L^*+K^*)$$

we can expand the elementary face weight w^{dual} of the dual model as

$$w^{\text{dual}} = A + Bv_1 + Cv_1v_2v_4 + Dv_2v_4 \tag{3.11}$$

with

$$A = \tfrac{1}{4}(S_1 + S_2 + S_3 + S_4); \qquad B = \tfrac{1}{4}(S_1 - S_2 - S_3 + S_4)$$
$$C = \tfrac{1}{4}(S_1 - S_2 + S_3 - S_4); \qquad D = \tfrac{1}{4}(S_1 + S_2 - S_3 - S_4)$$

Comparing (3.11) to the second part of (3.7), one obtains the duality relations:

$$\frac{v_H^{\text{D}} + v_L^{\text{D}}v_K^{\text{D}}}{1 + v_H^{\text{D}}v_L^{\text{D}}v_K^{\text{D}}} = \frac{B}{A}; \qquad \frac{v_L^{\text{D}} + v_H^{\text{D}}v_K^{\text{D}}}{1 + v_H^{\text{D}}v_L^{\text{D}}v_K^{\text{D}}} = \frac{C}{A}; \qquad \frac{v_K^{\text{D}} + v_L^{\text{D}}v_H^{\text{D}}}{1 + v_H^{\text{D}}v_L^{\text{D}}v_K^{\text{D}}} = \frac{D}{A} \tag{3.12}$$

At a first glance the model seems to be self-dual—at least it has the same interaction structure. A more careful study of this equations reveals that in general the high- (low-) temperature region H, K, $L \simeq 0$ (∞), although mapped into the same model, corresponds rather to some "unphysical" (complex) values of the couplings. On the disorder line (3.8) $S_2 \equiv 0$, so that some combination of the couplings H^{dual}, K^{dual}, L^{dual} must go to $-\infty$. This means that the disorder line is mapped by the duality into an order line lying on some low-temperature region or outside the physical region. A very similar situation has been encountered in the study of disorder lines in the triangular Ising model or the IRF model[60]; here the disorder line was found to be mapped into the nonphysical region (complex couplings).[51]

The same procedure can be applied to three-dimensional systems as well. Consider, for example, an Ising odel on a bcc lattice (or any close-

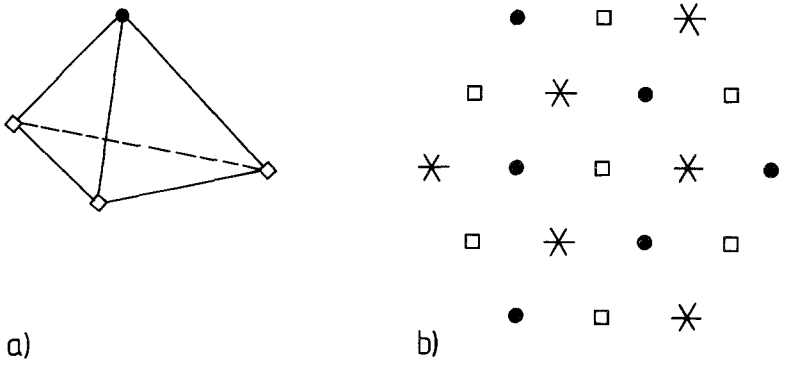

Fig. 9. The elementary tetrahedron and an upper view of the three-dimensional close-packed lattices. The spins denoted by crosses, circles, and stars form different layers of stacked-shifted triangular lattices.

packed 3-dimensional lattice) with interactions in *every second* elementary tetrahedron, as shown in Fig. 9. The interactions consist of an external field, a four-spin term coupling all the spins on the corners of the elementary tetrahedra, and, to close the subgroup, a three-spin interaction between the three spins at the base of the tetrahedron shown in Fig. 9a. Again, the CA condition (2.11) is given by Eq. (3.8) using the same arguments as previously. Models with only two-spin interactions [in $(1+1)$ dimensions the triangular lattice, in $(2+1)$ dimensions the hcp or other close-packed lattice] can be interpreted as a "staggered" model by assigning all couplings to every other (alternating) triangles or tetrahedra. The CA conditions are similar to (3.8). All these models have "dynamic" or global duality relations of the kind shown in the previous example. For symmetric CA, when the effective Hamiltonian corresponding to $\langle L_1 | R_1 \rangle$ is known and short-ranged, the "static" duality transformation might be used to predict the exact location of the phase transition.[57]

Before finishing this subsection, we mention that the duality transformation can be formulated also in terms of lattice-gas variables $n_i = 0, 1$, as illustrated in the following example.

Example 6. Duality Transformation in Terms of Lattice-Gas Variables. Let us consider again the triangular lattice of Example 5, but express now the energy of a basic triangle in terms of the occupation variables n, n', $n'' = 0, 1$ as

$$-\beta H = \sum_{\nabla} [\mu n + J_2 n(n' + n'') + J_3 n n' n''] \tag{3.13}$$

where $\sum_{\nabla}$ means a summation over the down-pointing triangles only. Introducing the notation $z = e^{\mu/kT}$, $\alpha = e^{J_2/kT}$, and $\beta = e^{J_3/kT}$ and using that $e^{xn} = 1 + (e^x - 1)n$, we can expand the Boltzmann factors as

$$e^{-\beta H} = \prod_{\nabla} \{[1 + (\alpha - 1)\, n(n' + n'')][1 + (\beta - 1)\, n n' n'']\, z^n\} \tag{3.14}$$

which corresponds to the high-temperature expansion in the spin variables. Introducing *three* sets of "link" variables corresponding to the products $t_1 \equiv nn'$, $t_2 \equiv nn''$, and $t_3 \equiv nn'n''$, one can now perform the summation over the old

$$\{n_x\}$$

variables. Summing up the term 1 from the product gives $(1+z)^{N_\downarrow}$ ($N_\downarrow$ is the number of down-pointing triangles); summing up the linear terms leads to two different kind of fugacities for $t_{1,2}$ and t_3, respectively: $\zeta_{1,3} =$

$(\alpha, \beta - 1)/(1+z)^2$. Interactions (usually short-ranged) are the result of summing up higher order terms. Sometimes two neighboring t variables are not compatible with any original configuration; in that case a nearest neighbor exclusion must be assumed. Note that for large negative values of the original couplings the dual fugacities ζ become negative, showing again that the "dynamic" duality relations will map the original model into the "unphysical" region of the dual model. This type of duality relation was used by Dhar[61] to calculate the generating function of directed animals in two and three dimensions.

3.4. Fully Integrable Cellular Automata

Of special interest are cellular automata that can be solved by the generalized Bethe *Ansatz* or by using the inversion relation.[19] Such models are called fully integrable in statistical physics and quantum field theory because one can solve in principle for every eigenvalue and eigenvector of the transfer matrix. Full integrability is related to the existence of commuting transfer matrices (or to the factorization of the scattering matrix S). For two-dimensional IRF models, the condition for two row-to-row transfer matrices with a different set of couplings to commute can be cast into the local Yang–Baxter generalized star–triangle equation (see Fig. 10):

$$\sum_{s_7 = \pm 1} w(s_1, s_2, s_7, s_6)\, w'(s_6, s_7, s_4, s_5)\, w''(s_7, s_2, s_3, s_4)$$
$$= \sum_{s_7 = \pm 1} w''(s_6, s_1, s_7, s_5)\, w'(s_1, s_2, s_3, s_7)\, w(s_7, s_3, s_4, s_5) \quad (3.15)$$

This equations must be true for any value of the spins $s_1, \ldots, s_6$, leading to an overdetermined set of nonlinear equations for the couplings contained

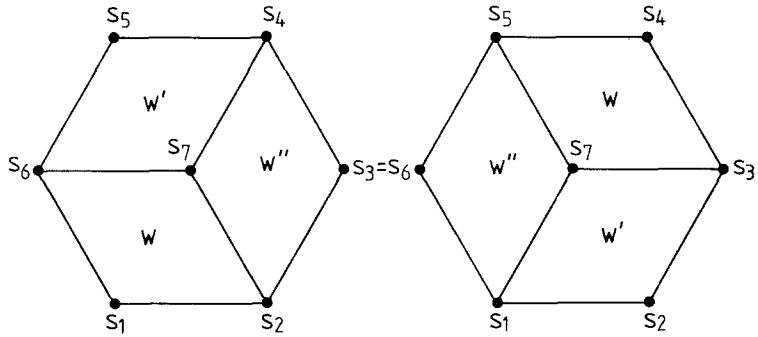

Fig. 10. The generalized star–triangle transformation. The faces denoted by w, w', w'' have different values for the couplings but the same interaction structure. On both sides one has to sum s_7.

in w, w', and w''. An exhaustive analysis of the solutions of these equations for even interactions has been performed.[72] The solutions that do not correspond to one-dimensional models in disguise basically correspond to three classes: the symmetric eight-vertex model, the (asymmetric) six-vertex model, and the free fermion model.[19] An exhaustive study of the CA solutions of the IRF models has also been done[60] and the conclusion is that there are no common points of the two manifolds except at $T=0$, with one notable exception: the free fermion model has a disorder line—actually one found among the first.[53] Along this disorder line the free fermion $d=1$ model reduces to the linear model defined in Section 3.2. Note that the kinetic Ising model with the Glauber transition probability corresponds to a free fermion model[46] and is also a typical example of a linear model.

One can generalize the star–triangle equations of the IRF model to three dimensions. For the interactions-round-a-cube (IRC) model one can derive that two plane-to-plane transfer matrices with a different set of couplings will commute if the *tetrahedron* equations[73] are satisfied. An interesting question is whether in three dimensions there exists a class of models generalizing the two-dimensional free-fermion models and whether such models have a common manifold with the linear CA models. A more important question is the problem of integrability conditions for (even two-dimensional) models with *interpenetrating faces.* It is known that for fully integrable models the commutation relations must be fulfilled also for finite matrices (here finite automata in the spacial direction)[72]; this seems to be the right direction for starting the study of fully integrable dynamics.

One cannot close this section without mentioning that from the point of view of cellular automata such exact results seem at first glance interesting but not important—especially for those who believe only in deterministic CA. My opinion is different. I think that these types of analytic results might be very useful: the fully integrable models, for example, have an infinite number of conserved charges (integrals of motion). We may soon learn how to encode information in these charges, which are not affected by the dynamics of the system and can be retrieved at any later time. Moreover, since these charges are macroscopic objects, this kind of information storage would be also resistant against local noise.

4. APPROXIMATE AND NUMERICAL METHODS

The main goal of this section is to show how different approximate methods borrowed from statistical physics may be adapted to the study of cellular automata. Many of the points one could emphasize in this context have been extensively presented before.[30,52],[15] For the sake of simplicity I

[15] For a review and further references see Kinzel.[74]

shall consider a model that generalizes the well-known problem of the directed percolation; for a review of the subject and its many ramifications see Kinzel.[74] The model has the structure shown in Fig. 3a with the probabilities given as

$$w(1\,|\,0,0)=p_0=0; \quad w(1\,|\,0,1)=w(1\,|\,1,0)=p_1; \quad w(1\,|\,1,1)=p_2 \tag{4.1}$$

$|000,\ldots,0\rangle$ is an absorbing state because $p_0=0$. The phase diagram of the model is shown in Fig. 11. In the $\langle 0\rangle$ phase the CA will always fall into the absorbing phase after a finite amount of time, while in the "infected" phase $\langle n\neq 0\rangle$ an "eternal" cluster, percolating in the time direction, is present. This cluster can be described as a linear combination of states having some nonzero average occupancy. In order to understand better this phase transition, the most obvious and simplest choice is to start with some kind of mean field approach.[74] Let us suppose that the main feature of the stationary state in the infected phase is represented only by the concentration of occupied sites and for the moment let us neglect all other correlations between the sites at equal times. Then one may write the mean field equation

$$n(t+1)=p_0[1-n(t)]^2+2p_1n(t)[1-n(t)]+p_2n(t)^2 \tag{4.2}$$

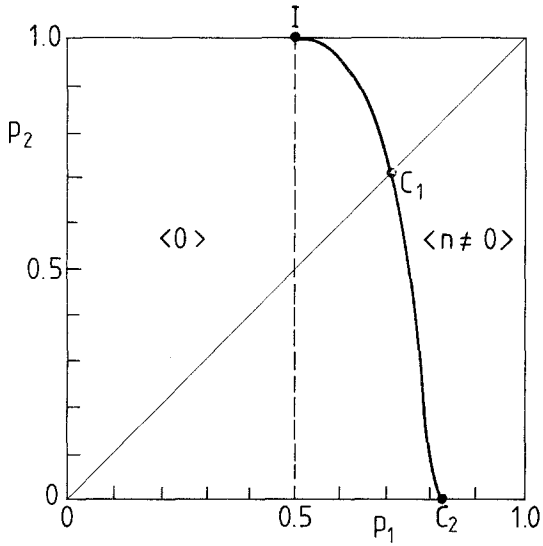

Fig. 11. The phase diagram for the generalized directed percolation problem. The mean field result is indicated by the broken line. Numerical results using finite-size transfer matrix calculations and renormalization group analysis are shown by the continuous line.[30,50] The time dependence of the model at the points I, C_1, and C_2 is compared in the following figures for simultaneous and sequential updating dynamics.

where we have tacitly assumed that the average occupancy is homogeneous and does not depend on the site i. For the directed percolation problem, $p_0 = 0$, and one obtains two possible stationary solutions, $\bar{n}_1 = 0$ and $\bar{n}_2 = (2p_1 - p_2)/(2p_1 - 1)$. The mean field critical line is $p_c = 1/2$; for $p_1 < p_c$ the first solution is stable, while for $p_1 > p_c$ the second one is stable. This is a phase transition corresponding to the directed percolation transition, with the mean field exponents $\nu = 1/2$, $z = 2$, $\gamma = 1$, etc.[74] The situation is quite interesting along the line $p_2 = 1$. If $p_1 = 1/2$, $n(t+1) = n(t)$ identically, while for $p_1 < 1/2$, $\bar{n}_1 = 0$, and for $p_1 > 1/2$, $\bar{n}_2 = 1$ is the stable solution. It is quite obvious that the phase transition on this line is quite different from the bifurcation-type transition at $p_1 = 1/2$, $p_2 < 1$. The former is an Ising-type transition (in the field direction), while the latter is in the universality class of directed percolation (or CA with one absorbing state). The mean field approach shown above is *exact* for the linear models introduced in Section 3.

As in the theory of fluids, one can derive an infinite set of coupled equations for the different correlation functions. By truncating this set of equations one may obtain a better estimate of the critical line—a very similar approach has been proposed for the *Life*[36] rules.[75],[16] Furthermore, it is possible in general (not only for the directed percolation problem) to use the variational methods developed in connection with the transfer matrix formalism.[21]

A very typical feature of the directed percolation problem is that the corresponding transfer matrix is reducible; all matrix elements corresponding to the probabilities of going out from the absorbing state are zero. The transition is not related to a spontaneous symmetry breaking as in usual second-order transitions, but seems to be only a function of this reducibility property of the transfer matrix. In order to check that indeed this is the case, we have considered a sequential updating procedure rather than the simultaneous one. This is based on the following simple observation: if the transfer matrix is

$$P^{\mathrm{e,o}}_{\mathbf{s},\mathbf{s}'} = \prod_{i=\mathrm{e,o}} w(s_i | s'_{i-1}, s'_{i+1}) \tag{4.3}$$

for even (e) and odd (o) time steps, respectively, then one can construct a different stochastic operator, namely

$$L^{\mathrm{e,o}}_{\mathbf{s},\mathbf{s}'} = \sum_{i=\mathrm{e,o}} w(s_i | s'_{i-1}, s'_{i+1}) \tag{4.4}$$

The even–odd updating procedure breaks the translated symmetry of the operators P and L. A remedy to this problem is a trick we shall also use

[16] For a different approach see Falk.[76]

later: take the original lattice (shown in Fig. 3a) and double the number of sites, so that one obtains the geometry shown in Fig. 3b. If furthermore one introduces the weights $w_{\text{new}}(n_1 \mid n_2, n_3, n_4) = w_{\text{old}}(n_1 \mid n_2, n_4)$, where w_{old} is given by (4.1) and w_{new} by

$$
\begin{aligned}
&w_{\text{new}}(1 \mid 0, 0, 0) = p_0 = 0; \\
&w_{\text{new}}(1 \mid 1, 0, 0) = w_{\text{new}}(1 \mid 0, 0, 1) = w_{\text{new}}(1 \mid 1, 1, 0) = w_{\text{new}}(1 \mid 0, 1, 1) = p_1 \\
&w_{\text{new}}(1 \mid 1, 0, 1) = w_{\text{new}}(1 \mid 1, 1, 1) = p_2
\end{aligned} \tag{4.5}
$$

one updates at *the same time* two *independent* but identical automata. In this formulation P becomes translational invariant, and so does the corresponding *Liouville* operator L:

$$
L_{\mathbf{s},\mathbf{s}'} = \sum_i w_{\text{new}}(s_i \mid s'_{i-1}, s'_i, s'_{i+1}) \tag{4.6}
$$

It is easy to check that L is also a stochastic operator normalized to N (number of spins in a row) rather than to 1. Such a change from simultaneous to sequential dynamics is called in statistical physics the "Hamiltonian limit" and it corresponds to an infinitely strong anisotropic limit of couplings in the space and time direction, finally leading to a continuous time variable. If the anisotropy operator is not relevant, that is the singular behavior of the models represented by (4.4)–(4.6) is the same, the Hamiltonian formulation has several technical advantages over the simultaneous dynamics (Euclidean formulation). Unfortunately, in the case of the directed percolation one cannot use the usual arguments supporting the Hamiltonian limit (see Ref. 77 for a review). In Figs. 12a–12c we show a comparison of the simultaneous dynamic behavior (4.4) and that of the sequential dynamic behavior (4.6) close to the points I, C_1, and C_2 of Fig. 11. The simulations were done using a Monte Carlo algorithm, with a time scale twice as long in the sequential case as in the simultaneous one. One can clearly see a similar behavior in both cases, with the point $p_2 = 1$ (Ising case) being different from the $p_2 < 1$ behavior.

The operator (4.6) is easier to diagonalize than the transfer matrix (4.4): we have calculated numerically the largest two eigenvalues of finite chains up to 18 sites by applying a powerful numerical technique based on the iteration of the Lánczos scheme.[78]

We measured along the line $p_1 = p_2 = p$ the *gap* of the problem $G \equiv \tau^{-1} = \ln(\lambda_1/|\lambda_2|)$, corresponding to the slowest relaxation mode. At a usual second-order phase transition the static problem has a diverging characteristic length $\xi \sim \xi_0(K - K^*)^{-\nu}$ as function of some parameter K (here $K = p$) and the fixed point K^*, while the gap behaves as $G \sim G_0(K - K^*)^{\Delta}$,

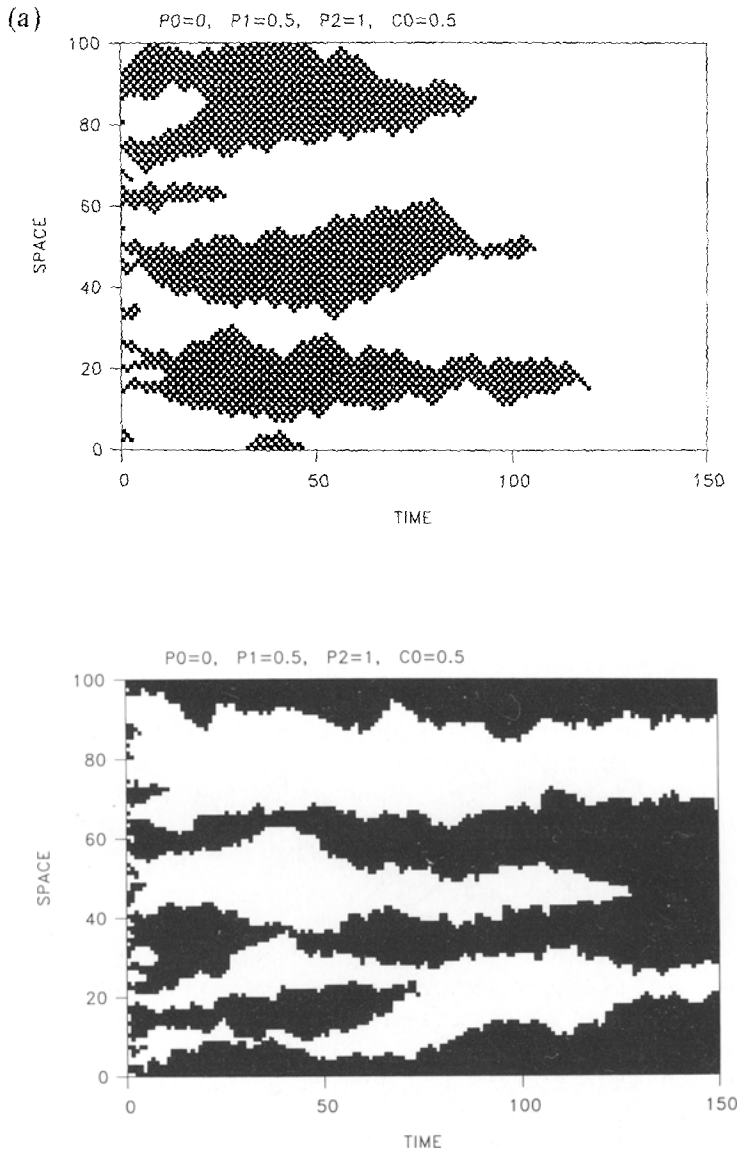

Fig. 12. Monte Carlo simulations comparing near-critical behavior on different regions of the phase diagram. Black dots are occupied sites; unoccupied sites are not shown. (a) Near the Ising point I ($p_1 = 1/2$, $p_2 = 1$). (b) Near the critical point C_1 ($p_1 = p_2 \sim p_c$). (c) Near the critical point C_2 on the line $p_2 = 0$. The top picture shows the simultaneous updating, the bottom picture the sequential one after a full sweep. Note that the values of the critical points (except I) are different in the two models.

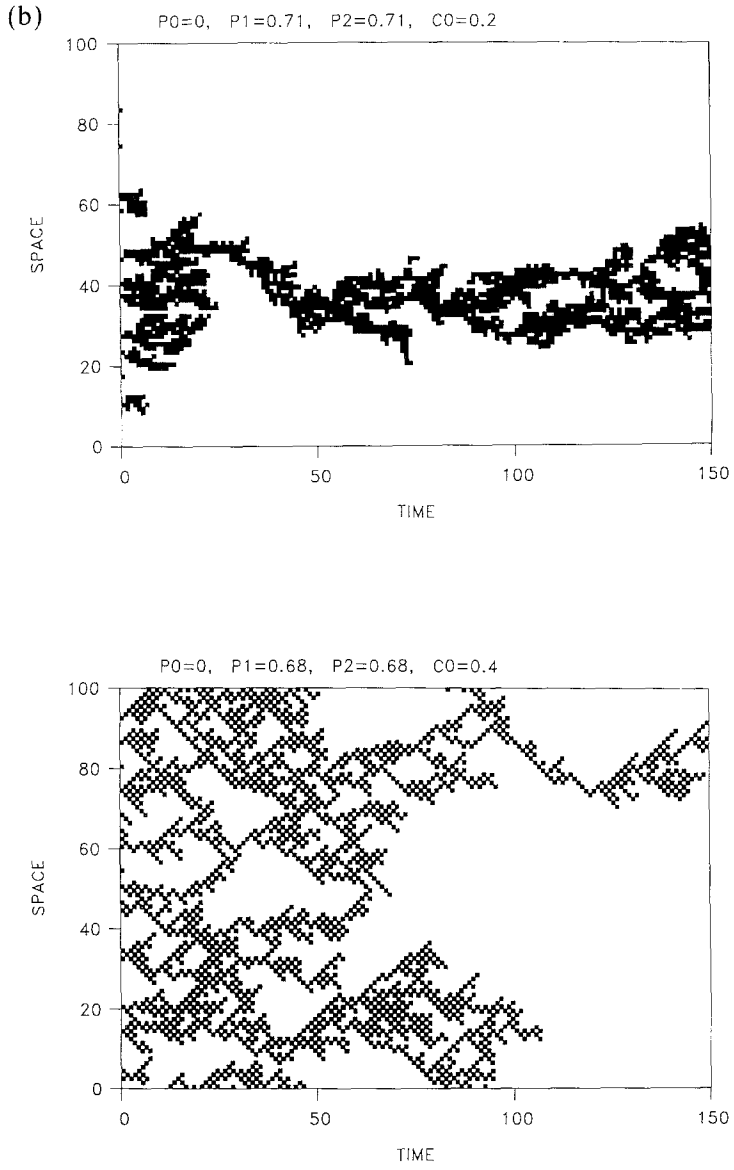

Fig. 12 (*continued*)

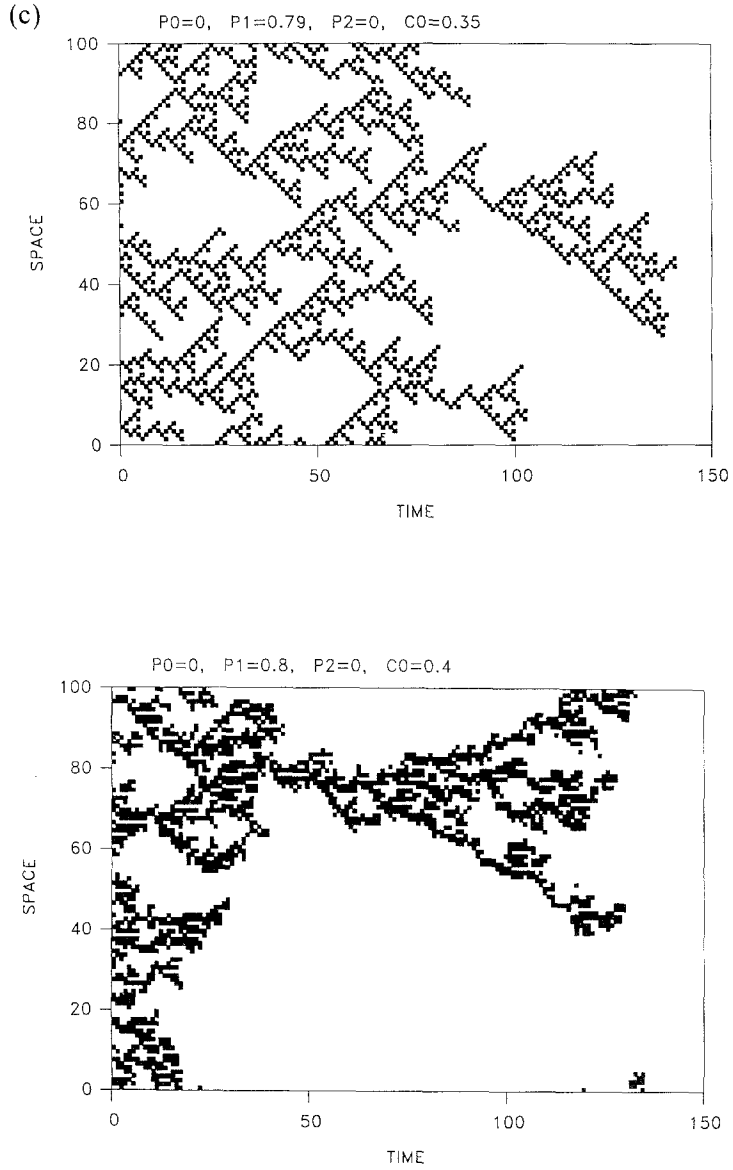

Fig. 12 (*continued*)

where $\Delta = z\nu$, and z is the dynamic exponent.[42] From the point of view of finite lattice scaling and phenomenological renormalization[24,25] this means that in the neighborhood of K^*, $G_N \sim N^{-z}$. Denote for two finite systems of size N and N'

$$b = \frac{N}{N'}; \quad Z_{N,N'} = \ln\left(\frac{G_{N'}}{G_N}\right)\Big/\ln\left(\frac{N}{N'}\right); \quad Z'_{N,N'} = \ln\left(\frac{G'_{N'}}{G'_N}\right)\Big/\ln\left(\frac{N}{N'}\right) \tag{4.7}$$

where b is the scale change and

$$G' = \left(\frac{\partial G}{\partial K}\right)_{K=K^*}$$

Here b is the scale change. The three parameters K^*, ν, and z can be calculated from sets of data involving systems of three finite sizes, N, N', and N'' as follows: (a) calculate K^* from $Z_{N,N'}(K^*) = Z_{N',N''}(K^*)$, leading also to: (b) $z = Z_{N,N'}$; (c) finally, $\nu^{-1} = z + Z'_{N,N'}$. These dynamic scaling relations are exactly the ones previously derived in the context of anisotropic scaling.[47]

The *beta function* is defined as

$$\beta(K) \equiv \lim_{b \to 1} \frac{dK'}{db} = \left[\frac{d}{dK}\ln(\xi^{-1})\right]^{-1}$$

(ξ is the *static* correlation length). In finite lattice calculations β can be approximated following Roomany and Wyld[24] as

$$\beta_{\text{dyn}}^{\text{RW}} = -\left(1 - \frac{1}{z}Z_{N,N'}\right)\left(\frac{G'_N G'_{N'}}{G_N G_{N'}}\right)^{1/2} \tag{4.8}$$

where now $G_N = G_N(K)$, $G_{N'} = G_{N'}(K')$, etc. The dynamics inherits the kind of global symmetry (such as invariance when all spins at time t and $t+\tau$ are flipped) possessed by the statics.

A plot of the quantity $Z_{N,N+1}$ as a function of $p = p_1 = p_2$ is presented in Fig. 13. A detailed analysis of data is cumbersome because the approach to the true critical value is not monotonic. However, using different sets of data and an improved version of the Romberg algorithm for extrapolation,[79] we have found a dynamic critical exponent slightly lower than the Euclidean value[30] $z = 1.58(1)$, which is, however, within the error bars of our estimate.

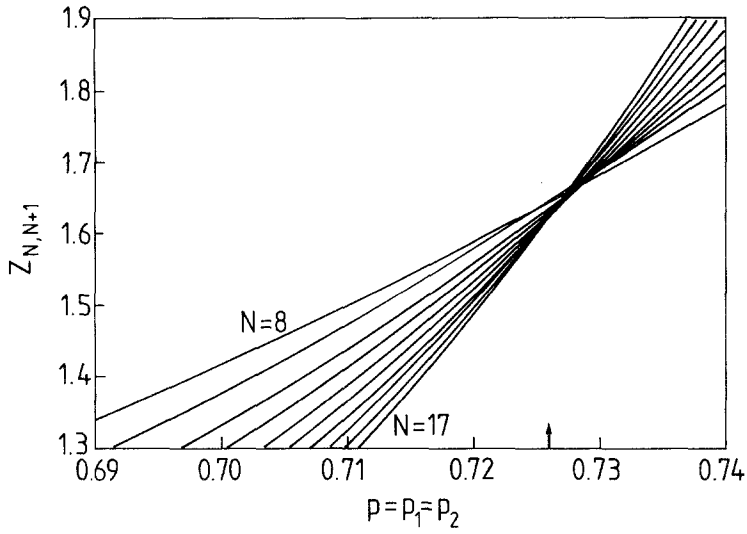

Fig. 13. Finite-size dynamic exponents $Z_{N,N+1}$ for $N=8$–17 from the exact diagonalization of the Liouville operator (4.6) for $p_1=p_2$. Note that the critical probability has shifted from the $p_c=0.706$ to $p_1=0.725$.

We must recall that these results were obtained by assuming the usual second-order mechanism in which the inverse of the gap between the two leading eigenvalues plays the role of the *single* most diverging correlation length. This assumption might prove to be wrong on two accounts: one is the possibility of an "entropy"-driven transition [see possibility (b) in Section 2]. As obvious from Example 4, a strip geometry might be missleading in such a case. The second one is the relation between the spin–spin correlation length and the *mean width* of the percolating cluster. The characteristic sizes of the largest clusters near the transition must diverge with the same exponents as the correlation length if scaling is true. Recently, counterexamples have been found for similar dynamic problems.[40] An investigation along these lines is under way.

5. CELLULAR AUTOMATA ENGINEERING

Cellular automata are interesting in themselves as simple models displaying a complex behavior or as discrete realizations of continuous differential equations. In many ways, modeling with cellular automaton rules seems a natural thing to do in biology, ecology, and computer science. Such a *phenomenological* approach may be very helpful in many cases by

explaining a general pattern of behavior in terms of some (hopefully) simple and local dynamic rules. A *taxonomic* approach classifying all possible simple deterministic rules in $(1+1)$ and $(2+1)$ dimensions is also useful, providing a *menu* of possibilities for potential applications. An alternative approach is to find the rules corresponding to some observed (or expected) pattern without having to rely on a possibly lengthy trial-and-error search. The main goal of the present section is to show how to use the analogy between statistical mechanics and cellular automata to find dynamic rules whose effect can be predicted *analytically* in advance. It is hoped that the examples, and the methodology, shown below might be useful for *practical* purposes, as functioning hardware or as mathematical prototypes of different biological models.

Our examples are centered around four main areas: first we consider the question of phase transitions in cellular automata. By using the techniques explained in the section dealing with disorder-type solutions, we give two examples: first we construct a cellular automaton that corresponds to the $T=0$ critical point of the antiferromagnetic triangular Ising model. This is a particularly interesting case, because the model is exactly soluble and the large-distance correlations are known to be isotropic. In the second example we construct a $(2+1)$-dimensional CA whose statics is given by the symmetric eight-vertex model: according to the exact solution,[19] the static exponents should change continuously with temperature.

The second main question under scrutinity is the question of conserved quantities. Examples of time development with constant energy and magnetization are given for $(1+1)$-dimensional CA and their critical behavior is discussed. Celular automaton rules preserving the *topological structure* of an initial configuration are presented, together with some applications.

The third and the fourth areas of interest, namely the question of a change in the limit cycle and the question of parallel cellular automaton networks, are closely related. In statistical mechanical systems one can construct short-range interaction models with an *infinite* number of (commensurate) ground states either by some clever topological constraints or by combining together two parallelly running cellular automata. This leads to sets of rules that are either deterministically or randomly changed in space and/or time. Their properties, including purely dynamic transitions without scaling, the presence of Cantor sets like attractors, etc., are briefly reviewed through some simple examples and show the degree of complexity one can obtain by increasing the hierarchy of parallel automaton networks.

5.1. Constructing CA with Different Critical Properties

Example 7. The Antiferromagnetic Triangular Ising Model. In this example we consider a $(1+1)$-dimensional cellular automaton defined on a triangular lattice as shown in Fig. 14. The time-developing operator involves now two time steps. At $T=0$ the ground state of the antiferromagnetic Ising model is fully frustrated. In every elementary triangle the spins try to avoid having alike neighbors. For topological reasons, however, this is not possible: the best that can be achieved is to have two alike and one different spin in every elementary triangle. This restriction is easily implemented by using the following rules:

$$
\begin{aligned}
&w\begin{pmatrix} 0 & \\ 0 & 0 \\ & \downarrow \\ & 1 \end{pmatrix} = p_0 = 1, \qquad w\begin{pmatrix} 0 & \\ 0 & 1 \\ & \downarrow \\ & 1 \end{pmatrix} = p_1 = 1 \\
&w\begin{pmatrix} 1 & \\ 0 & 0 \\ & \downarrow \\ & 1 \end{pmatrix} = p_2 = p, \qquad w\begin{pmatrix} 1 & \\ 0 & 1 \\ & \downarrow \\ & 1 \end{pmatrix} = p_3 = 0 \\
&w\begin{pmatrix} 0 & \\ 1 & 0 \\ & \downarrow \\ & 1 \end{pmatrix} = p_4 = 1, \qquad w\begin{pmatrix} 0 & \\ 1 & 1 \\ & \downarrow \\ & 1 \end{pmatrix} = p_5 = 1 - p \\
&w\begin{pmatrix} 1 & \\ 1 & 0 \\ & \downarrow \\ & 1 \end{pmatrix} = p_6 = 0, \qquad w\begin{pmatrix} 1 & \\ 1 & 1 \\ & \downarrow \\ & 1 \end{pmatrix} = p_7 = 0
\end{aligned}
\tag{5.1}
$$

These rules are dictated by the full frustration condition, except for the rules $p_2 = p$ and $p_5 = 1 - p$. Once we set the two first rows of spins to some initial values, the dynamic rules can be used to obtain a *given* ground-state configuration of the antiferromagnetic triangular Ising model. Such a configuration is shown in Fig. 15a for an initial random configuration of the two rows with initial concentration of $c_0 = 0.5$ and for $p = 0.382$. Starting with a different initial configuration and/or using different random numbers to decide the ties (p_2 and p_5), one obtains different possible ground

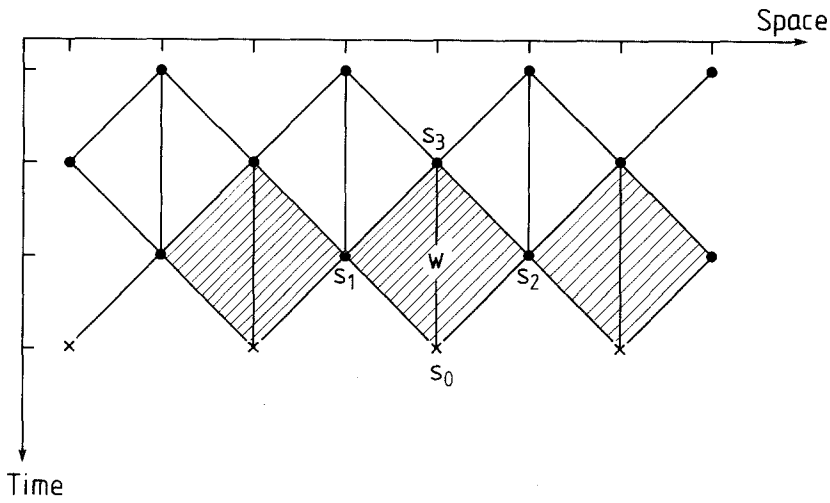

Fig. 14. The construction of the triangular lattice. The transfer matrix involves two time steps. An elementary square face $w(s_0|s_1, s_3, s_2)$ containing two triangles is also shown.

states of the Ising model. The magnetization per spin is also displayed on Fig. 15b as a function of time: its average value is 0, as it should, but strong fluctuations around this value are present due to the critical character of the model. Until now we have taken for granted that the rather obvious rules (5.1) are really describing the ground states of the triangular antiferromagnetic Ising model. In order *to prove* that this is indeed the case, one has to show that: (a) the dynamics given by (5.1) can reach *any* possible ground state (ergodicity) and (b) all such ground states have an *equal* probability to appear. A direct proof of these two points is rather difficult, we use the following trick to resolve the problem.

Consider the elementary square face shown in Fig. 14b. The question posed before can be rephrased as follows: Is it possible to define the couplings in the interaction form of the face weight w such as to lead to the weights (5.1) and at the same time to correspond to the triangular Ising model? In order to answer this question, let us introduce the notation shown in Fig. 14b and denote by α the *couplings* between the spins s_0 and s_1, s_2, and by K_3 the coupling between the spins s_0 and s_3. In order to satisfy the CA condition, let us first sum $\bar{w}(s_0|s_1, s_2, s_3)$ over s_0:

$$\sum_{s_0} \exp\{s_0[\alpha(s_1+s_2)+K_3 s_3]\} = \exp[A + Bs_3(s_1+s_2) + Cs_1 s_2] \quad (5.2)$$

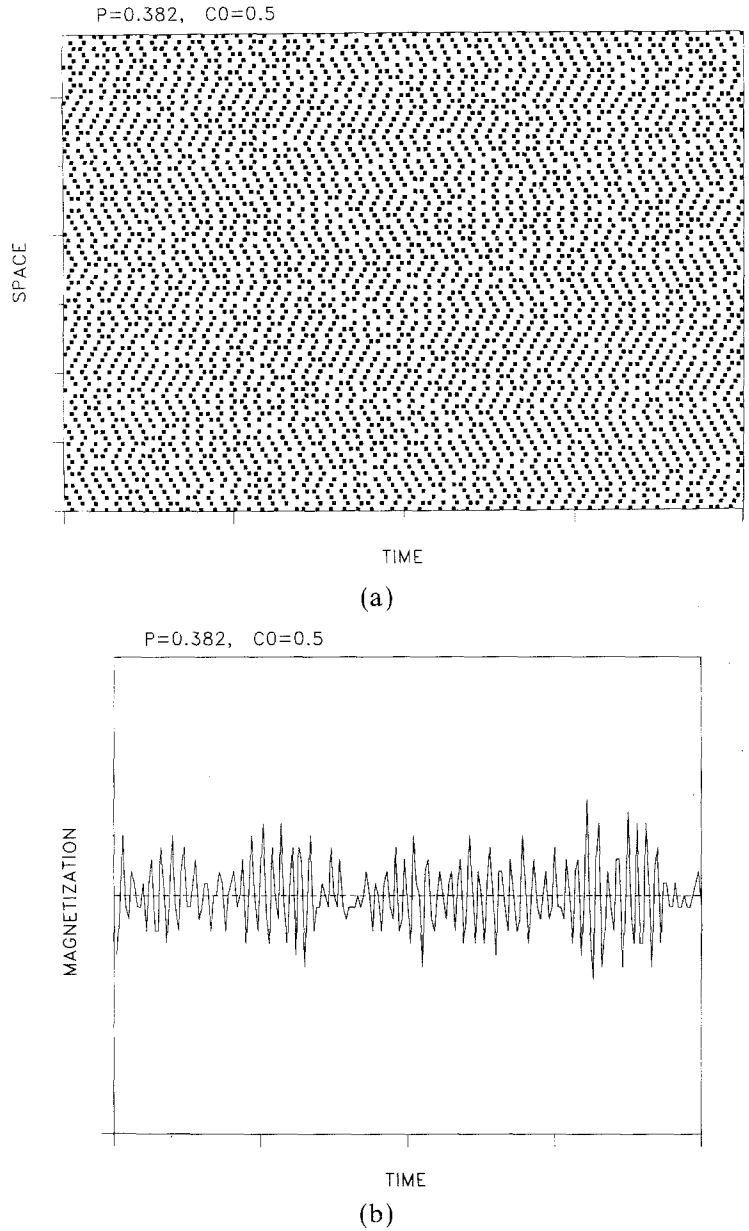

Fig. 15. (a) Monte Carlo simulation for 150 time steps of the CA given by the rules (5.1) for an automaton of size $N = 50$ with periodic boundary conditions, $p = 0.381966...$, $c_0 = 0.5$. An occupied site is represented by a black square; the empty sites are not shown. (b) The coverage/site as a function of time for the same configuration.

where

$$A = \tfrac{1}{4} \ln 2^4 \cosh(K_3 + 2\alpha) \cosh(K_3 - 2\alpha) \cosh^2(2K_3)$$
$$B = \tfrac{1}{4} \ln[\cosh(K_3 + 2\alpha)/\cosh(K_3 - 2\alpha)] \tag{5.3}$$
$$C = \tfrac{1}{4} \ln[\cosh(K_3 + 2\alpha) \cosh(K_3 - 2\alpha)/\cosh^2(2K_3)]$$

Therefore by construction

$$w(s_0 | s_1, s_2, s_3) = \exp\{-A - Bs_3(s_1 + s_2) - Cs_1 s_2 + s_0[\alpha(s_1 + s_2) + K_3 s_3]\} \tag{5.4}$$

will satisfy the CA condition (2.11). When considering the lattice obtained by gluing together all faces w, one easily see that the total coupling between spins s_0, $s_{1,2}$ is given by $K_1 = K_2 = \alpha - B$. Note that a coupling C between the spins s_1 and s_2 is produced; it is the effect of this coupling that must be studied in detail. Consider the limit $K_3 = -|K_3| \to \infty$, and suppose that $\alpha = -\beta |K_3| + \bar{\alpha}$. Calculating the value of B from (5.3) and asking that $K_1 = K_2 = K_3$, one obtains that $\beta = 1/2$ and

$$\exp(4\bar{\alpha}) = (\sqrt{5} - 1)/2$$

Using the values of $\bar{\alpha}$ and β, one can recalculate the values of the couplings using Eqs. (5.3). A remarkable result is that

$$C = \tfrac{1}{4} \ln \tfrac{1}{2}(3 + \sqrt{5}) = 0.2406059...$$

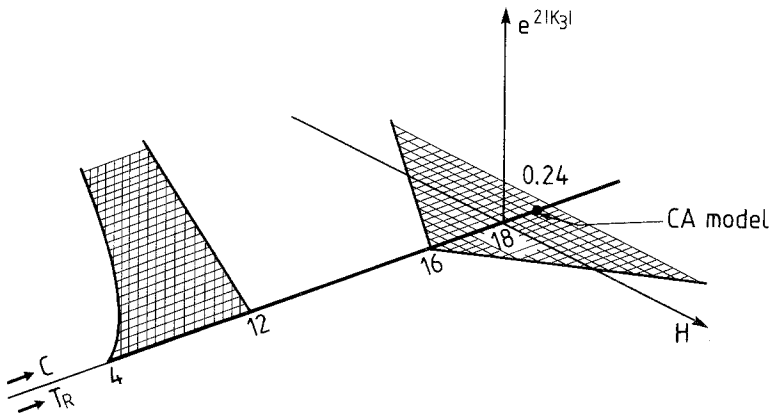

Fig. 16. The phase diagram of the triangular antiferromagnetic Ising model with next-nearest neighbor interactions and an external field.[80] Here $\exp(2|K_3|)$ corresponds to the temperature operator, C is proportional to the SOS model parameter T_R, H is the external field. Shaded regions are massless (critical) phases with continuously changing parameters. The parameter values corresponding to the CA rules (5.1) are indicated by an arrow.

is of order $O(1)$, and is not proportional to $|K_3|$. In leading order for $K_3 \to -\infty$, C *seems* to play no role whatsoever. A little further algebra shows that the parameter p in (5.1) is equal to

$$p = 2/(3+\sqrt{5}) = 0.381966...$$

the value used in the Monte Carlo simulation shown in Fig. 15.

The number of ground states of the isotropic antiferromagnetic triangular model is macroscopic. Therefore, even some $O(1)$ couplings like C may have an important effect in selecting a subset of configurations among the allowed ones. In the Boltzmann weight w, C enters always with a negative sign. For a moment suppose the opposite, so there is an attraction between (six) next nearest neighbours. This signals a preference for such a sixfoldcrystalline structure: $-C>0$ acts as an external field with sixfold symmetry. In a recent work it has been shown[80] that the triangular antiferromagnetic Ising model, including next-nearest neighbor couplings and also an external field, can be mapped into a solid-on-solid (SOS) model. As a result, it was possible to identify the spin-wave and vortex operators corresponding to C and to an external field. The resulting phase diagram[80] is shown in Fig. 16. The shaded regions correspond to massless (critical) phases with continuously changing exponents. T_R is the roughening temperature of the SOS model and is supposed to be proportional to C; at $C=0$, $T_R=18$. Although no exact relation is known between T_R and C, it can be argued that at large distances the spin–spin correlations decay as[80]

$$\langle s_i s_j \rangle \xrightarrow[r_{ij}\to\infty]{} AC(i,j)\, r_{ij}^{-2X_6} + B r_{ij}^{-2X_2} \tag{5.5}$$

where A and B are constants, r_{ij} is the distance between two sites i, j of the triangular lattice, and $C(i,j)$ is a modulating factor, which equals 1 if i and j are on the same sublattice (the triangular lattice has three sublattices) and $-1/2$ otherwise, X_p is the anomalous dimension of a spin-wave operator with charge p,[80]

$$X_p = T_R/2p^2 \tag{5.6}$$

For $C=0$ one recovers the known result[53] $2X_6 = 1/2$ and $2X_2 = 9/2$. Since in the CA model $C>0$, this implies that $T_R > 18$ and thus from (5.6) larger exponents X_p (faster decay).

When the value of p is changed in the dynamics rules (5.1), three $O(1)$ parameters are varied along a special trajectory. If $K_i = -|K_3| + \Delta_i$, $i=1, 2$, the three operators in question are Δ_1, Δ_2, and C. The anisotropies $\Delta_{1,2}$ correspond to irrelevant operators (they do not induce a transition) up

to the value $e^{2A_1} - e^{2A_2} = 1$, where a incommensurate–commensurate transition happens.[80] In the $C > 0$ direction there is no transition, only $T_R > 18$ increases. A small external field can be easily added by breaking slightly the symmetry $p_5 = 1 - p_2$ in (5.1). The temperature operator $\sim e^{2|K_3|}$ has the critical index $x_T = 18/T_R$ and it is related to relaxing the deterministic part of the rules (5.1).

There are many interesting features of this automaton: it is an example of a simultaneous dynamics at criticality; the model is "almost" soluble[80] with spin–spin correlations decaying isotropically at large distances. This isotropic behavior is highly unusual for cellular automaton models and leads to the value $z = 1$ for the dynamic exponent. Moreover, this example shows that a very fast, simultaneous simulation of such a nontrivial model is possible, gaining one full dimension over the usual Monte Carlo method. It is also encouraging that this model is rotational invariant at large distances; similar models would be of high interest for the simulation of lattice gauge theories.[17] However, this would require an exhaustive search for multicritical points in such models, similar to the one done for the IRF model.[60] That study was the basis for the present calculation: we are now moving on the critical surface predicted by the first two articles of Ref. 60.

Example 8. A (2+1)-Dimensional CA with a Continuous Change of Exponents. In this example we answer the question[18] of whether is it possible to construct a $(2+1)$ CA whose stationary distribution (or static behavior) is described by the symmetric eight-vertex model.[19] According to Section 3.1, one has then to construct a set of time-symmetric automaton rules whose static $\langle L_1 | R_1 \rangle$ partition function is identical to the one of the symmetric eight-vertex model in spin representation (an IRF model with diagonal and four-spin interactions). The main difficulty of such a construction is related to the four-spin coupling: it is not possible to break the square lattice into two sublattices that could be then updated alternately. As pointed out to me by D. Dhar after this work was completed, it is, however, possible to define four sublattices forming squares of twice the side of original lattice: in this way the spins of a given sublattice (generation) are not nearest or next-nearest neighbors to each other. His method implies a three-step time recursion, but is simple and applies to all IRF models. In what follows we present an alternative method, involving a two-step time recursion only, but requiring the full integrability of the static problem.

[17] An example of a Z_2 gauge-invariant $(3+1)$-dimensional cellular automaton was given by Rujàn and Patkòs,[81] which, however, breaks the time-space symmetry at the transition point.

[18] H. Hartman asked me this question during the Statphys' 16 meeting in Boston.

Consider a slice of the 3-dimensional sc lattice with all possible interactions within the elementary cubes (IRC model) as shown in Fig. 17a. We assume that by summing up all the spins indicated by a bullet and shown for one single cube in Fig. 17b, only a constant is generated [see Eq. (2.11)] independently of the values of the spins numbered by 5, 6, 7, 8. Considering an IRC model with even interactions symmetric under the $\pi/2$ rotations around the $s_1 s_8$ axis, one generates only three different even couplings between the spins $s_5,\ldots, s_8$, which reduce the number of independent IRC couplings by three. The "*Ansatz*" couplings K, L on the three lower sides of the cube represent the interactions within $\langle L_1|$ and are shown in "planar" form in Fig. 18b. Fortunately, the eight-vertex model satisfies the generalized star–triangle transformation and consequently obeys Eq. (3.15) (see Fig. 10) also for $w = w' = w''$. Applying this transformation several times, one can transform the lattice shown in Fig. 18a into the one shown in Fig. 18b, where apart from the "defect line" shown by the heavy lines, the structure is the one corresponding to the planar eight-vertex model. Its solution is exactly known.[19] I suspect that the effect of

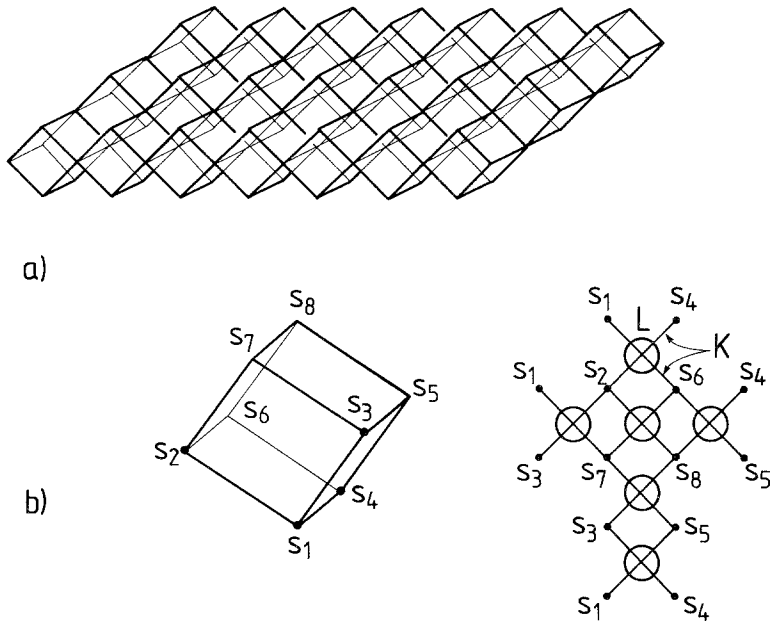

Fig. 17. (a) The diagonal-to-diagonal transfer matrix of a simple cubic IRC model in the (1, 1, 1) direction. (b) Notations used for a single cube: the spins $s_{1\text{-}4}$ are summed up. Note that the faces of the cube must have interactions corresponding to the underlying symmetric eight-vertex model: diagonal interactions (K) and four spin interactions (L), as indicated on the planar representation of the cube.

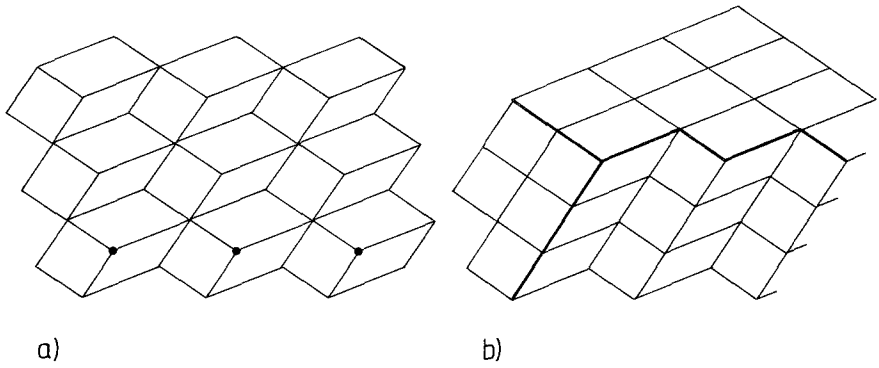

Fig. 18. (a) The $\langle L_1 | R_1 \rangle$ corresponding to an eight-vertex model defined on the (1, 1, 1) face of the cubic lattice, which can be transformed using the star–triangle transformation (3.15) into (b) an eight-vertex model on a square lattice with a "defect line" (heavy line).

this defect line is irrelevant in the thermodynamic limit, especially since it can be shifted far away from the region of interest.

I do not present here a detailed definition of the dynamic rules; the construction follows the same scheme as for the previous example, with the added inconvenience of many more parameters. As far as I know, there are no dynamic studies near the critical line of the symmetric eight-vertex model, where the exponents change continuously as a function of temperature: the present example might be used to devise a fast, simultaneous algorithm for such a simulation.

5.2. Conservation Laws and Topology-Invariant Dynamics

The following examples illustrate how one may devise rules conserving different macroscopic quantities. In an elegant paper Jen[82] considered recently the problem of finding deterministic CA rules leaving given one-dimensional strings invariant. She was also able to give the minimal spatial extension of rules whose *only* invariants were the given string and words formed from it. Here we emphasize mainly probabilistic rules leaving a given macroscopic quantity invariant, since such quantities are not affected by local random noise. As a first example, we consider a $(1+1)$-dimensional automaton that preserves the total magnetization of a one-dimensional string. The second example shows the same thing for an energy-conserving dynamics, while the third example introduces a local CA that "knows topology," in the sense that it preserves the topological structure of an initial configuration and, moreover, it is able to recognize some of its aspects.

Example 9. A Cellular Automaton Conserving Magnetization. Consider a checkerboard lattice (see Fig. 2a) in two dimensions and define the following rules for the transition probabilities of the dashed squares:

$$w_{\blacksquare}\begin{pmatrix} 0 & 0 \\ & \downarrow \\ 0 & 0 \end{pmatrix} = p_{0,0} = 1, \quad w_{\blacksquare}\begin{pmatrix} 0 & 0 \\ & \downarrow \\ 1 & 1 \end{pmatrix} = p_{1,1} = 0, \quad w_{\blacksquare}\begin{pmatrix} 1 & 0 \\ & \downarrow \\ 0 & 1 \end{pmatrix} = p_{2,2} = p \tag{5.7}$$

These rules, the normalization condition, and the symmetries

$$\begin{aligned} w_{\blacksquare}(n_1, n_2 | n_3, n_4) &= w_{\blacksquare}(n_2, n_1 | n_4, n_3) = w_{\blacksquare}(n_3, n_4 | n_1, n_2) \\ &= w_{\blacksquare}(1-n_1, 1-n_2 | 1-n_3, 1-n_4) \end{aligned} \tag{5.8}$$

define completely all the 16 weights, which can be alternately given in the following compact form:

$$w_{\blacksquare}(s_1, s_2 | s_3, s_4) = \tfrac{1}{4}[2 + (1-p)(s_1 s_3 + s_2 s_4) + p(s_1 s_4 + s_2 s_3)] \tag{5.9}$$

where $s_i = 1$ if a site is occupied and -1 if a site is empty. The magnetization is conserved by construction: all transitions changing the number of occupied sites are forbidden. The free parameter p is related to the ability of the "walls formed in the time direction by the occupied sites to diffuse to the right or to the left. Note that this model can be mapped in the usual way[83] into a staggered six-vertex model (or into a nonstaggered "diagonal-to-diagonal" six-vertex model).

In Fig. 19 we show a few simulations according to the rules (5.8). From (5.8) it is obvious that the rules are symmetric in the time direction; hence, according to Section 3.1, the statics of this model can be easily determined. Consider, for example, the spacelike correlation functions

$$\langle s_{i_1}, \ldots, s_{i_k} \rangle_{t \to \infty} = \frac{\sum_{\{s_i\}} s_{i_1}, \ldots, s_{i_k} \delta(\sum_j s_j - mN)}{\sum_{\{s_i\}} \delta(\sum_j s_j - mN)} = m^k \tag{5.10}$$

which reproduce the typical behavior of noninteracting spins in a field. However, since the rules are partially deterministic (completely deterministic if $p = 0$ or 1), some properties of the initial state (such as different correlations between sites) are carried on and are not "forgotten" during the dynamic simulation. The result (5.10) and the results below apply for a random initial distribution of the occupied sites. The disorder solution (5.10) tells us that the "stationary" distribution is that of noninteracting

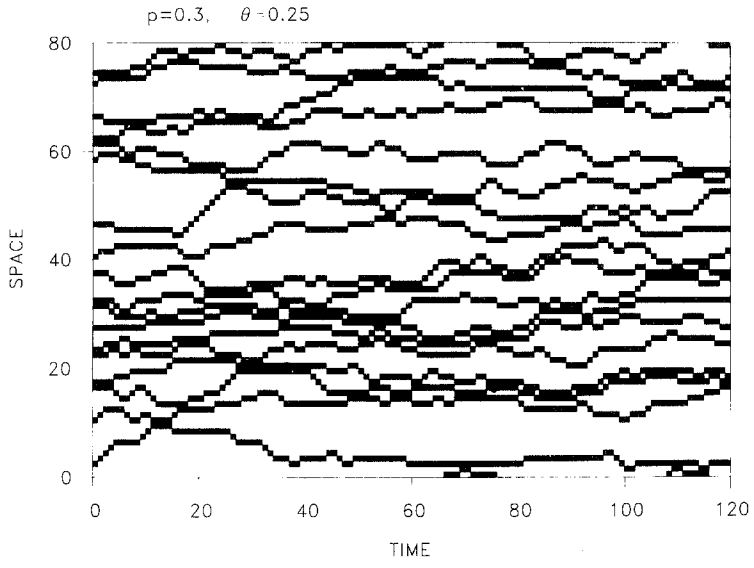

(a)

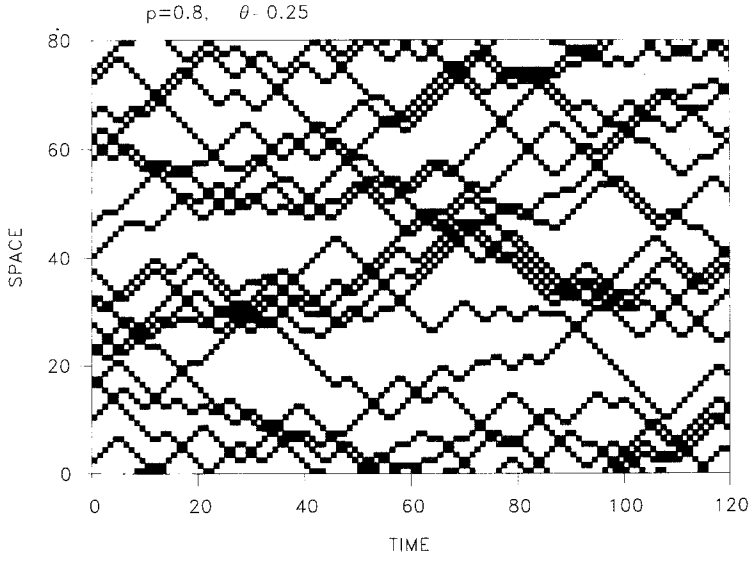

(b)

Fig. 19. Cellular automaton dynamics conserving magnetization: Monte Carlo simulations for different parameter values $N = 80$, $p \sim$ diffusitivity and $\theta =$ coverage: (a) $p = 0.3$, $\theta = 0.25$, (b) $p = 0.8$, $\theta = 0.25$.

spins. Equation (5.10) can be better understood by the following simple argument:

$$\langle s_i s_j \rangle = \left\{ \begin{array}{l} +1 \text{ with probability } n_+^2 + n_-^2 \\ -1 \text{ with probability } 2n_+ n_- \end{array} \right\} = (n_+ - n_-)^2 = m^2$$

where $n_{+,-}$ is the concentration of occupied (empty) sites. The calculation of correlations in the time direction is also simple. Consider first the trivial case $p = 0$ (frozen walls). Then it is obvious that $s_i(t) = s_i(t + \tau)$, so every correlation between spins at different times reduces to the ones already given by (5.10). The other deterministic case, $p = 1$, is only slightly more involved. Here the occupied sites always move to the right (left) if they occupy even (odd) lattices (see Fig. 18c) due to the staggered structure of the lattice (Fig. 2a). Therefore, correlations of spins lying in the "light cone" $v = \pm 1$ will cross only half of the occupied sites, so, for example, $\langle s_i(t)\, s_{i \pm vT}(t + T) \rangle = (m/2)^2$, etc. The other correlations again will have the form (5.10). For $0 < p < 1$ we expect the same result to hold, but with $v = p$.

Example 10. Energy-Conserving Dynamics. Consider a $(1 + 1)$-dimensional lattice with the elementary faces shown in Fig. 20. For every dashed face the transition probabilities are given as follows:

$$w(1\,|\,000) = 0; \qquad w(1\,|\,001) = p; \qquad w(1\,|\,010) = 1; \qquad w(1\,|\,011) = 1 - p \tag{5.11a}$$

and

$$w(n_1\,|\,n_2, n_3, n_4) = w(1 - n_1\,|\,1 - n_2, 1 - n_3, 1 - n_4); \qquad n_i = 0, 1$$

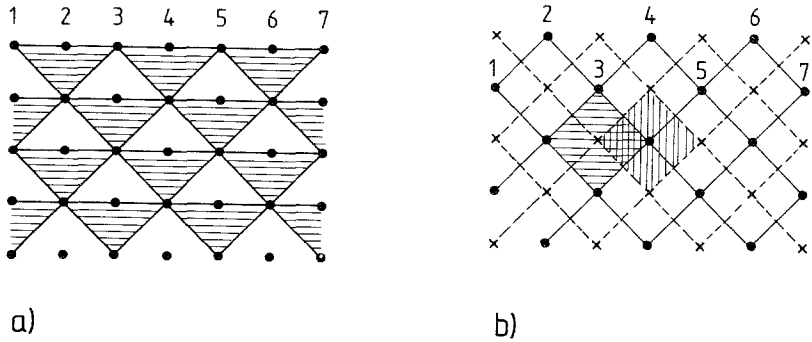

Fig. 20. (a) The $(1 + 1)$-dimensional lattice of a cellular automaton conserving energy. A full row of spins is set in two steps, as indicated by the shaded triangles. (b) The doubling of the lattice sites: first, the straight lines of the original lattice are bent into a zigzag form, then a second sublattice (denoted by crosses) is added, with the same rules. Note that the w triangles of (a) now have a diamond shape involving two time steps.

If instead of the $n=0, 1$ variables we use $\sigma=-1, +1$ variables, the face weight w has the simple form

$$w(\sigma_0|\sigma_1, \sigma_2, \sigma_3)=\tfrac{1}{2}[1+(1-p)\,\sigma_0\sigma_2+p\sigma_0\sigma_1\sigma_2\sigma_3] \qquad (5.11b)$$

This rules conserve the energy ($\sum_i \sigma_i\sigma_{i+1}$) of a row because the number of negative bonds (the number of times the spins change sign) is left invariant by construction in (5.11). Using the same trick as for oriented percolation (Section 4), it is again possible to double the lattice size in such a way as to have a simultaneous updating of two interpenetrating, but independent, sublattices. They are shown in Fig. 20b and for $p=1$ correspond to the $(1+1)$-dimensional case of the Q2R rules.[14-17] Let us now introduce the link (or dual) spins as $s_{i+1/2}=\sigma_i\sigma_{i+1}$ and let us call the negative bond variables *kinks*. If one follows the dynamic induced by (5.11) for the *kinks*, one easily recognize the rules as (5.7). Therefore, we have here an example of what we called a *static duality transformation* in Section 3.3. All results obtained in the previous example can be translated for the present case by performing an inverse transformation from the bond variables.

This analogy is illustrated graphically in Fig. 21. In Figs. 21a and 21b we show two simulations performed with the same values of the parameters

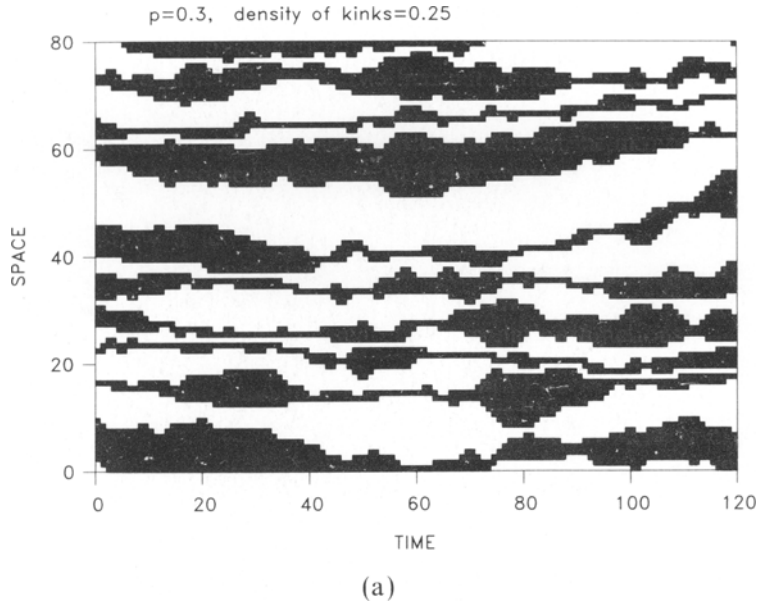

Fig. 21. Numerical simulation for an energy-conserving automaton of size $N=80$. (a) $p=0.3$, (b) $p=0.8$; in both cases the density of negative bonds (kinks) $c_0=0.25$, (c) same simulation as in (b), but only the evolution of kinks is shown.

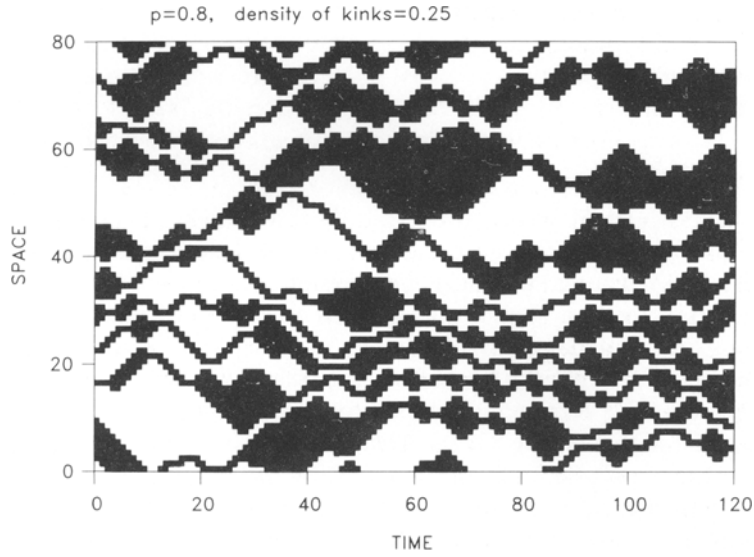

(b)

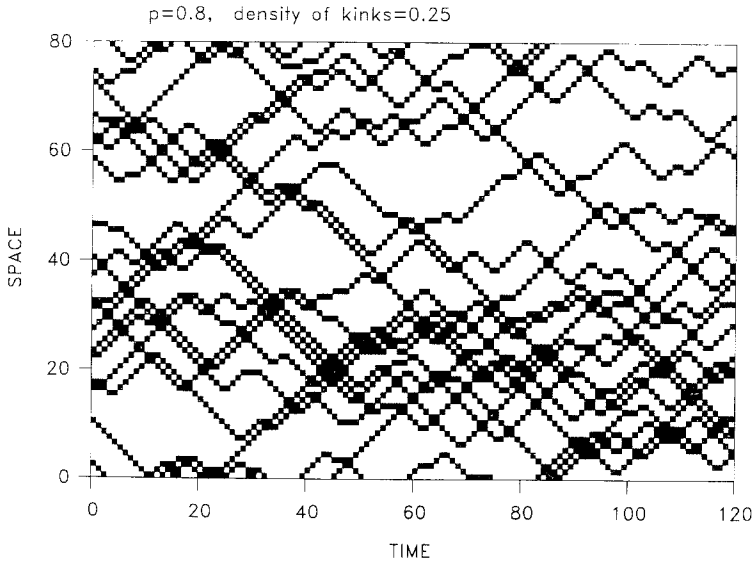

(c)

Fig. 21 (*continued*)

as in Figs. 19a and 19b, except that the coverage θ represents the density of kinks. To make the analogy more visible, we have replotted Fig. 21b by showing only the kinks: it leads to a picture similar to Fig. 19b, the difference being caused by the fact that one uses the (same) set of random numbers in a different way (for $p=1$, for example, the two figures are identical).

At this point it seems worthwhile to discuss what happens in higher dimensions, especially because the topology of the one-dimensional lattice is trivial. Consider a (spacial) d-dimensional Ising model and define a "loose" spin to be a spin whose internal field is exactly zero. Therefore, flipping this spin does not change the total energy of the system. The celebrated Q2R (or flip if two—from the nearest four = quatre—neighbors are up) rule[14–17] corresponds exactly to the prescription to flip all possible loose spins of the system. The problem here is that on the constant-energy surface there are also configurations without any loose spins, so the Q2R rule cannot be ergodic. Consider, for example, the elementary low-temperature excitations consisting of small domains of spins pointing upward immersed in a large, compact domain of spins pointing downward: some examples are shown in Fig. 22a. In general, one finds that loose spins can be found at the corners or along walls oriented on the (1, 1) direction of compact clusters.

If one is really interested in a microcanonical simulation of the Ising model,[84] one also has to consider dynamic processes that would move around a single flipped spin. Define a "loose cluster" of spins as a cluster

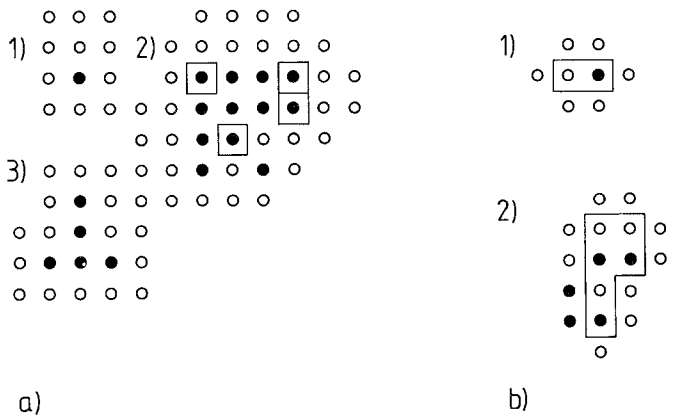

Fig. 22. (a) Some typical low-temperature configurations without loose spins (1) or with localized loose spins (2, 3). (●) Up spins, (○) down spins, loose spins (clusters) are framed. (b) Some examples of "loose" clusters; the two-spin cluster (1) moves the elementary low-temperature excitation one step to the left.

whose total external field vanishes—flipping such a cluster does not change the energy. In principle all such clusters must be flipped. From a practical point of view, however, one may try to keep as dynamical rules only flipping the single-spin and two-spin loose clusters. A two-spin loose cluster is shown in Fig. 22b; when flipping the internal two spins, the overturned spin moves one step to the left. In order to show that by including also flips of loose 2-clusters the dynamics becomes ergodic, one would have to prove that flipping an arbitrarily large loose cluster can be done by successive elementary flips, or to prove that the measure of loose clusters without this property is zero in the thermodynamic limit. Although we have not sought such a proof, similar numerical procedures applied to the staggered six-vertex model[85] suggest that such an extended dynamics leads to the expected results.

The rules (5.11a) have another interesting feature: they preserve the *topology* of any initial configuration in the sense that the number of clusters is conserved by the dynamics. One can try to generalize such constraints to higher dimensions. A lattice quantum mechanical model leaving invariant the topology ("topodynamics") has been proposed by Aharonov and Schwartz[86] and has been recently generalized to a stochastic dynamics.[87] We present briefly here the main idea and some applications in two (spatial) dimensions.

Example 11. A Cellular Automaton That Leaves the Topological Structure Invariant. Consider a square lattice and define a lattice-gas variable in every elementary square. A square can be occupied (black) or unoccupied (white). Two such squares (sites) are said to be *connected* only if they have a common edge. A *cluster* is a set of connected sites (including the single site); a *loop* is defined as usual as being a set of empty sites encircled by a cluster of occupied sites (see Fig. 23a). In Fig. 24a we show a 60×60 lattice where the sites have been occupied at random with the probability $c_0 = 0.55$, close to the site-percolation thereshold $p_c^{\text{site,sq}} = 0.592$.[88] It is obvious that we have many clusters, loops, double loops (eights), perhaps loops within loops, etc. We ask the following question: is it possible to design a *local* CA rule that (a) leaves invariant the topological structure of such a configuration and (b) is able to recognize clusters, loops, and possibly their hierarchy. We mention here that it was the inability of *Perceptrons* (linear, one-step CA) to perform such a task[89] that hampered the extensive research efforts in that field.

Consider a site and its nearest and next-nearest neighbors (Fig. 23b). The central square (spin) is set at time $t+1$ as a function of its own value and of its environment defined above at time t. The rules are such that no connection is made and no connection is broken within the (3×3) window

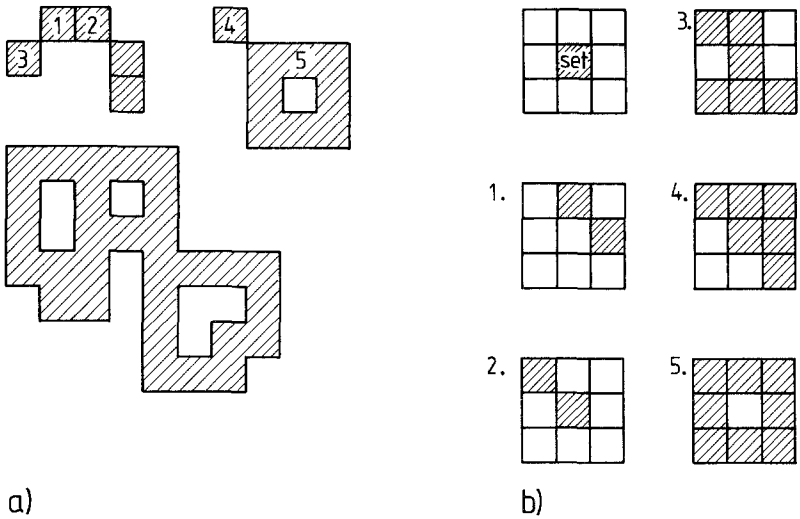

Fig. 23. (a) Clusters and loops on the square lattice. The squares indicated by 1 and 2 are connected, 1 and 3 not. The canonical form of a cluster (4) and that of a loop (5) are also shown. (b) The elementary window of the CA rules and three different possibilities: (1) the center spin must remain 0 in order to not connect two clusters; (3) the center spin must remain 1 in order to not disconnect a cluster; (4) the center spin can be taken away ($1 \to 0$) from an existing cluster without changing the topological structure; (2) a cluster is identified; (5) a loop is identified.

(Fig. 23c). Still, we are left with many rules that basically may add or take away with some probability a site to (from) a cluster. This probability p plays here the role of the chemical activity (external field). If $p = 1$ (0), one has a deterministic rule we call the "take" ("add") rule. By taking away such irrelevant sites with large probability (actually, $p = 1$ = "take" rule), one obtains the picture shown in Fig. 24b, since the system tries to minimize its energy and the field prefers the white sites. It is evident that now all *loopless* clusters have reached their "canonical" form—a single occupied site. Once this stage is reached, the dynamics is stopped and the number of clusters is counted using the local 3×3 window. The loops also tend to have the "canonical" form consisting of one empty site encircled by a full cluster. However, a loop whose "membrane" is already minimal (one layer of occupied sites) cannot be reduced any longer, even if the "ground state" of the system would prefer loops of minimal size. In some sense, the situation is similar, but not equivalent, to the one encountered in spin glasses. The dynamics has many fixed points corresponding to metastable states separated by large energy barriers. If one also wants to count the numbers of loops, the clusters are set to empty and the rules are

reversed: now we add sites whenever possible. The interior of the loops is then reduced to an elementary square, again recognizable within the (3×3) window. When no more sites can be added, the dynamics stops (Fig. 24c); again the loops are counted and filled up. The process is inverted again (Fig. 24d), until nothing is left. With this algorithm one can count the number of clusters, the number of loops, the number of clusters within loops, the number of loops within loops, etc.

The pictures shown in Fig. 24 were obtained using a sequential updating. One can convince oneself that a simultaneous updating procedure is possible after splitting the square lattice into nine sublattices, such that the (3×3) windows do not interpenetrate—that could result in an unwanted cancellation of clusters consisting of two sites. This also means that a specially designed chip could make these operations in a number of steps that does not depend on the size of the lattice but only on the *topological complexity* of the presented pattern. The CA rules have many potential applications in a wide range of areas, including statistical physics, some of which were presented recently.[87]

5.3. Cellular Automata with Many Limit Cycles: Cellular Automata Networks

Here we address the following question: is it possible to devise dynamic rules such that the automaton will display a very large (possible infinitely large) number of limit cycles? Is it possible to change the behavior from one limit cycle to another limit cycle by changing one (or a few) parameters?

We have seen that limit cycles in (*finite*) cellular automata correspond to commensurate phases in statistical physics. Let us consider first the problem of having a large (possibly infinite) number of commensurate phases in a statistical mechanical model. The real problem is, of course, to find a subclass of such models that *satisfy also the CA condition (2.11)*. Among the most striking discoveries made in the last few years was the fact that many lattice systems with competing interactions actually display a very complex, highly nonanalytic phase diagram. One of the first models of this type was the axial-next-nearest-neighbor-Ising (ANNNI) model in three dimensions.[19] Other representative models are a one-dimensional antiferromagnetic lattice-gas model with long-range interactions[91] or the one-dimensional random energy Ising model in a field.[92] In order to have an infinite number of phases we need either quite high dimensionality, so

[19] Rather than try to list all the relevant work, we only cite the recent paper by Luck and Petritis.[102]

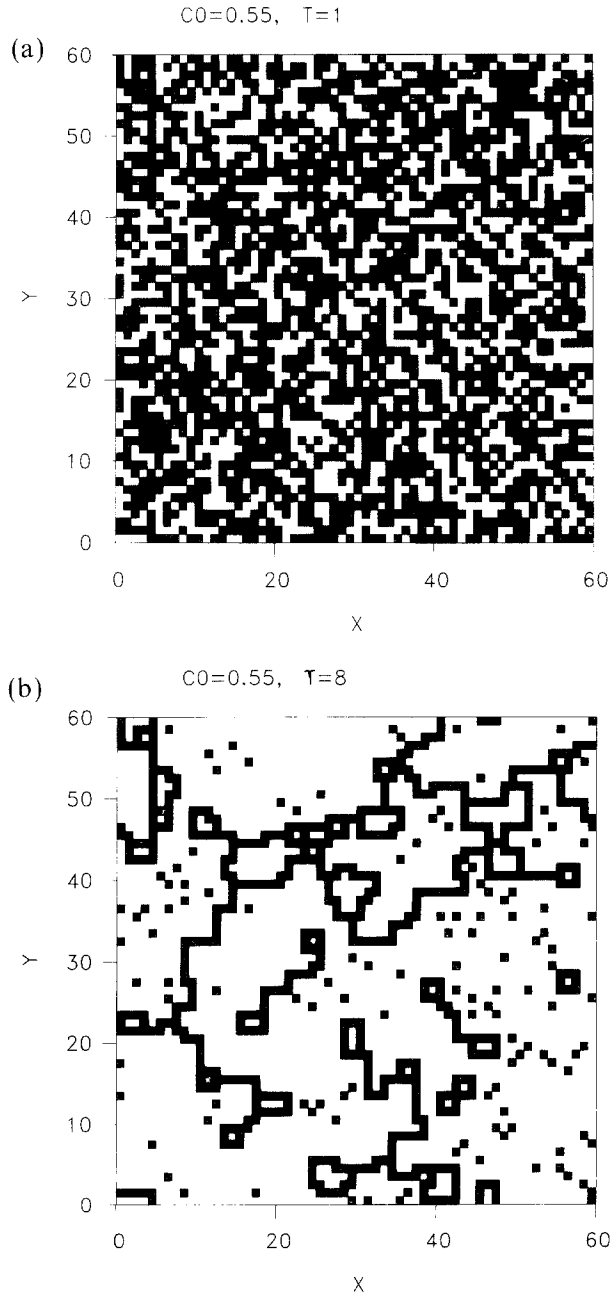

Fig. 24. (a) All sites of 60×60 square lattice are set to 1 with the probability $p = 0.55 < p_c = 0.592$ (site percolation). (b) After $T = 8$ sweeps the "take" dynamics has reduced all loopless clusters to canonical form. The clusters are counted (there are 120 clusters) and set to zero before the rules are inverted to "add." (c) The "add" dynamic stops again when one cannot add any further spin without breaking the topological structures. The picture is a negative one (white and black are inverted). Note again that the *isolated* black squares are the centers of the loops. The loops are counted (there are 36 loops) and filled up. (d) After inverting again the rules, six clusters are left.

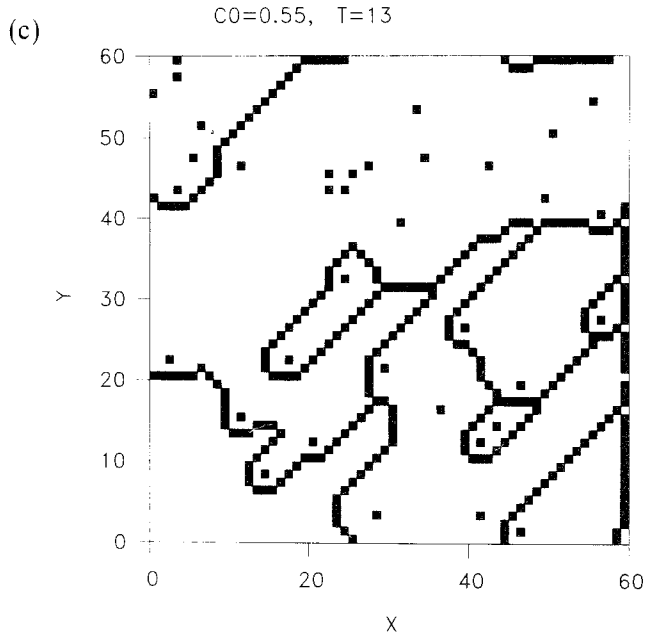

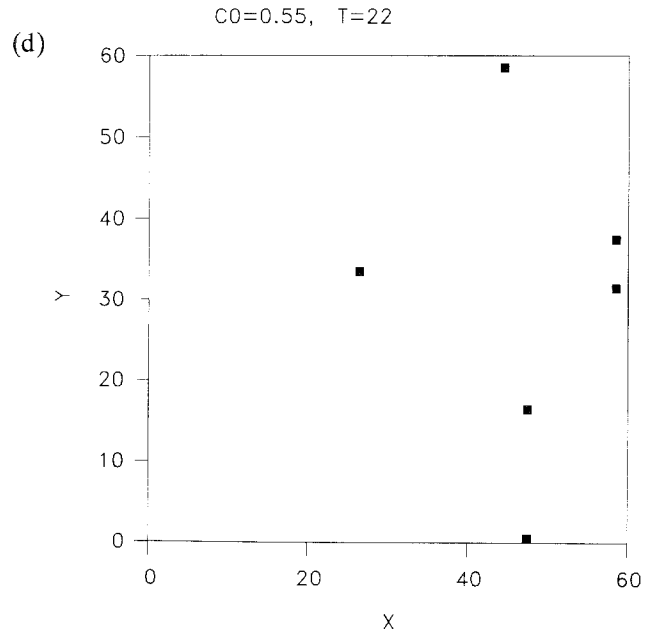

Fig. 24 (*continued*)

that the mean field approach is qualitatively correct (the ANNNI model exhibits infinitely many phases only in three or higher dimensions), long-range interactions, or quenched randomness. In the next example we show how to construct the *dynamics* of a model, which due to some *topological* effects occurring in non-Bravais lattices has an infinite number of $T=0$ (simple) ground states. Note that the *dynamics* does not have to show long cycles—we are dealing here only with many commensurate phases occurring in the stationary (equilibrium) state.

Example 12. A (2+1)-Dimensional Cellular Automaton with Infinitely Many Phases. In a recent paper Kanamori[93] has shown that a lattice-gas model defined on a honeycomb lattice and including nearest, next-to-nearest, and third-neighbor interactions shows an infinity of ground states for some specified region of the parameters. We consider here a simplified version of his model, which we will treat following the general approach proposed by Villain.[94] Consider a honeycomb lattice with lattice-gas variables $\{n_i=0, 1\}$. The nearest neighbor interactions are infinitely repulsive, so that two occupied sites cannot be nearest neighbors (nearest-neighbor-exclusion = nne). In addition, the interactions *per elementary hexagon* contain an *attractive* interaction between third neighbors (J_3) and an external field H (the activity is $z=e^{H/kT}$) acting on *occupied sites*. Let us consider the low-temperature region of the phase diagram. If the field is very large compared to J_3, then every second site (one sublattice) of the honeycomb lattice will be occupied, so as to minimize the energy of the nne lattice gas. If, however, J_3 increases in value, the system will form the kind of walls shown in Fig. 25. Following Villain,[94] we calculate the energy/occupied site for triangles of length L as follows:

$$-\varepsilon = -\frac{E}{\text{number of sites}}$$

$$= -\varepsilon_\infty + \frac{2}{L(L-1)}\left[\frac{3(L-1)}{2}(J_3-H)-\frac{3}{6}3H\right] \tag{5.12}$$

Here $L(L-1)/2$ is the number of occupied sites in a triangle of side L, and $3(L-1)$ is the perimeter. Every edge is common to two and every corner to six triangles. The gain in energy when forming a wall of unit length is proportional to J_3 for every hexagon (see Fig. 25), from which one must extract a lost field unit H, while at the vertex one loses $3H$ compared to the energy of a configuration without walls $\varepsilon_\infty = \varepsilon(L=\infty)$ (note again that the field and the attractive third-neighbor iteraction act only on occupied sites). Since the presence of vertices is unfavorable, one may suspect a

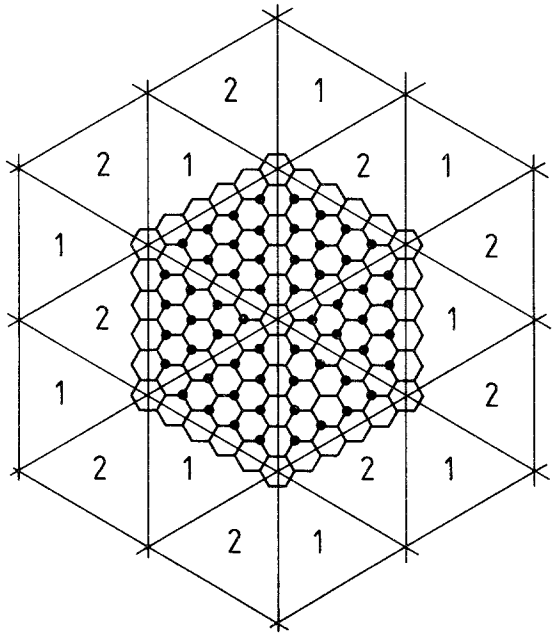

Fig. 25. A typical ground state of alternating "triangles" of occupied sublattice 1 and 2. The length of the triangles is $L=5$; the occupied sites are denoted by dots. The walls separating the different sublattices are indicated by the continuous lines and form a regular triangular lattice.

striped structure with no wall crossings to have a lower energy. A closer look at this layered structure, however, shows that for topological reasons the energy/unit length of *parallel* walls is proportional to $3H-J_3$, implying that in the region of interest ($H\sim J_3$) the stripped structure cannot occur.

Minimizing the (5.12) expression for ε in L, one obtains that L changes continuously with the parameter $\rho=J_3/H$:

$$\rho=1+\frac{2L-1}{(L-1)^2} \tag{5.13}$$

Since L can change only in integer units, the critical value for a change from a commensurate phase characterized by L to one characterized by $L+1$ is

$$\rho_c(L, L+1)=1+2/(L-1), \qquad L>2 \tag{5.14}$$

Now that we have the statistical physical model with the desired property, we turn to the implementation of dynamic CA rules that will have as underlying statics the above-mentioned model. Consider the two

sublattices of the honeycomb lattice and suppose that we move one of these sublattices upward in the time direction (see Fig. 26a). It is clear that the resulting three-dimensional lattice will be a close-packed lattice[57] and that when setting the dynamic rules every spin n_0 will be a function of the spins on the previous time slice only (Fig. 26b):

$$w(n_0 \mid n_1, n_2, n_3; n_4, n_5, n_6) \underset{\alpha \to 0}{=} \alpha^{n_0(n_1+n_2+n_3)} \beta^{n_0(n_4+n_5+n_6)} z^{n_0} / (\alpha^{n_1+n_2+n_3} \beta^{n_4+n_5+n_6} z + 1) \quad (5.15)$$

where $\beta = e^{J_3/kT}$ and $z = e^{H/kT}$.

These rules should reproduce the ground-state structures discussed above; they represent an example of a $(2+1)$-dimensional CA that changes its equilibrium structure. Since the transition between commensurate phases is usually of first order, one may expect the usual interesting dynamical phenomena (especially when $\alpha = 0$) related to long-lived metastable states, creation of domain walls, etc. It seems thus useful to apply in the context of this problem the method of simulated annealing[95]—heating the system ($\alpha > 0$) and then cooling it slowly ($\alpha \to 0$).

From the point of view of cellular automaton theory it would be very nice if one could devise $(1+1)$-dimensional rules that would construct the

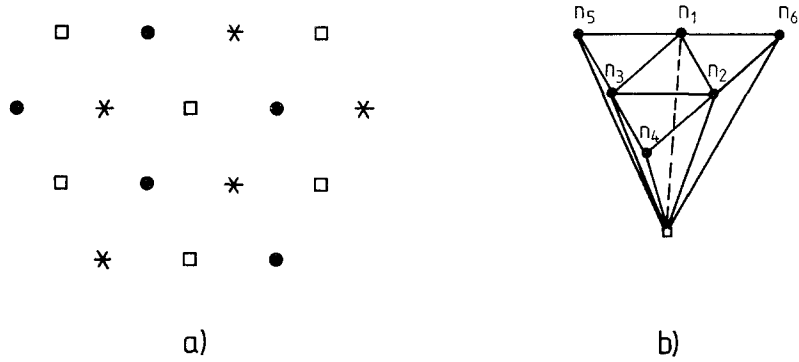

Fig. 26. (a) The updating of the honeycomb lattice happens by alternating in time the sublattices of the honeycomb lattices. An upper view of the resulting lattice is shown: points deoted by crosses, solid circles, and squares form vertically stacked triangular lattices denoted by A, B, and C, respectively. The above considerations apply for any three-dimensional close-packed lattice consisting of vertical sequences A, B, A, B, C,..., the only restriction being that identical triangular lattices cannot be nearest neighbors in the time direction. (b) The dynamic rules: the spin n_0 is set according to the rules (5.15), depending on the values of its one-time-step predecessors, denoted by n_1, n_2, n_3 = nearest neighbors and n_4, n_5, n_6 = third neighbors.

kind of ground-state structure shown in Fig. 25. Such rules are possible, but somewhat artificial—one has to put by hand the horizontal walls by changing the rules every $2L$ time steps.

However, we think that this simple extension of the hcp model is very interesting and it might be of interest in relation to experiments with materials intercalated in graphite.[96] Equation (5.15) provides a very fast algorithm for the numerical study of the static and dynamic properties of this model.

Example 13. A (0+1)-Dimensional Cellular Automaton with Many Limit Cycles. There is, however, a straightforward way of constructing cellular automata with different limit cycles. Let us generalize the dichotomic variables n_i or s_i to some *Q-state* variables, $l_i = 1, 2, ..., Q$, where $Q = q_1 q_2 \times \cdots \times q_k$. Construct a transfer matrix which is a $q_1 \times q_1$ cyclic (but not symmetric) hypermatrix. Every block of the hypermatrix consists again of $q_2 \times q_2$ cyclic hyperblocks, etc. Such a model is an obvious generalization of the *chiral clock model.*[97] The hypercyclic structure involves that the transfer matrix is doubly stochastic and (apart from a trivial norm factor) already describes the dynamics of this general Z_Q model. By changing the values of different couplings (or elements of the matrix), many limit cycles are obtainable.

Another possibility of creating models with different cycles is to use the *decoration* method, as, for example, in the case of the "mock"-ANNNI models.[98] Starting with a checkerboard lattice as shown in Fig. 2 containing only one- and two-spin interactions, decorate every vertical bond with a string of n spins. The interactions along the string are such that by summing up all spins except the two end spins one recovers the original couplings. The dynamics for such a problem can be defined in many ways, either as setting at the same time the whole decorated spin string, or only the last two spins—the CA condition is recovered after summing up first the decorating spins. Such a model can exhibit[98] a large number of commensurate phases (now in the time direction!), corresponding to different limit cycles. We shall not go into details, because such models are rather artificial; we prefer to move toward more interesting models, where the presence of many limit cycles is due to deterministic or random changes in the rules in time and/or space.

Example 14. Hierarchic Linear Models. In this example we try to generalize the notion (and the solution) of linear models treated in Section 3.3 to *inhomogeneous* automata, that is, to automata whose rules change in *space*, but, once fixed, remain the same in time. At the same time, we present a new type of solution for the $(1+1)$-dimensional case, strongly related to the theory of fully developed chaos. For the sake of simplicity,

consider a linear model corresponding to the Glauber choice of transition probabilities[46]:

$$w(s_i|s'_{i-1}, s'_{i+1}) = \frac{1}{2}\left[1 + \frac{\gamma}{2} s_i(s'_{i-1} + s'_{i+1})\right]; \qquad \gamma = \tanh 2K \quad (5.16)$$

where K is the coupling of the one-dimensional Ising model. The order parameter of this model is the magnetization. According to Eq. (3.5), in the magnetization sector one has to diagonalize the matrix [see Eq. (3.5)]

$$2(\lambda/\gamma)\langle s_i\rangle_\lambda = \langle s_{i-1}\rangle_\lambda + \langle s_{i+1}\rangle_\lambda \quad (5.17)$$

where we have used the time generating function

$$\langle s_i\rangle_\lambda = \sum_t \lambda^t \langle s_i\rangle_t$$

and (see Section 2) the relaxation time is given by $\tau = -1/\ln \lambda$. The usual renormalization group approach is to make a decimation both in *space* and *time*. A decimation in space leads to the new coupling constant given by

$$v' = v^2; \qquad v = \tanh K \quad (5.18)$$

which has a stable fixed point at $v = 0$ and an unstable one at $v = 1$. A decimation in time corresponds to eliminating every second unknown in Eq. (5.17), leading to

$$2\frac{\lambda}{\gamma}\left(2\frac{\lambda}{\gamma} - \frac{\gamma}{\lambda}\right)\langle s_i\rangle_\lambda = \langle s_{i-2}\rangle_\lambda + \langle s_{i+2}\rangle_\lambda \quad (5.19)$$

In the *renormalization group interpretation* one has first to express γ in Eq. (5.19) in terms of γ' corresponding to v' of Eq. (5.18) and only then to identify the new frequency λ'. This method allows for the study of the distribution of relaxation times *only* near the fixed points, since during the iterations v moves toward its fixed-point value. We know, however, that the problem is exactly soluble for *any* γ. The alternative approach is to "renormalize" only the dynamics, but not the statics.[99] After decimating the *infinite* set of dynamic equations (5.17), one obtains the same set of equations (γ is now *unchanged*), but with a different λ, given by (5.19). If originally λ was a proper eigenvalue, it must be so after decimation. Introducing $\bar{\omega} = 2(\lambda/\gamma)$, we obtain the mapping induced by the decimation procedure as

$$\bar{\omega}' = \bar{\omega}^2 - 1 \qquad \text{or} \qquad \omega' = 4\omega(1-\omega); \qquad \omega = 2 - 4\bar{\omega} \quad (5.20)$$

leading to the well-known quadratic map for fully developed chaos,[99] whose stationary probability distribution satisfies

$$P(\omega) = \int d\omega' \, P(\omega') \, \delta[\omega - 4\omega'(1-\omega')] \tag{5.21}$$

and is well known.[99] This way one recovers, with minimal effort, the exact *density of relaxation times* at any γ. The main reason why this method works is that the decimation procedure is "incommensurate" with the spectrum of $\{\lambda\}$, so the map (5.20) is like a Poincaré map, and every eigenvalue λ will appear with its correct weight when (5.20) is indefinitely iterated. For analytic (and numerical) studies it is often more convenient to calculate the *integrated probability density*, $\mu(x) = \int_{-\infty}^{x} dy \, P(y)$. The fast convergence is illustrated by a few successive approximations of Eq. (5.21) shown in Fig. 27, for $\gamma = 0.8$. Although we know that the band is $[-\gamma, \gamma]$, we deliberately started with a flat distribution $P(\bar{\omega})$ in the interval $[-1, 1]$. The points inside the band are trapped there; the points outside the band

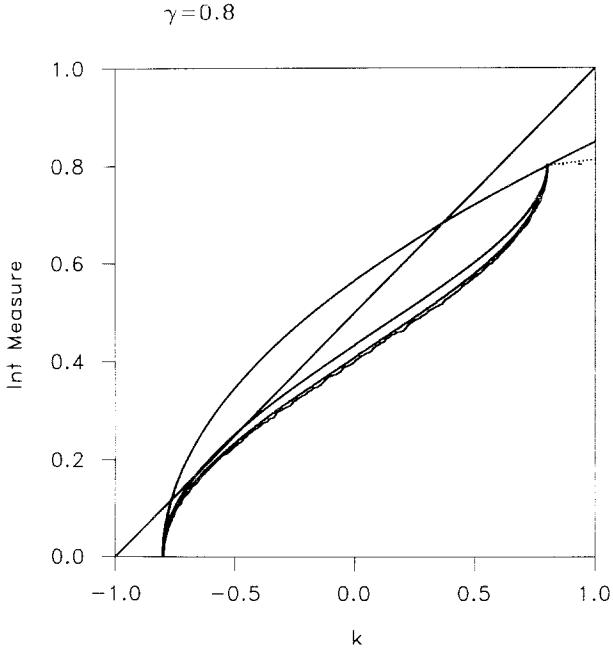

Fig. 27. The integrated density of relaxation times: the numerical iteration of Eq. (5.21) for $\gamma = 0.8$. The original probability density is a flat distribution defined on the interval $[-1; +1]$; its integrated measure is linear. In a few iterations, shown by the consecutive lines, the exact result is reached. Note that the points lying outside the band $[-\gamma; \gamma]$ will escape to $+\infty$; this explains why μ is less than 1.

are iterating to $+\infty$, as clearly shown in Fig. 27. Therefore, even if we had not known in advance the extension of the band, the numerical iteration of Eq. (5.21) shows it clearly.

Let us next consider the possible extensions of this method for the more general case when γ is some function of the space site index i, so that instead of (5.17) one has

$$2\frac{\lambda}{\gamma(i)}\langle s_i\rangle_\lambda = \langle s_{i-1}\rangle_\lambda + \langle s_{i+1}\rangle_\lambda \tag{5.22}$$

Note that such a choice is possible because in the linear model under consideration $w(s_i|s'_{i-1}, s'_i, s'_{i+1})$ depends in general on four independent parameters, two of them fixed by the linear model condition (3.4). Equation (5.22) is equivalent to a one-dimensional tight-binding Anderson model, to a Schrödinger equation with inhomogeneous potentials, or to a harmonic chain with different masses. A decimation transformation will not preserve, in general, the form (5.22) if $\gamma(i-1)\neq\gamma(i+1)$. The most general structure still invariant under such a decimation procedure is the hierarchical lattice shown in Fig. 28. Note that $\gamma(i)$ may assume now n different values on a lattice consisting of 2^n lattice sites. Following the notation of Fig. 28, let us number this set of values by the order of iteration: $\gamma_0, \gamma_1, \ldots, \gamma_m, \ldots$. By eliminating all $\langle s_i\rangle_\lambda$ variables corresponding to γ_0 values, one obtains a new set of equations similar to (5.19), but involving γ_0 and γ_m. The dynamic renormalization is achieved by assigning to each such equation a "frequency" equal to $2\lambda'/\gamma_{m-1}$. Supposing that the original lattice was infinite, the whole set of equations (5.22) is recovered in this way. The resulting map is

$$\lambda'(m) = \lambda^2(\gamma_{m-1}/\gamma_0\gamma_m) - \gamma_{m-1}; \qquad m = 1, 2, \ldots \tag{5.23}$$

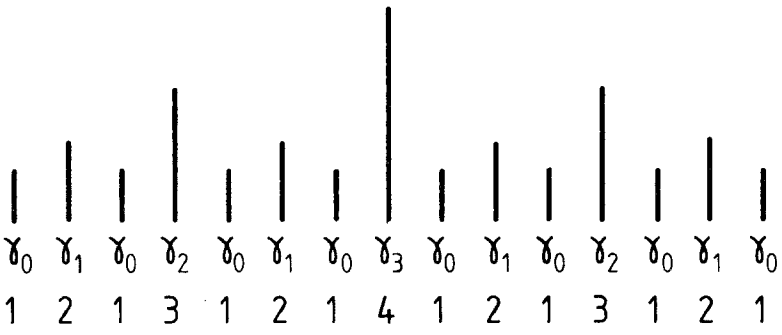

Fig. 28. The hierarchic structure: the dynamic variables are eliminated in the order indicated.

Note that (5.23) is a *multivalued map*: if λ was a proper eigenvalue of the infinite set of equations (5.22), then every $\lambda'(m)$ must be also an eigenvalue, but with the weight 2^{-m}! Except for the hierarchical structure, there is no further condition on the distribution of $\{\gamma_m\}$. For a given distribution (random or deterministic) $R(\{\gamma_m\})$ of the parameters γ_m the stationary distribution of the map (5.23) is given by the iteration of the following integral equation:

$$P(\lambda) = \int d\lambda' \, P(\lambda') \int \prod_m d\gamma_m \, R(\{\gamma_m\}) \sum_{m=1}^{\infty} 2^{-m} \delta\left(\lambda - \lambda'^2 \frac{\gamma_{m-1}}{\gamma_0 \gamma_m} - \gamma_{m-1}\right) \quad (5.24)$$

Again, instead of the density of relaxation times $P(\lambda)$, it is sometimes more convenient to consider the *integrated measure* $\mu(\lambda)$:

$$\mu(\lambda) = \int_{-\infty}^{\lambda} d\lambda' \, P(\lambda')$$

which provides a powerful tool for obtaining the *full density of relaxation times*. A rough attempt at such an iteration is shown in Fig. 29 for $\gamma_0 = 0.7$ and using $\gamma_i = (\gamma_{i-1} + \Delta)/(1 + \gamma_{i-1}\Delta)$ as a deterministic rule ($\Delta = 0.4$). In contrast to Fig. 27, many points *inside* the physical interval $[-1, 1]$ are escaping out because the branches of the four-valued map shown in Fig. 29a are not fully chaotic any longer: the spectrum also has a continuous-singular component.

In spite of this complicated behavior, the dynamic phase transitions occurring in such a system can be understood using physical arguments analogous to the Lifschitz theory of fluctuating states or to the mechanism of Griffiths singularities in disordered systems. If some of the "barriers" γ_m are very close to one, the corresponding relaxation times are very long: they provide the most important contributions to the density of states near the upper edge ($\lambda_c = 1$) of the "band" of relaxation times. If, in addition, the probability of occurrence (weight) of such barriers is known, one can write down the tail of the density of states as the weighted sum of such contributions. By changing some parameters, the form of the band tail may change, thus inducing a dynamic phase transition, where the long-time behavior changes from an exponential decay to an algebraic decay.[39] The interest reader is refered to the references in question for further details.

Equation (5.22) can be rewritten also in a transfer-matrix form

$$\begin{bmatrix} \langle s_{i+1} \rangle_\lambda \\ \langle s_i \rangle_\lambda \end{bmatrix} = T_i \begin{bmatrix} \langle s_i \rangle_\lambda \\ \langle s_{i-1} \rangle_\lambda \end{bmatrix}; \qquad T_i = \begin{bmatrix} 2\lambda/\gamma(i) & -1 \\ 1 & 0 \end{bmatrix} \quad (5.25)$$

If λ is an eigenvalue, then one has

$$\begin{bmatrix} \langle s_{N+1} \rangle_\lambda \\ \langle s_N \rangle_\lambda \end{bmatrix} = \left(\prod_{i=1}^{N} T_i \right) \begin{bmatrix} \langle s_2 \rangle_\lambda \\ \langle s_1 \rangle_\lambda \end{bmatrix} \quad (5.26)$$

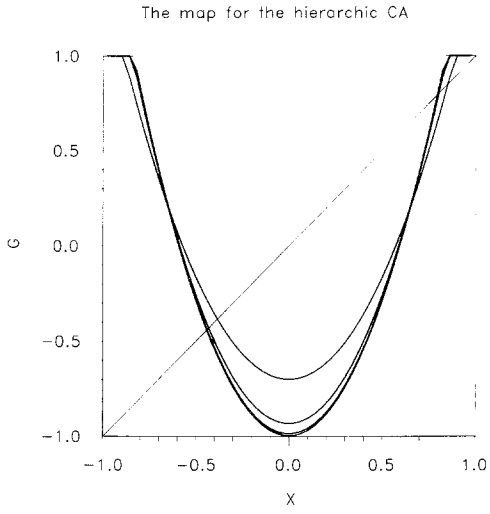

(a)

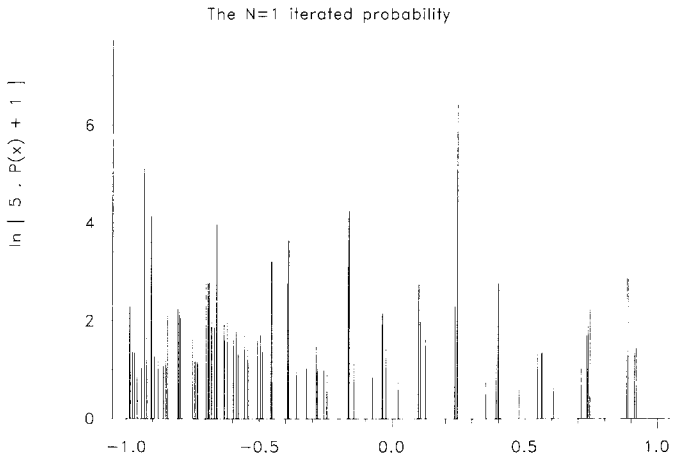

(b)

Fig. 29. Three consecutive iteration steps of Eq. (5.24) for $\gamma_0 = 0.7$, $\Delta = 0.4$. Note that the four branches of the map (a) do not correspond to fully developed chaos. This means that many points from the $[-\gamma_0; \gamma_0]$ interval can now escape (b–d). See also the "tail" structure near the point $\lambda = -1$. Further iterations are necessary to establish the full spectrum.

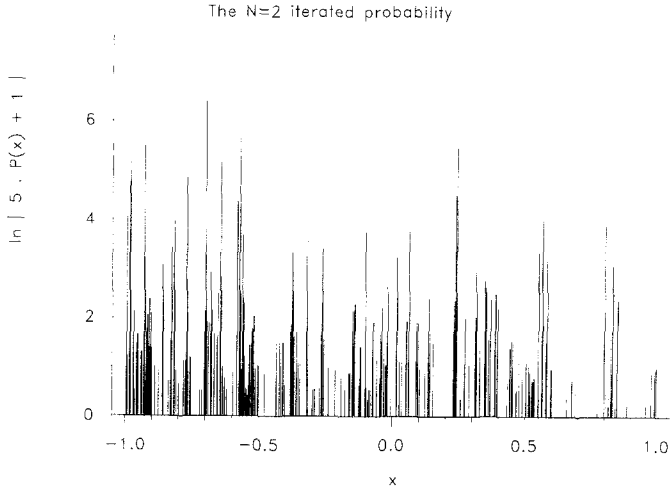

(c)

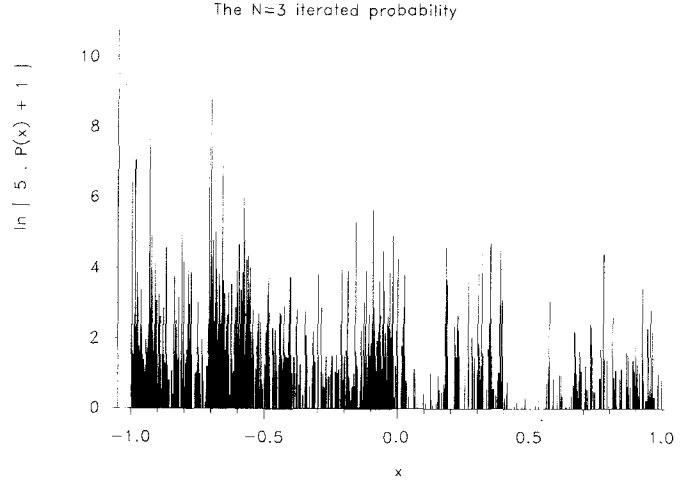

(d)

Fig. 29 (*continued*)

An alternative way of solving for the spectrum is to use the node-counting theorem to calculate the integrated density of states $\mu(\lambda)$ by counting the number of sign changes of $\langle s_i \rangle_\lambda$ during the iteration (5.25). This method is more flexible than the decimation procedure when dealing with different deterministic or random distributions of $\gamma(i)$'s. However, for the hierarchic structure shown in Fig. 28, Eq. (5.19) seems to be conceptually simpler and has a better convergence rate, due to the large number of sites eliminated in one iteration step.

Example 15. (0+1)-Dimensional Cellular Automaton Networks with Time-Dependent Rules. In this last example we consider the dynamics of one-site automaton, whose rules are set in different time steps by the output of a parallel [also $(0+1)$-dimensional] automaton. This is the simplest possible example of a functionally hierarchic network of automata. Let us call the "driver" the automaton setting up the rules for the "slave." The slave automaton has a transition matrix

$$P_\tau = \begin{bmatrix} a(\tau) & 1-b(\tau) \\ 1-a(\tau) & b(\tau) \end{bmatrix} \tag{5.27}$$

corresponding to the (time-dependent) weight

$$w_\tau(1 \mid n') = 1 - a(\tau) + [b(\tau) - a(\tau) + 1]n'; \qquad n' = 0, 1$$

where the parameters $\{a(\tau), b(\tau)\}$ are given by the output of the driver automaton running one time step ahead. If the driver automaton is deterministic, one may call it a *substitutional* automaton; if the driver is a probabilistic one, one has a *quenched* automaton. The quantity of interest, which enters in the calculation of all stationary properties, is the *limit distribution* of the product matrix

$$P_\infty = \lim_{\tau \to \infty} \prod_\tau P_\tau \tag{5.28}$$

Examples of deterministic drivers are the Morse sequences and generalizations,[100] which have recently attracted a great deal of interest.[101] In all these cases it is possible to define an "alphabet" consisting of two (or more) different matrices P_a and P_b (two possble dynamic rules). One builds up words going from right to left—because of the matrix product properties—according to some simple substitution rules. The Morse sequence can be constructed in many different ways: one way is to take a given word and to concatenate (to its left) the complementary word obtained by interchanging P_a and P_b. This is done until one obtains an

infinite word X, which is invariant under this operation. A different way is to define the substitution

$$\sigma(P_a) = P_b P_a; \qquad \sigma(P_b) = P_a P_b; \qquad X = \lim_{n \to \infty} \sigma^{(n)}(P_a) \tag{5.29}$$

Similarly, one can define other substitutions, some corresponding to incommensurate (quasiperiodic) sequences, which were studied very actively recently in connection with quasicrystals. For a one-dimensional Penrose tiling the substitution rules are

$$\sigma(P_a) = P_b P_a; \qquad \sigma(P_b) = P_b P_b P_a \tag{5.30}$$

A different possibility for this particular substitution is to use the Fibonacci sequence generated by the automaton given in Example 2.[102]

These deterministic models can be treated by a properly defined renormalization group transformation and usually display a very complicated phase diagram at $T = 0$, with infinitely many ground states.[103] In terms of the substitution rules, the different ground states of these models are represented in terms of our stochastic matrices (the product of two stochastic matrices is also a stochastic matrix) as

$$\sigma^{(k)}(P_a) = \sigma_x \text{ or } \mathbf{e}; \qquad \sigma^{(k)}(P_b) = \sigma_x \text{ or } \mathbf{e} \tag{5.31}$$

where $\sigma^{(k)}$ means the kth iteration of the substitution, while σ_x and $\mathbf{e}$ are the Pauli matrix and the unit matrix, respectively. In linear $(1+1)$-dimensional CA one may use again the substitution rules for the set $\{\gamma(i)\}$ in Eq. (5.22). We note here that exactly this type of equation has been discussed for a "Fibonacci" driver in Ref. 102.

The situation is quite similar for *randomly* driven automata, which can choose independently at every time step from, say, two set of rules with some given (quenched) probability. The driving automaton is in this case a quasirandom number generator.[11] There is here a subtle point perhaps worth mentioning. Suppose one has a one-dimensional Ising model with quenched randomness; for example, the energy coupling J has the distribution $R(J_i) = p\delta(J - J_0) + (1-p)\,\delta(J + J_0)$. In the statistical mechanical problem the partition function is given by the trace of a product such as (5.28) of (2×2) transfer matrices. Although each transfer matrix can be separately mapped into a stochastic matrix, this does not solve the problem for a random product of such matrices: two new types of diagonal matrices (corresponding to the two different left eigenvectors) appear whenever there is a change from a suite of P_a's to a suite of P_b's and vice versa. The random chain problem can be discussed also from a "dynamic" point of view.[37,38] A mapping between statistical physics and

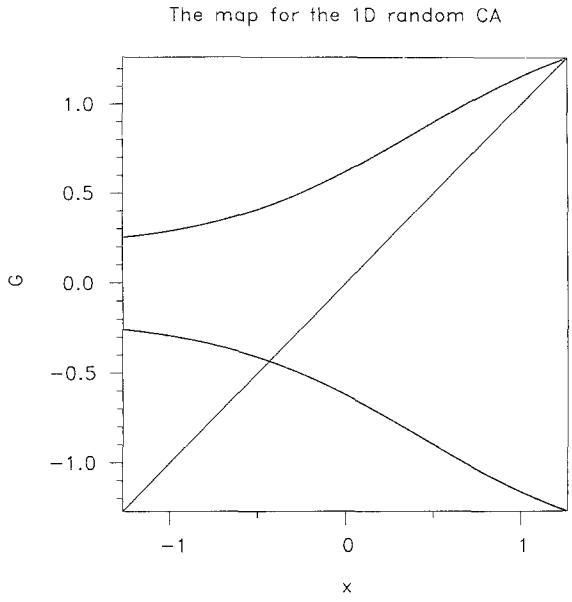

(a)

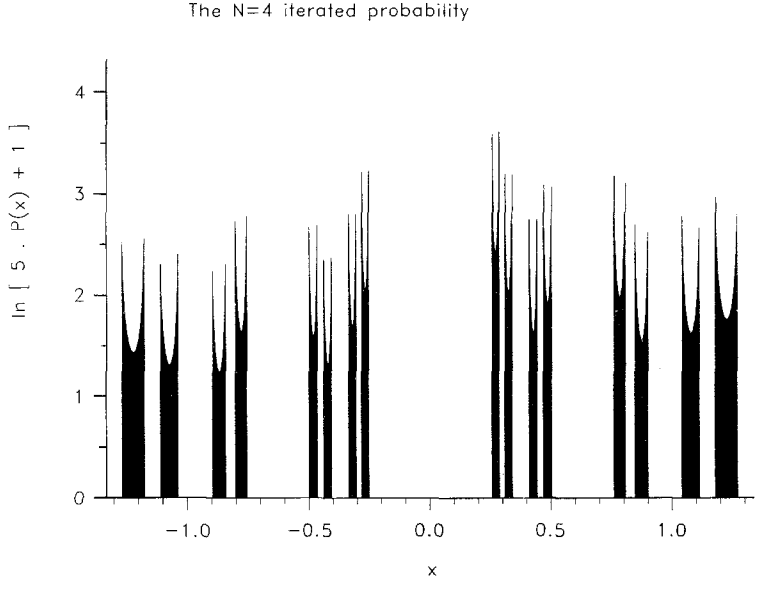

(b)

Fig. 30. Constructing the limit distribution $P(x)$ defined by the recursion (5.32).[37,38] (a) For the map shown here ($a_1 = 0.9525745 = 1 - a_2$, $b_1 = 0.4013122 = 1 - b_2$) a Cantor support is obtained. The probability of finding the matrix P_a (upper branch of the map) is $p = 0.6$. (b) The fourth iterated $P(x)$, starting from a flat distribution. (c) The support is the whole interval for the map shown here (same $a_{1,2}$ as before, $b_{1,2}$ are interchanged) but (d) the distribution is still singular after four iteration steps. Note that $\ln[5P(x) + 1]$ is plotted.

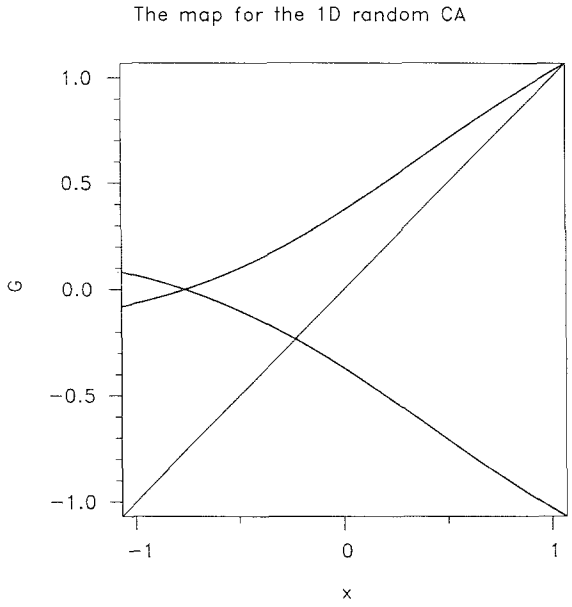

(c)

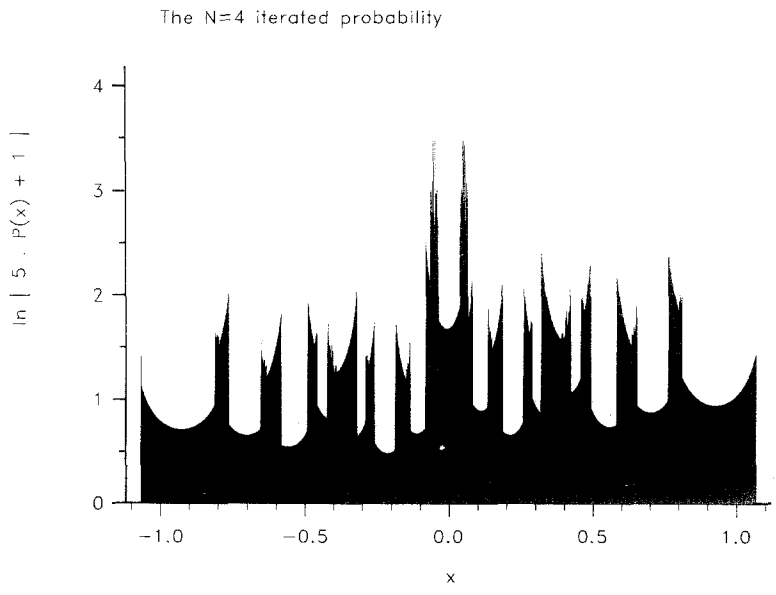

(d)

Fig. 30 (*continued*)

stochastic matrices (CA) can be most easily done by requiring that the two-valued $\mapsto$ induced by the right iteration

$$P_\tau \begin{bmatrix} 1 \\ \exp(-2x) \end{bmatrix} \sim \begin{bmatrix} 1 \\ \exp(-2x') \end{bmatrix} \tag{5.32}$$

is the same as for the statistical physical model. In Figs. 30a and 30c we show the two maps one obtains, respectively, for the values

$$a_1 = 0.952575 = 1 - a_2, \qquad b_1 = 0.4013122 = 1 - b_2$$

and

$$a_1 = 0.952575 = 1 - a_2, \qquad b_2 = 0.4013122 = 1 - b_1$$

which are similar to maps one obtains for the random-energy Ising model in an external field. The probability of choosing the upper branch is $p = 0.6$. Starting from a flat distribution, one obtains after four iterations the distributions shown in Figs. 28b and 28d. A change from a fractal support to a support over the whole confining interval is evident. The limit probability distribution is, however, highly nonanalytic in both cases. The one-dimensional random-energy Ising model in a field has an infinte number of phase transitions at $T = 0$ for the critical field values $H_c = 2J_0/n$, $n > 0$ is integer. Physically, this corresponds to the condition that the energy required to flip a cluster of n down-spins in the direction of the field vanishes. A similar phenomena will happen for the CA (5.29). Note that this kind of "spreading" of the probability distribution has been identified recently also for the Kauffman model[104] of cell differentiation when a probabilistic element is added to the original rules (chose at random in *space* one of all possible deterministic rules involving a fixed number of neighbors and iterate in time according to the chosen rules). The behavior of such automata is very similar to those of spin glasses.[105]

6. CONCLUSIONS: THE PROBABILISTIC COMPUTER

This paper has two distinct parts: in the first part we explained the analogy between the transfer matrix formalism for short-range statistical mechanical models and the discrete time-developing operator of cellular automata. Viewed from this perspective, cellular automata are a special class of statistical mechanical models obeying the restriction (2.11). The bulk and surface properties of these statistical models correspond to long-time (stationary) and transient dynamic behavior, respectively, of probabilistic cellular automata. Deterministic, or almost deterministic, automata correspond to special configuration constraints or special ways

to take the $T \to 0$ limit in the statistical physical models. Many standard methods of statistical mechanics can thus be used in understanding and predicting the temporal behavior of cellular automata. Some exact results were derived in Section 3, including a discussion of "disorder"-like solutions, fully integrable models, duality transformations, etc. Possible mechanisms of phase transitions have been reviewed following the known classification of stochastic matrices; the "universality" of such a mechanism has been tested in Section 4.

In the Second part of this paper I have tried to show how statistical physics can be used to devise different dynamic rules whose behavior is totally or partially known in advance. Along the path I have presented some intriguing examples that are the subject of further research, while other examples seem to have direct practical applications. I consider this work as a first step toward a much more ambitious program, namely the design of a fully parallel, probabilistic machine. In setting up this goal we have first to define what we expect from such a machine and what specific tasks cannot be achieved by other means. From the beginning it is clear that the main emphasis here is not on the speed of *numerical* calculations, not even on their precision. What we want is a new *organizational principle*, leading to a qualitatively different, intelligent machine. After all, we are also probabilistic "machines," and understanding the functional basis of such highly hierachical, parallel networks might help also understand the way *we* think. The main requirement on this new type of machine must be the ability to learn. This implies a decentralized structure which tries different avenues[106] in solving a given problem, treating its own structure (architecture) on an equal footing with programs and data, and storing the optimal solution. I think here of different layers of cellular automata, running in parallel at different levels, some creating "wires" (see Figs. 19 and 21), some transporting information along the wires, and finally some executing operations when wires "meet." This requires also a completely new concept of memory—a memory that is not labeled with addresses, but where information is locally stored and retrieved according to its level of processing and its content. The memory might have a layered structure in itself, giving in one end an *abstract* classification of data, while still being able to recover on the other end the full details of the particular objects with which it is presented.

For the moment all this is only little more than speculation—and physics is not especially fond of speculation. My belief is that a gradual approach, solving parts of the problem at a time, is possible. On the other hand, it is not hard to predict that statistical physics will play an increasingly relevant role in neurobiology, computer science, and related fields.

ACKNOWLEDGMENTS

Working out and writing this paper took me much longer than is usually admissible. I apologize to my family for being an always absent father and husband and I thank Director J. Villain for his understanding.

I learned a great deal from discussions with many people, especially B. Derrida, E. Domany, H. Falk, H. Hartman, J. M. Maillard, G. Marx, J. Oitmaa, and D. Stauffer. Among them, I am, however, most indebted to Wolfgang Kinzel, who introduced me to the fascinating field of cellular automata and to Michel Kerszberg, who constantly challenged my views on physics, physicists, and Nature. I am grateful to W. Wolff for a careful reading of the manuscript.

REFERENCES

1. J. von Neumann, *Theory of Self-Reproducing Automata* (edited and completed by A. W. Burks) (University of Illinois Press, 1966).
2. E. F. Codd, *Cellular Automata* (Academic Press, 1968); A. W. Burks, *Essays on Cellular Automata* (University of Illinois Press, 1970).
3. L. Bienenstock, F. Fogelman, and G. Weisbuch (eds.), *Disordered Systems and Biological Organization* (Springer-Verlag, 1986); D. J. Depew and B. H. Weber (eds.), *Evolution at a Crossroads* (MIT Press, 1985); R. L. Dobrushin, V. I. Kryukov, and A. L. Toom (eds.), *Locally Interacting Systems and their Application in Biology* (Springer-Verlag, 1978); B. Batchelor (ed.), *Pattern Recognition* (Plenum Press, 1978); T. Poggio, V. Torre, and C. Koch, *Nature* **317**:314 (1985), and references therein.
4. J. E. Hopcroft and J. D. Ullman, *Introduction to Automata Theory, Languages, and Computation* (Addison-Wesley, 1979); F. Fogelman-Soulie, Y. Robert, and M. Tschuente (eds.), *Automata Networks in Computer Science, Theory and Applications* (Manchester University Press, 1986); R. Vollmar, *Algorithmen in Zellularautomaten* (B. G. Teubner Verlag, Stuttgart, 1979).
5. S. Wolfram, *Theory and Applications of Cellular Automata* (World Scientific, 1986).
6. S. Wolfram, *Rev. Mod. Phys.* **55**:601 (1983); G. Y. Vichniak, in *Disordered Systems and Biological Organization*, L. Bienenstock, F. Fogelman, and G. Weisbuch, eds. (Springer-Verlag, 1986).
7. H. J. Hilhorst, A. F. Bakker, C. Bruin, A. Compagner, and A. Hoogland, *J. Stat. Phys.* **34**:987 (1984); H. Herrmann, in *Proceedings of the Statphys' 16* (North-Holland, 1986).
8. W. A. Little, *Math. Biosci.* **19**:101 (1974); W. A. Little and G. L. Shaw, *Math. Biosci.* **39**:281 (1978); J. J. Hopfield, *Proc. Natl. Acad. Sci. USA* **79**:2554 (1982); P. Peretto, *Biol. Cybern.* **50**:51 (1984); D. J. Amit, H. Gutfreund, and H. Sampolinsky, *Phys. Rev. A* **32**:1007 (1985).
9. E. Domany, R. Meir, and W. Kinzel, *Europhys. Lett.* **2**:175 (1986); E. Domany and R. Meir, to be published.
10. B. A. Huberman and T. Hogg, *Phys. Rev. Lett.* **52**:1024 (1984); *J. Stat. Phys.* **41**:115 (1985); U.S. Patent No. 4591980; D. d'Humieres and B. A. Huberman, *J. Stat. Phys.* **34**:361 (1984).
11. T. G. Lewis and W. H. Payne, *J. Assoc. Comput. Mach.* **20**:456 (1973); S. Kirkpatrick and E. P. Stoll, *J. Comp. Phys.* **40**:517 (1981).

12. M. H. Kalos, *Phys. Rev.* **128**:1781 (1962); D. M. Ceperley and M. H. Kalos, in *Monte Carlo Methods in Statistical Physics*, K. Binder, ed. (Springer, 1979); J. H. Hetherington, *Phys. Rev. B* **30**:2713 (1984).
13. J. Hardy, O. de Pazzis, and Y. Pomeau, *J. Math. Phys.* **14**:470 (1973); U. Frisch, B. Hasslacher, and Y. Pomeau, *Phys. Rev. Lett.* **56**:1505 (1986); D. d'Humieres, P. Lallemand, and U. Frisch, *Europhys. Lett.* **2**:291 (1986).
14. Y. Pomeau, *J. Phys. A* **17**:L415 (1984).
15. G. Vichniac, in *Theory and Applications of Cellular Automata*, S. Wolfram, ed. (World Scientific, Singapore, 1986).
16. H. Herrmann, *J. Stat. Phys.* **45**:154 (1986).
17. E. Goles and G. Y. Vichniac, *J. Phys. A* **19**:L961 (1986).
18. D. A. Ackley, G. E. Hinton, and T. J. Sejnowski, *Cognitive Sci.* **9**:147 (1985); G. E. Hinton, T. J. Sejnowski, and D. A. Ackley, Boltzmann machines: Constraint satisfaction networks that learn, Technical Report CMU-CS-84-119, Carnegie-Mellon University (May 1984).
19. R. J. Baxter, *Exactly Solved Models in Statistical Mechanics* (Academic Press, 1982).
20. O. Perron, *Math. Ann.* **64**:248 (1907); S. B. Frobenius, *Preuss. Akad. Wiss.* 471 (1908); E. Seneta, *Non-negative Matrices* (Wiley, 1973); P. Ròzsa, *Linear Algebra and Applications* (Müszaki Kiadò, 1974) (in Hungarian).
21. H. A. Kramers and G. H. Wannier, *Phys. Rev.* 60:263 (1941); R. J. Baxter, *J. Stat. Phys.* **19**:461 (1978); P. Rujàn, *Physica A* **96**:379 (1979); R. J. Baxter and P. J. Forrester, *J. Phys. A* **17**:2675 (1984).
22. F. Haake and K. Thol, *Z. Phys. B* **40**:219 (1980).
23. C. Domb and M. S. Green (eds.), *Phase Transitions and Critical Phenomena*, Vol. 6 (Academic Press, 1976).
24. P. Nightingale, *J. Appl. Phys.* **53**:7927 (1982); H. H. Roomany and H. W. Wyld, *Phys. Rev. D* **21**:3341 (1980).
25. M. N. Barber, in *Phase Transitions and Critical Phenomena*, Vol. 8, C. Domb and J. L. Lebowitz (eds.) (Academic Press, 1983).
26. F. Alcaraz, M. N. Barber, J. Kuti, and P. Rujàn, to be published.
27. P. Rujàn, in *Non-linear Equations in Classical and Quantum Field Theory*, N. Sanchez, ed. (Springer-Verlag, 1985), p. 286; J. M. Maillard, in *Proceedings of the 2nd UC Conference on Statistical Physics* (March 26–29 1986, Davis, California).
28. C. H. Bennett and G. Grinstein, *Phys. Rev. Lett.* **55**:657 (1985).
29. H. A. Kramers and G. H. Wannier, *Phys. Rev.* **60**:252 (1941).
30. W. Kinzel, *Z. Phys. B* **60**:205 (1985).
31. G. Grinstein, C. Jayaprakash, and Y. He, *Phys. Rev. Lett.* **55**:2527 (1985).
32. S. Redner, *J. Stat. Phys.* **25**:15 (1981).
33. Z. Ràcz, *Phys. Rev. B* **21**:4012 (1980); R. J. Baxter, I. G. Enting, and S. K. Tsang, *J. Stat. Phys.* **22**:465 (1980).
34. S. J. Chang and J. Wright, *Phys. Rev. A* **23**:1419 (1981).
35. S. Wolfram, *Commun. Math. Phys.* **96**:15 (1984).
36. M. Gardner, *Sci. Am.* **223**(4):120 (1970); E. R. Berlekamp, J. H. Conway, and R. K. Guy, *Winning Ways*, Vol. 2 (Academic Press, 1982); M. Gardner, *Wheels, Life and Other Mathematical Amusements* (Freeman, 1982).
37. P. Grassberger, *Physica D* **10**:52 (1984).
38. C. Fan and B. McCoy, *Phys. Rev.* **182**:614 (1969); J. F. Fernandez, *Phys. Rev. B* **16**:5125 (1977); R. Bruinsma and G. Aeppli, *Phys. Rev. Lett.* **50**:1494 (1983); G. Györgyi and P. Rujàn, *J. Phys. C* **17**:4207 (1984).
39. C. L. Henley, *Phys. Rev. Lett.* **54**:2030 (1985); D. Kutasov, A. Aharony, E. Domany, and

W. Kinzel, *Phys. Rev. Lett.* **56**:2229 (1986); A. Maritan and A. L. Stella, *J. Phys. A* **19**:L269 (1986).
40. Z. Ràcz, *Phys. Rev. Lett.* **55**:1707 (1985); Z. Ràcz and M. Plischke, *Acta Phys. Hung.* (May 1987).
41. J. Marro, J. L. Lebowitz, H. Spohn, and M. H. Kalos, *J. Stat. Phys.* **38**:725 (1985).
42. P. C. Hohenberg and B. I. Halperin, *Rev. Mod. Phys.* **49**:435 (1977).
43. F. Y. Wu, Unpublished results.
44. R. Balian and G. Toulouse, *Ann. Phys. (N.Y.)* **83**:28 (1974).
45. T. D. Lee and C. N. Yang, *Phys. Rev.* **87**:410 (1952); M. E. Fisher, *Phys. Rev. Lett.* **40**:1610 (1978); D. A. Kurtze, *J. Stat. Phys.* **30**:15 (1983).
46. R. J. Glauber, *J. Math. Phys.* **4**:294 (1963); B. U. Felderhof, *Rep. Math. Phys.* **1**:215 (1972); **2**:151 (1972); E. Siggia, *Phys. Rev. B* **16**:2319 (1979); see also H. Falk, *J. Math. Phys.* **26**:692 (1985).
47. W. Kinzel and J. Yeomans, *J. Phys. A* **14**:L163 (1981).
48. H. Yahata, *Prog. Theor. Phys.* **52**:871 (1974); T. Schneider, M. Zannetti, and R. Badii, *Phys. Rev. B* **31**:2941 (1985); T. Schneider and M. Schwartz, *Phys. Rev. B* **31**:7484 (1985).
49. E. Domany and J. E. Gubernatis, *Phys. Rev. B* **32**:3354 (1985); A. Aharony, E. Domany, R. M. Hornreich, T. Schneider, and M. Zannetti, *Phys. Rev. B* **32**:3358 (1985).
50. E. Domany and W. Kinzel, *Phys. Rev. Lett.* **53**:311 (1984).
51. C. J. Hamer, *J. Phys. A* **15**:L675 (1982); H. Takano and Y. Saito, *Prog. Theor. Phys.* **73**:1369 (1985).
52. B. J. Adler and T. E. Wainwright, *Phys. Rev.* **127**:359 (1962); J. Orban and A. Bellemans, *J. Chem. Phys.* **49**:363 (1968); K. Binder and L. P. Landau, *Phys. Rev. B* **21**:1941 (1980).
53. J. Stephenson, *J. Math. Phys.* **11**:420 (1970); *Can. J. Phys.* **48**:2118 (1970); *Phys. Rev. B* **1**:4405 (1970).
54. T. R. Welberry and G. H. Miller, *J. Appl. Cryst.* **6**:87 (1973); **8**:636 (1982); *Acta Cryst. A* **34**:120 (1978).
55. I. Peschel and V. J. Emery, *Z. Phys. B* **43**:241 (1981); J. Kurmann, H. Thomas, and G. Müller, *Physica A* **112**:235 (1982).
56. I. G. Enting, *J. Phys. A* **10**:1023, 1737 (1977); **11**:555, 2001 (1978); A. M. W. Verhagen, *J. Stat. Phys.* **15**:219 (1976); P. Rujàn, *J. Stat. Phys.* **29**:231, 247 (1982); **43**:615 (1984); I. Peschel and F. Rys, *Phys. Lett. A* **91**:187 (1982); R. J. Baxter, *J. Phys. A* **17**:L911 (1984).
57. E. Domany, *Phys. Rev. Lett.* **52**:871 (1984).
58. M. T. Jaeckel and J. M. Maillard, *J. Phys. A* **18**:641,2271 (1985); F. Y. Wu, *J. Stat. Phys.* **40**:613 (1985).
59. W. Selke, in *Lecture Notes in Physics*, Vol. 206, A. Pekalski and J. Sznajd, eds. (Springer-Verlag, 1984).
60. P. Rujàn, *J. Stat. Phys.* **29**:231,247 (1982); **43**:615 (1984).
61. D. Dhar, *Phys. Rev. Lett.* **49**:959 (1982); **51**:853 (1983).
62. V. Hakim and J. P. Nadal, *J. Phys. A* **16**:L213.
63. B. Derrida and J. P. Nadal, *J. Phys. (Paris) Lett.* **45**:L701 (1984).
64. J. M. Maillard and R. Rammal, *J. Phys. A* **16**:353; **18**:833 (1985).
65. I. G. Enting, *J. Phys. A* **11**:2001 (1978); A. Georges, D. Hansel, P. Le Doussal, and J. M. Maillard, *J. Phys. A* **19**:L329,1001 (1986).
66. D. Dhar and J. M. Maillard, *J. Phys. A* **18**:L383 (1985).
67. M. Y. Choi and B. A. Huberman, *J. Phys. A* **17**:L765 (1984).
68. C. Fan and F. Y. Wu, *Phys. Rev.* **179**:560 (1969); E. Müller-Hartmann and J. Zittartz, *Z. Phys. B* **27**:261 (1977); J. Villain and P. Bak, *J. Phys. (Paris)* **42**:657 (1981).
69. J. L. Cardy, *J. Phys. A* **15**:L593 (1982).

70. R. Savit, *Rev. Mod. Phys.* **52**:453 (1980).
71. H. Giacomini, *J. Phys. A* **18**:1499,1505,1579 (1985).
72. I. M. Krichever, *Funct. Anal. Appl. Math.* **15**:92 (1981); K. Sogo, M. Uchimani, Y. Akutsu, and M. Wadati, *Prog. Theor. Phys.* **68**:508 (1982); J. M. Maillard and T. Garel, *J. Phys. A* **17**:1251,1257 (1984).
73. A. B. Zamolodchikov, *Commun. Math. Phys.* **69**:165 (1979); **79**:489 (1981); M. T. Jaeckel and J. M. Maillard, *J. Phys. A* **15**:1309 (1982).
74. W. Kinzel, in *Percolation Structures and Processes*, G. Deutscher, R. Zallen, and J. Adler, eds. (Adam Hilger, Bristol, 1983).
75. L. S. Schulmann and P. E. Seiden, *J. Stat. Phys.* **27**:83 (1982); H. Gutowitz, J. Victor, B. Knight, *Physica D*, to be published.
76. H. Falk, *Physica A* **119**:580 (1983).
77. J. Kogut, *Rev. Mod. Phys.* **51**:659 (1979).
78. A. Patkós and P. Rujàn, *J. Phys. A* **18**:1765 (1985).
79. F. Beleznay, *J. Phys. A* **19**:551 (1986).
80. H. W. Blötte and H. J. Hilhorst, *J. Phys. A* **15**:L631 (1982); B. Nienhuis, H. J. Hilhorst, and H. W. Blötte, *J. Phys. A* **17**:3559 (1984).
81. P. Rujàn and A. Patkós, *Phys. Lett. B* **129**:437 (1983).
82. E. Jen, *J. Stat. Phys.* **43**:243 (1986).
83. E. H. Lieb and F. Y. Wu, in *Phase Transitions and Critical Phenomena*, C. Domb and M. S. Green, eds. (Academic Press, 1972); P. W. Kasteleyn, in *Fundamental Problems in Statistical Mechanics III*, E. G. D. Cohe, ed. (North-Holland, 1975).
84. M. Creutz, *Ann. Phys. (N.Y.)* **167**:62 (1986).
85. M. Novotny, *J. Appl. Phys.* **53**:7997 (1982).
86. Y. Aharonov and M. Schwartz, *Phys. Rev. Lett.* **48**:1137 (1982); *Phys. Lett. B* **157**:57 (1985); in *Quantum Concepts in Space and Time*, O. Penrose, ed. (Oxford Press, 1986).
87. P. Rujàn and M. Schwartz, to be published.
88. J. W. Essam, in *Phase Transitions and Critical Phenomena*, Vol. 2, C. Domb and M. S. Green, eds. (Academic Press, 1972); D. Stauffer, *Phys. Rep.* **54**:1 (1979).
89. M. Minsky and S. Papert, *Perceptrons* (MIT Press, 1969).
90. P. Bak, *Rep. Prog. Phys.* **45**:587 (1982).
91. V. L. Pokrovsky and G. V. Uimin, *J. Phys. C* **11**:3535 (1978); J. Hubbard, *Phys. Rev. B* **17**:494 (1978); S. Aubry, in *Solitons and Condensed Matter Physics*, A. R. Bishop and T. Schneider, eds. (Springer-Verlag, 1979); P. Bak and R. Bruinsma, *Phys. Rev. Lett.* **49**:249 (1982).
92. B. Derrida, Y. Pomeau, and J. Vannimenus, *J. Phys. C* **11**:4749 (1978).
93. J. Kanamori, *J. Phys. Soc. Japan* **53**:250 (1984).
94. J. Villain, *Ferroelectrics* **66**:143 (1986).
95. S. Kirkpatrick and G. Toulouse, *J. Phys. (Paris)* **46**:1277 (1985), and references therein.
96. M. S. Dresselhaus, G. Dresselhaus, J. E. Fischer, and M. J. Moran (eds.), *Intercalated Graphite*, Vol. 20 (Elsevier, 1983); M. S. Dresselhaus and G. Dresselhaus, *Adv. Phys.* **30**:139 (1981).
97. S. Ostlund, *Phys. Rev. B* **24**:398 (1981); D. A. Huse, *Phys. Rev. B* **24**:5180 (1981).
98. D. A. Huse, M. E. Fisher, and J. Yeomans, *Phys. Rev. B* **23**:180 (1981).
99. R. Rammal and G. Toulouse, *J. Phys. (Paris) Lett.* **44**:L13 (1983); J. V. Josè, *J. Phys. A* **16**:L205 (1983); S. Grossmann, in *Non-Equilibrium Cooperative Phenomena in Physics and Related Fields*, M. G. Velarde, ed. (ASI-Series, Plenum Press, 1983); R. B. Stinchcombe, in *Scaling Phenomena in Disordered Systems* (NATO Advanced Study Institute, 1985).

100. M. Keane, *Z. Wahr. Verw. Geb.* **10**:335 (1968); F. M. Dekking, *Z. Wahr. Verw. Geb.* **41**:221 (1978).
101. F. Axel, J. P. Allouche, M. Klèman, M. Mendès-France, and J. Peyrière, *J. Phys. Coll.* **C3**:181 (1986).
102. J. M. Luck and D. Petritis, *J. Stat. Phys.* **42**:289 (1986), and references therein.
103. J. Luck, *J. Phys. A* **20**:1259 (1987); C. Godrèche, J. M. Luck, and H. Orland, *J. Stat. Phys.* **45**:777 (1986).
104. B. Derrida, in *Chance and Matter* (Les Houches Summer School, July 1986); B. Derrida and Y. Pomeau, *Europhys. Lett.* **1**:45 (1986); B. Derrida and D. Stauffer, unpublished.
105. B. Derrida and H. Flybjerg, *J. Phys. A* **19**:L1003 (1986).
106. M. Kerszberg and A. Bergman, in *Computer Simulation in Brain Science* (Copenhagen, 1986).